

**Investigating the ameliorative potential of *Aspalathus linearis* and *Cyclopia intermedia*
against lipid accumulation, lipolysis, oxidative stress and inflammation**

Mokadi Peggy Mamushi



*Thesis presented in fulfilment of the requirements for the degree of Masters in Science (Medical
Physiology) in the Faculty of Medicine and Health Science at Stellenbosch University*

SUPERVISOR: Dr C Pheiffer

CO-SUPERVISORS: Dr BU Jack and Prof SS Du Plessis

March 2020

DECLARATION

By submitting this thesis electronically, I declare that the entirety of the work contained therein is my own, original work, that I am the authorship owner thereof (unless to the extent explicitly otherwise stated) and that I have not previously in its entirety or in part submitted it for obtaining any qualification.

.....

Miss Mokadi Peggy Mamushi

March 2020

.....

Date

Copyright © 2020 Stellenbosch University
All rights reserved

ABSTRACT

Background

Despite the availability of several treatment regimens, obesity continues to be one of the greatest health challenges of the 21st century. In recent years, plant polyphenols have attracted increasing attention as nutraceuticals that are able to prevent or treat obesity and its co-morbidities. However, the first-line screening of these compounds is hampered by the shortage of *in vitro* experimental models that mimic the complex pathophysiology of obesity (excess lipid accumulation, basal lipolysis, inflammation and oxidative stress) *in vivo*. The aim of this study was two-fold. Firstly, establish a 3T3-L1 adipocyte *in vitro* model that more closely mimics obesity *in vivo*, and secondly to investigate the ameliorative properties of *Aspalathus linearis*, *Cyclopia intermedia* and their major polyphenols against these conditions.

Methods

For the experimental model, 3T3-L1 pre-adipocytes were differentiated in 5.5 mM, 25 mM or 33 mM glucose concentrations for 7 or 14 days. Lipid accumulation, basal lipolysis, oxidative stress, inflammation, mitochondrial activity and gene expression were assessed using Oil Red O staining, glycerol release, 2',7'-dichlorofluorescein-diacetate fluorescence to quantify reactive oxygen species, monocyte chemoattractant protein-1 secretion, the 3- [4, 5-Dimethylthiazol-2-yl]-2, 5 diphenyltetrazolium bromide assay and quantitative real time polymerase chain reaction, respectively. The ameliorative effects of *Aspalathus linearis* (Afriplex GRTTM) and *Cyclopia intermedia* (CPEF) against these conditions were investigated by acute and chronic treatment of the optimised experimental model with various concentrations of these plant extracts and their major polyphenol Aspalathin and Mangiferin respectively.

Results

Collectively lipid accumulation, basal lipolysis, oxidative stress, inflammation and expression of associated genes were higher after differentiation in 33 mM for 14 days compared to lower glucose concentrations and 7 days, thus these conditions were selected as the experimental model. Neither acute nor chronic treatment with 0.1 to 100 µg/ml of *Aspalathus linearis* and *Cyclopia intermedia*, and 0.1 to 100 µM of Aspalathin and Mangiferin significantly decreased lipid content. However, all treatments decreased basal lipolysis and increased mitochondrial activity.

Conclusion

Differentiation of 3T3-L1 pre-adipocytes in 33 mM glucose for 14 days increased basal lipolysis, oxidative stress and inflammation compared to lower glucose concentrations and differentiation for 7 days. *Aspalathus linearis*, *Cyclopia intermedia*, Aspalathin and Mangiferin ameliorated the increased basal lipolysis under these conditions. This study showed that differentiation in 33 mM glucose for 14 days may offer potential as an experimental model that more closely mimics obesity *in vivo* and may thus improve first-line screening for anti-obesity therapeutics. *Aspalathus linearis*, *Cyclopia intermedia* and their major polyphenol Aspalathin and Mangiferin, respectively may have potential as antilipolytic agents that are able to ameliorate obesity-associated basal lipolysis.

OPSOMMING

Agtergrond

Ten spyte van die beskikbaarheid van verskeie behandelingsregimes, bly vetsug steeds een van die grootste gesondheidsuitdagings van die 21ste eeu. In die onlangse verlede het polifenole, afkomstig vanaf plante, toenemende aandag getrek as funksionele voedingsmiddels wat vetsug en die ko-morbiditeit daarvan kan voorkom of behandel. Die eerste-lyn-sifting van hierdie verbindings word egter belemmer deur die tekort aan *in vitro* eksperimentele modelle wat die komplekse patofisiologie van vetsug (oortollige lipiedakkumulاسie, lipolise, inflammasie en oksidatiewe stres) *in vivo* kan naboots. Die doel van hierdie studie was tweeledig. Die eerste doelwit was om 'n 3T3-L1-adiposiet *in vitro*-model op te stel wat vetsug *in vivo* naboots, en tweedens om die verligtingseienskappe van *Aspalathus linearis*, *Cyclopia intermedia* en hul belangrikste polifenole teen hierdie toestande te ondersoek.

Metodes

Vir die eksperimentele model is 3T3-L1 pre-adiposiete vir 7 of 14 dae in 5.5 mM, 25 mM of 33 mM glukosekonsentrasies gedifferensieer. Lipiedakkumulاسie, lipolise, oksidatiewe stres, inflammasie, mitochondriale aktiwiteit en geenuitdrukking is onderskeidelik bepaal met behulp van “Oil Red O”-kleuring, gliserolvrystelling, 2', 7'-dichlorfluoresceïne-diasetaat fluoressensie om reaktiewe suurstofspesies te bepaal, monosiet chemo-aantrekkingskrag proteïen-1 sekresie, die 3-[4, 5-dimetieltiazol-2-yl]-2, 5 difenieltetrazoliumbromied-toets en kwantitatiewe reële tyd polimerase kettingreaksie. Die verbeteringseffekte van *Aspalathus linearis* (Afriflex GRT™) en *Cyclopia intermedia* (CPEF) op hierdie toestande is ondersoek deur die akute en chroniese behandeling van die geoptimaliseerde eksperimentele model met verskillende konsentrasies van hierdie plantekstrakte en hul belangrikste polifenole, Aspalathin en Mangiferin, onderskeidlik.

Resultate

Lipiedakkumulاسie, lipolise, oksidatiewe stres, inflammasie en uitdrukking van gepaardgaande gene was gesamentlik hoër na differensiasie in 33 mM glukose vir 14 dae in vergelyking met laer glukosekonsentrasies en 7 dae; dus is hierdie toestande as die eksperimentele model gekies. Nie akute of chroniese behandeling met 0,1 tot 100 µg/ml *Aspalathus linearis* en *Cyclopia intermedia*,

en 0,1 tot 100 μM Aspalathin en Mangiferin het die lipiedinhoud beduidend verlaag nie. Al die behandelings het egter lipolise verminder en mitochondriale aktiwiteit verhoog.

Gevolgtrekking

Differensiasie van 3T3-L1 pre-adiposiete in 33 mM glukose vir 14 dae het lipolise, oksidatiewe stres en inflammasie verhoog, vergeleke met laer glukosekonsentrasies en differensiasie vir 7 dae. *Aspalathus linearis*, *Cyclopia intermedia*, Aspalathin en Mangiferin het die verhoogde lipolise onder hierdie toestande verlig. Hierdie studie bewys dat die differensiasie in 33 mM glukose vir 14 dae potensiaal bied as 'n eksperimentele model wat vetsug *in vivo* naboots en sodoende eerste-lyn-sifting vir terapie teen vetsug kan verbeter. *Aspalathus linearis* en *Cyclopia intermedia* en hul belangrikste polifenole, Aspalathin en Mangiferin, toon dus potensiaal as antilipolitiese middels wat vetsug-geassosieerde lipolise kan verlig.

ACKNOWLEDGEMENTS

Firstly, I would like to thank our almighty God for if it was not by His grace and mercy, I would have not made it this far. He provided me with strength and protection during the research. Most importantly he blessed me with the humblest, loving, caring and beautiful souls that made my journey easy and educational.

I would also like to thank my main supervisor, Dr Carmen Pheiffer, for giving me the opportunity to do a NRF internship with her. I never thought that a girl from the deep rural area of Limpopo, who could not even speak one sentence in English could ever land an opportunity to work alongside the best researchers at the Biomedical Research and Innovation Platform of the South African Medical Research Council. Dr Pheiffer took me in with my flaws and made me into the scientist I am today. She was always patient and understanding even when she should not have been. She was a good mentor to me, ignited my love for research and sparked my interest to pursue a MSc under her supervision.

Thank you to my co-supervisor, Dr Babalwa Jack for her dedication towards my studies. She exceeded expectations, helping me with my experiments, presentations, funding applications and many more. Dr Jack trained me in Tissue Culture and was always prepared to work after hours and on weekends when needed. She taught me with love and compassion, and always remained calm and patient with me. I published my first review with her, with the little knowledge of laboratory work I had when I started my studies. I am greatly indebted to Dr Jack, she is an inspiration to me and someone that I will strive to become.

I would like to acknowledge Asive Myataza, whom I call my living angel. She was always there for me, even before I came to Cape Town. She hosted me upon my arrival in Cape Town and has been with me ever since. She helped me financially, physically, spiritually and emotionally. She became the sister I never had, she compliments me even when I know I failed big time and she boosted my confidence so much.

Thank you to, Yoonus Ebrahim, Stephanie Dias and Tarryn Willmer, my team members (Epigenetics group), who also contributed to my development by providing stimulating discussions during our journal clubs and research meetings, and for helping me prepare for seminar presentations. I would especially like to thank Yoonus for training me in quantitative real time PCR.

I would also like to thank Prof Johan Louw for assisting with tuition fees.

I acknowledge Prof Stefan du Plessis, my co-supervisor, for his scientific input and support throughout this study.

Lastly, I would like to acknowledge the South African Medical Research Council (Research and Capacity Division), Stellenbosch University, Ethel and Ernst Eriksen trust, Harry Crossley and the National Research Foundation for funding and support (NRF-Grant- holder linked bursary- Grant number: 113459).

TABLE OF CONTENTS

Page No.

ABSTRACT	i
OPSOMMING	iv
ACKNOWLEDGEMENTS	vi
TABLE OF CONTENTS	viii
LIST OF TABLES	xi
LIST OF FIGURES	xii
LIST OF ABBREVIATIONS	xiii
1. Introduction	2
1.1 Background	2
1.2 Problem statement.....	3
1.3 Rationale	4
1.4 Hypothesis.....	4
1.5 Aims	5
1.6 Objectives	5
2. Literature review	7
2.1 Obesity definition.....	7
2.2 Epidemiology of obesity	8
2.2.1 Global prevalence	8
2.2.2 Prevalence in South Africa	9
2.3 Risk factors for obesity	9
2.4 Adipose tissue	10
2.4.1 White adipose tissue	10
2.4.2 Brown adipose tissue	12
2.5 Obesity intervention.....	13
2.5.1 Lifestyle modification	15
2.5.2 Pharmacotherapy.....	15
2.5.3 Bariatric surgery.....	16
2.6 Natural products as anti-obesity agents	16
2.6.1 <i>Aspalathus linearis</i>	17

2.6.2 <i>Cyclopia</i> spp.....	19
2.7.1 <i>In vivo</i> models.....	22
2.7.2 <i>In vitro</i> models.....	22
3. Materials and methods.....	25
3.1 Study design.....	25
3.2 Materials.....	26
3.3 Cell culture.....	27
3.3.1 Thawing and culturing of 3T3-L1 cells.....	27
3.3.2 Sub-culture of 3T3-L1 cells.....	28
3.3.3 3T3-L1 pre-adipocyte differentiation.....	30
3.3.4 Cell culture media collection.....	31
3.3.5 Treatment with GRT, CPEF, Aspalathin and Mangiferin.....	32
3.4 The 3- [4, 5-dimethylthiazol-2-yl]-2, 5 diphenyltetrazolium bromide assay.....	34
3.5 Oil red o assay.....	34
3.6 Glycerol release assay.....	35
3.7 The 2',7'-dichlorfluorescein-diacetate (DCFH-DA) fluorescent assay.....	36
3.8 Enzyme-linked immunosorbent assay (ELISA).....	36
3.9 Gene expression analysis.....	37
3.9.1 RNA extraction.....	37
3.9.2 RNA quantification.....	38
3.9.3 RNA integrity.....	39
3.9.4 Reverse transcription.....	40
3.9.5 Quantitative real-time PCR.....	41
3.10 Data and statistical analysis.....	43
4. Results.....	45
4.1 Development of the <i>in vitro</i> model.....	45
4.1.1 Lipid accumulation.....	45
4.1.2 Basal lipolysis.....	45
4.1.3 Oxidative stress.....	48
4.1.4 Inflammation.....	48
4.1.5 Mitochondrial activity.....	51
4.1.6 Gene expression.....	51

4.2 Treatment with GRT, CPEF, Aspalathin and Mangiferin	58
4.2.1 Acute treatment	58
4.2.2 Chronic treatment.....	58
4.3 Summary of results	65
5. Discussion.....	68
5.1 Model development	68
5.1.1 Lipid accumulation	68
5.1.2 Basal lipolysis	69
5.1.3 Oxidative stress	70
5.1.4 Inflammation.....	71
5.1.5 Mitochondrial activity.....	72
5.2 Treatment	73
5.2.1 Lipid accumulation	73
5.2.2 Basal lipolysis	74
5.2.3 Mitochondrial activity.....	75
5.3 Strengths and limitations.....	75
5.4 Conclusion	76
5.5 Future work.....	77
6. Bibliography	78
7. Appendix.....	95
7.1 Aseptic technique.....	95
7.2 Reagents and kits	96
7.3 List of equipment and software.....	98
7.4 Preparation of medium and buffers.....	100
7.5 Assays	102
7.5.1 Preparation of the ORO and CV stains	102
7.5.2 Preparation of the MTT	102
7.6 Treatments.....	103
7.7 Supplementary data.....	104
7.8 Outputs from study	106

LIST OF TABLES

	Page No.
Table 2.1 Classification of obesity and metabolic risk.....	8
Table 2.2 An overview of the current obesity therapeutic strategies.....	14
Table 3.1 Cell densities used for seeding 3T3-L1 pre-adipocytes.....	30
Table 3.2 Reaction components used for reverse transcription	40
Table 3.3 Reaction components for qRT-PCR reactions.....	42
Table 3.4 Taqman probes.....	42
Table 4.1 RNA concentrations, total yield and purity	53
Table 4.2 RNA integrity	54
Table 4.3 Assessment of genomic DNA contamination.....	55
Table 4.4 Amplification efficiency	55
Table 4.5 Results for model development	65
Table 4.6 Results of treatment	66
Table 7.1 List of reagents.....	96
Table 7.2 List of kits	97
Table 7.3 List of equipment and consumables.....	98
Table 7.4 List of software	99
Table 7.5 Preparation of medium.....	100
Table 7.6 Preparation of DMEM without phenol red.....	100
Table 7.7 Sorenson's buffer	101
Table 7.8 Treatments	103

LIST OF FIGURES

	Page No.
Figure 2.1 Risk factors for obesity.....	10
Figure 2.2 Mechanisms relating adipocyte hypertrophy to metabolic disease	13
Figure 2.3 Chemical structure of Aspalathin	18
Figure 2.4 Chemical composition of <i>Aspalathus linearis</i> (Afriflex GRT)	19
Figure 2.5 Chemical structure of Mangiferin	20
Figure 2.6 Chemical composition of <i>Cyclopia intermedia</i> (CPEF).....	21
Figure 3.1 Experimental overview.....	26
Figure 3.2 Cell counting	29
Figure 3.3 Experimental protocol for model development.....	31
Figure 3.4 Treatment experimental outline.....	33
Figure 4.1 Effect of glucose and differentiation times on lipid accumulation.....	46
Figure 4.2 Effect of glucose and differentiation times on basal lipolysis.....	47
Figure 4.3 Effect of glucose and differentiation times on oxidative stress.....	49
Figure 4.4 Effect of glucose and differentiation times on MCP1 secretion.....	50
Figure 4.5 Effect of glucose and differentiation times on mitochondrial activity	52
Figure 4.6 Effect of glucose and differentiation times on adipogenesis, lipid metabolism and adipokine genes.....	56
Figure 4.7 Effect of glucose and differentiation times on gene expression of oxidative stress markers.....	57
Figure 4.8 Effect of acute treatment on lipid content	59
Figure 4.9 Effect of acute treatment on glycerol release	60
Figure 4.10 Effect of acute treatment on mitochondrial activity	61
Figure 4.11 Effect of chronic treatment on lipid accumulation	62
Figure 4.12 Effect of chronic treatment on glycerol release.....	63
Figure 4.13 Effect of chronic treatment on mitochondrial activity	64

LIST OF ABBREVIATIONS

ACACA	Acetyl-CoA carboxylase alpha
ADM	Adipogenesis inducing media
ADSCs	Adipocyte derived stem cells
ADIPOQ	Adiponectin
AMM	Adipogenesis maintenance media
AT	Adipose tissue
ATCC	American type culture collection
BAT	Brown adipose tissue
B2M	Beta-2-microglobulin
BMI	Body mass index
BSA	Bovine serum albumin
cDNA	complimentary DNA
CO ₂	Carbon dioxide
CPEF	Crude polyphenol enriched fraction
CV	Crystal violet
CVD	Cardiovascular disease
DCF	2',7'-dichlorfluorescein
DCFH-DA	2',7'-dichlorfluorescein-diacetate
DEX	Dexamethasone
DIO	Diet induced obesity
DMSO	Dimethyl sulfoxide
DNA	Deoxyribonucleic acid
DPBS	Dulbecco's phosphate buffered saline
FA	Fatty acid
FBS	Foetal bovine serum
FDA	Food and drug administration
GATA	GATA-binding factor 2
GRT	Green rooibos tea
HBSS	Hanks buffered salt solution

HPLC	High performance liquid chromatography
HSL	Hormone sensitive lipase
HRP	Horseradish peroxidase
Hrs	Hours
IBMX	3-isobutyl-1-methylxanthine
IL6	Interleuken-6
Kg	kilogram
LMIC	Low- and middle-income countries
M	Meters
MCP1	Monocyte chemotactic protein-1
Min	Minutes
MSCs	Mesenchymal stem cells
MRI	Magnetic resonance imaging
MTT	3- [4, 5-Dimethylthiazol-2-yl]-2, 5 diphenyltetrazolium bromide
NOX	Nicotinamide adenine dinucleotide phosphate (NADPH) oxidase
NRF1	Nuclear respiratory factor 1
ORO	Oil Red O
PBS	Phosphate buffered saline
PCR	Polymerase chain reaction
PPAR γ	Peroxisome proliferator-activated receptor gamma
qRT-PCR	Quantitative real-time polymerase chain reaction
RNA	Ribonucleic acid
ROS	Reaction oxygen species
RPL13	Ribosomal protein L13a
RT	Reverse transcription
SA	South Africa
SAT	Subcutaneous adipose tissue
Sec	Seconds
spp.	Species
SREBF1	Sterol regulatory element-binding transcription factor 1
T2D	Type 2 diabetes

T75	75 cm ² tissue culture flask
TNF α	Tumour necrosis factor alpha
UK	United Kingdom
UCP1	Uncoupling protein-1
UN	United Nations
USA	United States of America
VAT	Visceral adipose tissue
WAT	White adipose tissue
WC	Waist circumference
WHO	World Health Organisation
WHR	Waist hip ratio

Chapter 1

1. Introduction

1.1 Background

Obesity is a multifactorial disorder characterised by the excessive accumulation of fat to the extent that it negatively affects health (Hruby & Hu, 2015). Recent estimates show that approximately 641 million individuals worldwide (8.9%) are obese, with obesity rates projected to reach 20% by 2025 (NCD-RisC, 2016). Obesity increases the risk of developing chronic disorders such as insulin resistance, type 2 diabetes (T2D), cardiovascular disease (CVD) and cancer (Haslam & James, 2005). Although obesity was historically associated with developed countries, high rates are now reported in low- and middle-income countries (LMIC), driven by factors such as urbanisation, sedentary lifestyles and unhealthy diets (Ford, Patel & Narayan, 2017; Fox, Feng & Asal, 2019). Effective interventions are required to reduce the burden of obesity on health systems, particularly those in LMIC that are already over-burdened and under-resourced and least able to respond to the escalating obesity crisis.

The mechanisms that underly the development of obesity and its complications are not yet fully elucidated, although several studies show that excessive energy intake leads to adipose tissue enlargement by hypertrophy (Jo et al., 2009; Sun, Kusminski & Scherer, 2011; Jung & Choi, 2014). Adipocyte hypertrophy is associated with increased lipid accumulation, basal lipolysis, oxidative stress and inflammation. Excessive lipid accumulation and basal lipolysis leads to fatty acid (FA) secretion, with harmful effects on peripheral tissues such as the liver and muscle where it induces insulin resistance (Boden, 2011; Wang, Scherer & Gupta, 2014). Furthermore, adipocyte hypertrophy induces reactive oxygen species (ROS) and oxidative stress (Boden, 2011; Wang, Scherer & Gupta, 2014). In addition, adipocyte hypertrophy is associated with chronic low-grade inflammation (Shoelson, Herrero & Naaz, 2007; Boutens & Stienstra, 2016), which is mediated by the increased secretion of monocyte chemoattractant protein 1 (MCP1). This cytokine attracts pro-inflammatory M1 macrophages to adipose tissue and decreases secretion of anti-inflammatory adipokines such as adiponectin (Jung & Choi, 2014). Together, all these co-morbidities of obesity induce metabolic disease (Jung & Choi, 2014; Gambero & Ribeiro, 2015).

Despite the availability of several anti-obesity strategies such as lifestyle modifications (mainly diet and exercise), pharmaceutical compounds and surgery for the morbidly obese, there is still a lack of safe, effective and long-term therapies. In recent years, plant polyphenols have attracted increasing attention as nutraceuticals that are able to prevent or treat obesity and its co-morbidities (Sun, Wu & Chau, 2016). *Aspalathus linearis* and *Cyclopia* species, more commonly known as rooibos and honeybush respectively, are indigenous South African plants that are widely consumed as herbal teas due to their pleasant aroma and taste (Joubert et al., 2008). Furthermore, these herbal teas are attracting increased interest due to their health promoting properties. Previous studies have shown that they are able to prevent the development of obesity (Dudhia et al., 2013; Pfeiffer et al., 2013; Sanderson et al., 2014; Jack et al., 2017), insulin resistance (Mazibuko et al., 2013), T2D (Muller et al., 2012; Chellan et al., 2014) and CVD (Dludla et al., 2014). Moreover, a dihydrochalcone C-glycoside, Aspalathin, which is the main flavonoid of rooibos was shown to improve lipid metabolism in insulin resistant 3T3-L1 adipocytes (Mazibuko et al., 2015), while Mangiferin, a xanthone C- glycoside from honeybush was shown to ameliorate insulin resistance by inhibiting inflammation and regulating adipokine secretion in adipocytes cultured under hypoxic conditions (Yang et al., 2017).

1.2 Problem statement

Obesity is considered one of the greatest health challenges of the 21st century. Obesity increases the risk of developing chronic metabolic diseases such T2D, CVD and cancer, thereby significantly decreasing life expectancy (Peeters et al., 2003; Haslam & James, 2005). Effective interventions are required to reduce the burden of obesity on health systems, particularly those in LMIC that are already over-burdened and under-resourced and least able to respond to the escalating obesity crisis. Lifestyle modifications such as improved diet and physical activity are the most effective anti-obesity strategies (Lagerros & Rössner, 2013). However, these lifestyle modifications are difficult to adhere to, thus increasing reliance on therapeutics, which unfortunately are plagued by several side effects (Sweeting, Hocking & Markovic, 2015). There is an urgent need to identify more effective and safer anti-obesity treatments.

1.3 Rationale

In recent years, plant polyphenols have attracted increasing attention as nutraceuticals that are able to prevent or treat obesity and its co-morbidities. In particular, *Aspalathus linearis*, *Cyclopia intermedia* and their major polyphenol Aspalathin and Mangiferin, respectively have been shown to possess ameliorative properties against these conditions (Muller et al., 2012; Dudhia et al., 2013; Mazibuko et al., 2013; Pheiffer et al., 2013; Chellan et al., 2014; Dlodla et al., 2014; Sanderson et al., 2014; Jack et al., 2017; Yang et al., 2017). The use of animal models to screen these compounds are restricted due to ethical concerns, thus, *in vitro* experimental models are widely used as first-line screening tools (Nilsson et al., 2012; Denayer, Stöhrn & Van Roy, 2014; Barrett, Mercer & Morgan, 2016). However, *in vitro* models do not reflect the complex pathophysiology of obesity (excess lipid accumulation, basal lipolysis, inflammation and oxidative stress) *in vivo*, which may hamper bioactivity testing (Ruiz-Ojeda et al., 2016; Langhans, 2018). It is therefore imperative to develop an *in vitro* model that mimics the pathophysiology of obesity *in vivo* (excess lipid accumulation, basal lipolysis, inflammation and oxidative stress) in order to improve the screening of anti-obesity therapeutics.

1.4 Hypothesis

1. We hypothesised that differentiating 3T3-L1 adipocytes in higher glucose concentrations for an extended period of time (compared to standard culture conditions) will exacerbate the co-morbidities associated with obesity (increased lipid accumulation, basal lipolysis, oxidative stress and inflammation).
2. Treatment with *Aspalathus linearis*, *Cyclopia intermedia* and their major polyphenols (Aspalathin and Mangiferin) will have ameliorative effects against increased lipid accumulation, basal lipolysis, oxidative stress and inflammation.

1.5 Aims

The aims of this study are two-fold.

- To develop a 3T3-L1 adipocyte *in vitro* model that more closely mimics obesity *in vivo* (increased lipid accumulation, basal lipolysis, oxidative stress and inflammation compared to standard conditions).
- To assess the ameliorative effects of *Aspalathus linearis*, *Cyclopia intermedia* and their major polyphenol Aspalathin and Mangiferin, respectively, against increased lipid accumulation, basal lipolysis, oxidative stress and inflammation.

1.6 Objectives

Aim 1

- To differentiate 3T3-L1 pre-adipocytes in 5.5 mM, 25 mM or 33 mM glucose concentrations for 7 or 14 days; and
- To assess lipid accumulation, basal lipolysis, oxidative stress, inflammation, mitochondrial activity and gene expression.

Aim 2

- Acute and chronic treatment of the optimised model with *Aspalathus linearis* (Afriplex GRT™), *Cyclopia intermedia* (CPEF) and their major compound Aspalathin and Mangiferin, respectively; and
- To assess lipid accumulation, basal lipolysis, oxidative stress, inflammation, mitochondrial activity and gene expression in the treated adipocytes.

Chapter 2

2. Literature review

2.1 Obesity definition

The World Health Organisation (WHO) defines obesity as a complex metabolic disease characterised by the excessive accumulation of body fat to the extent that it negatively affects health (WHO, 2018). The body mass index (BMI) is the most commonly used method for assessing obesity; it is calculated by dividing an individual's weight in kilograms (kg) by the square of their height in meters (m) (kg/m^2) (Nuttall, 2015). The WHO guidelines for the classification of obesity and metabolic risk are shown in Table 2.1 (WHO, 2000). However, the use of BMI to assess obesity is widely criticised. BMI is affected by gender and ethnicity and is not able to discriminate between muscle and fat mass. Methods that have been recommended as an alternative to BMI include waist circumference (WC), waist to hip ratio (WHR) and skinfold thickness (Kuriyan, 2018; Osayande, Azekhumen & Obuzor, 2018; Eghan et al., 2019). Values of WC ≥ 88 cm for women and ≥ 102 cm for men are associated with a high metabolic risk (Table 2.1) (Kuriyan, 2018). WHR measures the ratio of the WC to the hip circumference; ratios ≥ 0.80 for women and ≥ 0.95 for men are associated with metabolic risk (Table 2.1). Skinfold thickness measures the thickness of subcutaneous tissue (skin layer) at sites such as the triceps, biceps or right hipbone with specialised callipers (Cornier et al., 2011; Kuriyan, 2018). More sensitive, but costly and technically challenging techniques due to their reliance on specialised equipment, include bioelectrical impedance analysis, computed tomography, dual-energy X-ray absorptiometry, magnetic resonance imaging and underwater weighing (Borga et al., 2018; Cornier et al., 2011; Kuriyan, 2018; Lee et al., 2018).

Table 2.1 Classification of obesity and metabolic risk

Assessment Method	Measurement and classification	Health risk
BMI (kg/m²)	< 18.5 kg/m ² (underweight)	-
	18.5 - 24.9 kg/m ² (Normal)	Normal
	25.0 - 29.9 kg/m ² (Overweight)	Increased
	30.0 - 34.9 kg/m ² (Obesity)	High
	35.0 - 39.9 kg/m ² (High obesity)	Very high
	≥ 40.0 kg/m ² (Extreme obesity)	Extremely high
Waist-to-hip ratio: Waist (cm) / Hip (cm)	Females ≥ 0.8	High
	Males ≥ 0.95	High
Waist Circumference: Waist (cm)	Females < 80 cm	Low
	≥ 80 cm	High
	≥ 88 cm	Very high
	Males < 94 cm	Low
	≥ 94 cm	High
	≥ 102 cm	Very high

Table taken from WHO, 2000.

2.2 Epidemiology of obesity

2.2.1 Global prevalence

Globally, the prevalence of obesity has nearly tripled since 1975 (WHO, 2018). Recent estimates show that approximately 641 million individuals worldwide (8.9%) are obese, with the prevalence of obesity projected to reach 20% by 2025 (NCD-RisC, 2016). According to the WHO, approximately 41 million children under the age of five years were overweight or obese in 2016. The prevalence of overweight and obesity dramatically increased from 4% in 1975 to 18% in 2016 among children and adolescents aged between five and nineteen years (WHO, 2018).

2.2.2 Prevalence in South Africa

Although obesity was historically associated with developed countries, in recent years, high rates of obesity are reported in LMIC (Ng et al., 2014; Ford, Patel & Narayan, 2017), thus placing a major burden on the already struggling and over-burdened health systems of these countries. Between 1980 and 2015, the prevalence of overweight and obesity has nearly doubled in Africa (Chooi, Ding & Magkos, 2019). South Africa, a middle-income country at the southernmost tip of Africa, has the highest rates of obesity in Africa. In 2013, approximately 69.3% of women older than 20 years were overweight, of whom 42% were obese. Although rates were lower in men (38.8% overweight and 13.5% obese), they are nevertheless higher than the global average (Ng et al., 2014). Similar trends were also observed in children and adolescents, with obesity rates of 9.6% and 7.0% in girls and boys respectively.

2.3 Risk factors for obesity

Obesity is a multifactorial disease caused by a prolonged positive energy imbalance, resulting from increased energy intake and reduced energy expenditure (Hill, Wyatt & Peters, 2012). Obesity occurs due to the interplay of a number of factors including diet, physical activity, age, genetics and epigenetics (Figure 2.1), although the consumption of high calorie diets and the lack of physical activity are considered the main drivers of the current obesity pandemic (Hill, Wyatt & Peters, 2012). Furthermore, societal factors including socio-economic status and urbanisation have also contributed to the increased prevalence of obesity in developing countries (Micklesfield et al., 2013). Other risk factors for obesity include medications such as antidepressants, glucocorticoids, psychological factors and neuroendocrine-related factors (Grundy et al., 2014; Thaker, 2017; Blüher, 2019).

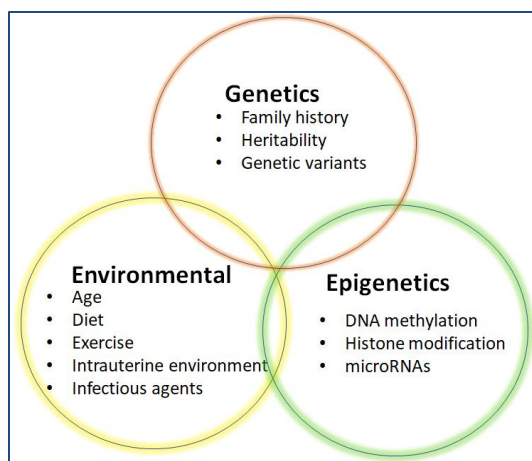


Figure 2.1 Risk factors for obesity

Overweight and obesity results from an energy imbalance due to the interplay of a multitude of risk factors.

2.4 Adipose tissue

Adipose tissue is a loose connective tissue that is mainly composed of adipocytes or fat cells, although other cell types present include fibroblasts, mesenchymal stem cells (MSCs), macrophages and vascular endothelial cells (Esteve Ràfols, 2014; Lynes & Tseng, 2018; Luong, Huang & Lee, 2019). Adipose tissue is widely distributed throughout the body and represents 15-20% of body weight in normal-weight healthy men, and 25-30% in normal-weight healthy women (Gallagher et al., 2000). There are two types of adipose tissue, namely white adipose tissue (WAT) and brown adipose tissue (BAT), which vary according to location, cellular structure and physiological function (Saely, Geiger & Drexel, 2012; Lee, Mottillo & Granneman, 2014).

2.4.1 White adipose tissue

The WAT is the most common type of adipose tissue, composed of densely packed mature adipocytes (35-75%), pre-adipocytes, MSCs, T regulatory cells, endothelial precursor cells and macrophages (Esteve Ràfols, 2014; Lynes & Tseng, 2018; Luong, Huang & Lee, 2019). Adipocytes within WAT are spherical in morphology and contain a single large lipid droplet that occupies up to 85% of the cell, a flattened peripheral nucleus and few mitochondria in the

periphery of the cytoplasmic area (Tandon, Wafer & Minchin, 2018). The main function of WAT is to regulate energy balance by storing excess energy as triacylglycerol and releasing energy in the form of FAs into the circulation when needed (Cinti, 2005; Church, Horowitz & Rodeheffer, 2012). WAT expands by two mechanisms, namely hypertrophy which increases adipocyte size, or hyperplasia, which increases adipocyte number (Jo et al., 2009). Adipocyte hypertrophy is implicated in the pathogenic mechanisms underlying obesity (Figure 2.2) (Lee, Wu & Fried, 2010; Sun, Kusminski & Scherer, 2011; Kahn, Wang & Lee, 2019; Longo et al., 2019). Adipocyte hypertrophy leads to increased basal lipolysis and FA secretion, increased inflammation through secretion of MCP1 and pro-inflammatory macrophage infiltration, and increases ROS and oxidative stress, conditions implicated in the pathophysiological mechanisms of metabolic disorders (Figure 2.2) (Boden, 2011; Sun, Kusminski & Scherer, 2011; Jung & Choi, 2014; Boutens & Stienstra, 2016). Obesity increases the risk of T2D, CVD and several types of cancer (Haslam & James, 2005). Globally, overweight and obesity contributes to about 44%, 23% and 7–41% of T2D, CVD and cancers, respectively (Frühbeck et al., 2013). Paradoxically, not all obese individuals develop chronic disease. Approximately 10-25% of obese individuals are metabolically healthy, while a similar percentage of normal weight individuals are metabolically unhealthy and have an increased risk of developing chronic disease (Blüher, 2010; Denis & Obin, 2013; Smith, Mittendorfer & Klein, 2019). This suggests that fat distribution rather than fat mass define metabolic risk (Goossens, 2017; Kwon, Kim & Kim, 2017; Grundy, Williams & Vega, 2018), and underscores the role of genetics and environmental factors in the development of obesity and metabolic disorders.

Other than being a fat reservoir, WAT also functions as a cushion to protect vital organs against mechanical stress and acts as an insulator, which controls heat conduction through the skin (Zwick et al., 2018). Emerging evidence suggest that WAT is a major endocrine organ that plays a role in regulating whole-body metabolic homeostasis via the secretion of adipokines (Kershaw & Flier, 2004; Coelho, Oliveira & Fernandes, 2013). These molecules play a vital role in regulating physiological processes such as appetite, energy balance, lipid and glucose metabolism and systemic immunity (Coelho, Oliveira & Fernandes, 2013; Musi & Guardado-Mendoza, 2014; Booth et al., 2016; Choe et al., 2016). WAT is mainly distributed within visceral adipose tissue

(VAT) and subcutaneous adipose tissue (SAT) depots (Choe et al., 2016; Mittal, 2019). VAT is characterised by ectopic fat deposition around organs and is associated with higher metabolic risk. Several lines of evidence show that increased accumulation of VAT leads to impaired insulin action, increased inflammation and oxidative stress, and the development of metabolic disease (Alexopoulos, Katritsis & Raggi, 2014; Janochova, Haluzik & Buzga, 2019; Longo et al., 2019). Conversely, SAT is characterised by fat distribution in the femoral, hips and gluteal regions and is considered metabolically benign. SAT is a metabolic buffer that prevents lipotoxicity induced lipid overflow and ectopic fat accumulation in other tissues (Ibrahim, 2010). Inadequate SAT expansion leads to visceral and ectopic fat deposition, adipokine dysregulation and insulin resistance (Longo et al., 2019).

2.4.2 Brown adipose tissue

In contrast to WAT that functions as an energy reservoir, BAT induces non-shivering thermogenesis (Keipert & Jastroch, 2014; Jastroch, Oelkrug & Keipert, 2018). Adipocytes within BAT are smaller and contain many mitochondria with increased expression of mitochondrial uncoupling protein 1 (UCP1), which gives BAT its unique ability to generate heat via adaptive thermogenesis (Saely, Geiger & Drexel, 2012; Keipert & Jastroch, 2014; Lee, Mottillo & Granneman, 2014; Jastroch, Oelkrug & Keipert, 2018). BAT is mainly present in babies and decreases with age (Yoneshiro et al., 2011; Gonçalves et al., 2017; Zoico et al., 2019). Beige adipocytes are a relatively newly discovered adipocyte found interspersed within white adipocytes (Wu et al., 2012; Sepa-Kishi & Ceddia, 2018; Lizcano, 2019; Zoico et al., 2019). Under basal conditions, beige adipocytes are morphologically indistinguishable from white adipocytes, although they share similar functions with both white and brown adipocytes (Sepa-Kishi & Ceddia, 2018). Beige adipocytes are activated upon cold exposure, chronic endurance exercise or β -adrenergic stimulation, and subsequently assume a brown adipocyte-like morphology with higher mitochondria content and multiple small lipid droplets (Sepa-Kishi & Ceddia, 2018). Activated beige adipocytes have higher expression of UCP1 and enhanced thermogenic capacity, thus leads to improved lipid and glucose metabolism (Wu et al., 2012; Sepa-Kishi & Ceddia, 2018; Lizcano, 2019).

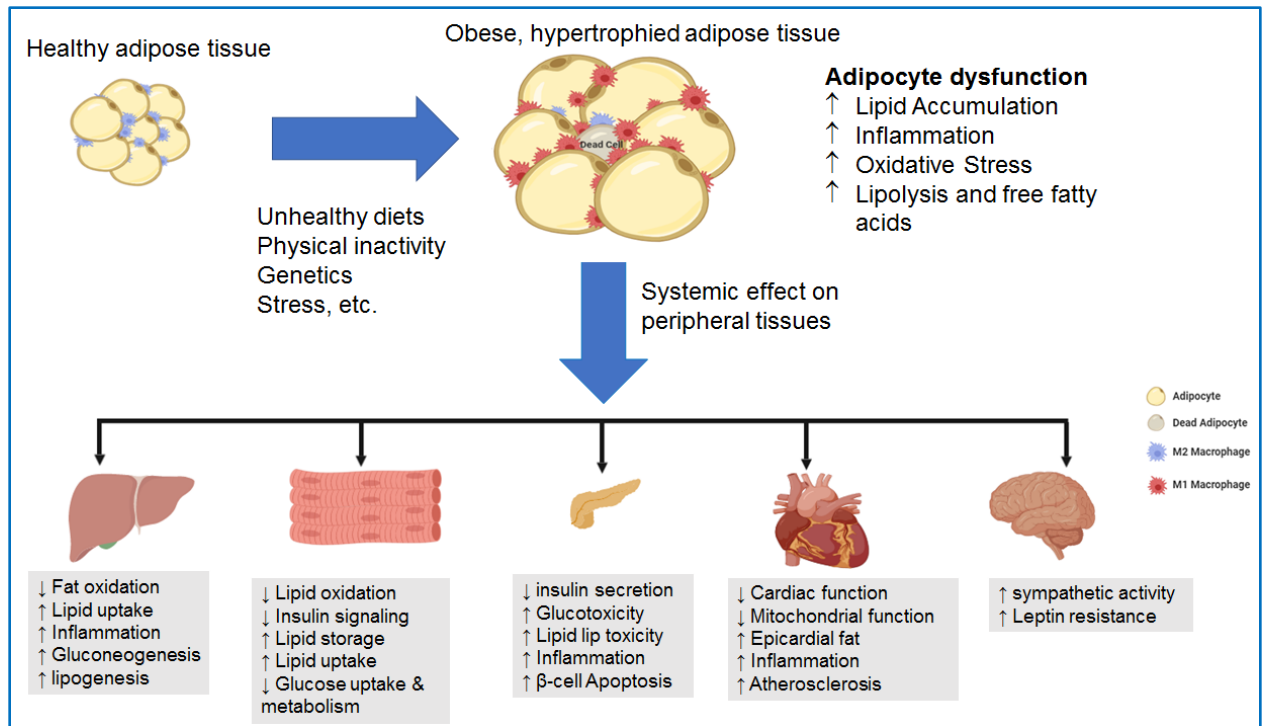


Figure 2.2 Mechanisms relating adipocyte hypertrophy to metabolic disease

Healthy adipose tissue is characterised by anti-inflammatory M2 macrophages. Factors such as unhealthy diets, physical inactivity, genetics and stress leads to adipocyte hypertrophy. Hypertrophied adipocytes recruit pro-inflammatory M1 macrophages, increasing inflammation and oxidative stress and impairing lipid metabolism. These conditions have systemic effects on peripheral tissues such as the heart, liver, muscle, pancreas and brain, leading to the development of chronic diseases. Arrow up (↑) indicates increase and arrow down (↓) signifies decrease. Figure taken and modified from (Jack et al., 2019).

2.5 Obesity intervention

Current intervention strategies for obesity include lifestyle modification, pharmacotherapy and surgery for the morbidly obese (Table 2.2).

Table 2.2 An overview of the current obesity therapeutic strategies

Treatment Strategy	Therapy	Mechanism/Activity	References
Lifestyle modification	Diet	Prevents excessive fat accumulation	(Fock & Khoo, 2013; Lagerros & Rössner, 2013)
Pharmacological drugs	Physical activity	Increase metabolic rate	(Adan, 2013; Sweeting, Hocking & Markovic, 2015; Wharton, 2016; Patel & Stanford, 2018)
	Orlistat ^a (Xenical, Alli)	Reduces fat absorption (pancreatic lipase inhibition)	
	Lorcaserin ^a (Belviq)	Appetite suppressant and promotes satiety (5-HT _{2c} receptor agonist)	
	Phentermine/topiramate ER ^a (Qsymia)	Appetite suppressant (noradrenalin releaser and anticonvulsant/neurostabilizer)	
	Phentermine HCl ^b (Adipex, Lomaira)	Appetite suppressant (noradrenalin releaser/sympaticomimetic)	
Weight-loss surgery/ Bariatric surgery ^c	Naltrexone SR/bupropion SR ^a (Contrave)	Appetite suppressant (norepinephrine/dopamine reuptake inhibitor and opioid receptor antagonist)	(Kissler & Settmacher, 2013; Piché et al., 2015; Kassir et al., 2016; Wolfe, Kvach & Eckel, 2016)
	Liraglutide ^a (Saxenda)	Appetite suppressant (GLP-1 receptor agonist)	
	Gastric sleeve; Adjustable gastric band; Roux-en-Y gastric bypass; Biliopancreatic diversion with duodenal switch	Restricts food intake and reduces nutrient absorption by decreasing stomach size or changing the anatomy of gastrointestinal area; Appetite suppression due to physiological or hormonal changes; Increases energy expenditure	

^a Approved by FDA for long-term use.

^b Approved by FDA only for short term use (≤ 12 weeks) and low dose.

^c Only recommended for morbidly obese (BMI ≥ 40 kg/m²).

Table abbreviations: β 3-AR, beta-3 adrenergic receptor; ER, extended release; FDA, Food and Drug Administration; GLP-1, glucagon-like peptide 1; 5-HT_{2c}, serotonin receptor; SR, sustained release; HCl, hydrochloride. Table taken and modified from (Jack et al., 2019).

2.5.1 Lifestyle modification

Lifestyle modifications such as calorie restriction and increased physical activity are the most effective first-line treatment strategies used in the management of overweight and obesity and have both been shown to induce significant weight loss (Table 2.2) (Fock & Khoo, 2013; Lagerros & Rössner, 2013). A low-calorie diet (800-1500 kcal/day) was shown to decrease bodyweight by 10% in obese individuals over a period of 3-12 months, while a very low-calorie diet (\leq 800 kcal/day) induced a 21.3% weight loss over a period of 6 months (Anderson, Luan & Høie, 2004; Fock & Khoo, 2013). A combination of diet and physical activity induced a 10.4% weight loss compared to diet (9.1%) or physical activity (2.1%) alone (Wing et al., 1998). However, studies have shown variability in an individual's response to diet and exercise, which is most likely due to genetic variation (Bray, 2008). Furthermore, despite the success of lifestyle modification, adherence is poor, increasing reliance on pharmacological agents to manage obesity.

2.5.2 Pharmacotherapy

Pharmacotherapy is prescribed to individuals who are unable to control obesity with lifestyle modifications (Adan, 2013; Sweeting, Hocking & Markovic, 2015; Wharton, 2016; Patel & Stanford, 2018). Orlistat was approved by the Food and Drug Administration (FDA) for the long-term treatment and management of obesity in 1990 and is the oldest anti-obesity drug on the market (Hvizdos & Markham, 1999; Sweeting, Hocking & Markovic, 2015; Patel & Stanford, 2018). It inhibits pancreatic lipase, thus decreasing intestinal fat absorption and promoting faecal fat excretion (Hvizdos & Markham, 1999). However, Orlistat has several gastrointestinal adverse effects such as oily stools, flatulence, increased defaecation, while some studies have shown that Orlistat interferes with nutrient and drug absorption (Adan, 2013; Patel & Stanford, 2018). Other anti-obesity drugs, including Lorcaserin, Phentermine/topiramate, Naltrexone/bupropion and Liraglutide have been approved by the FDA over the past few years and are currently used for the long-term treatment and management of obesity, while Phentermine hydrochloride is approved by the FDA only for short term use and at low dose (Table 2.2) (Adan, 2013; Sweeting, Hocking & Markovic, 2015; Wharton, 2016; Patel & Stanford, 2018). Several new drugs or drug combination therapies that target the central nervous system, the gastrointestinal tract or adipose tissue metabolism (either preventing the pathophysiology associated with adipose tissue dysfunction or

promoting energy expenditure via thermogenesis) are currently under preclinical investigation or in clinical development and may be approved for obesity treatment in the next few years (Barja-Fenández et al., 2014; Kakkar & Dahiya, 2015).

2.5.3 Bariatric surgery

Bariatric surgery, a collective term for gastrointestinal surgical procedures performed on severely obese patients who have at least one obesity-associated co-morbidity (Table 2.2), is considered the most effective treatment for reducing excess body weight (Kissler & Settmacher, 2013; Piché et al., 2015; Wolfe, Kvach & Eckel, 2016). The currently established bariatric procedures include the sleeve gastrectomy, adjustable gastric band, laparoscopic Roux-en-Y gastric bypass, and biliopancreatic diversion with duodenal switch (Table 2.2) (Kissler & Settmacher, 2013; Piché et al., 2015; Wolfe, Kvach & Eckel, 2016). These surgical procedures restrict food intake and reduce nutrient absorption by decreasing stomach size or changing the anatomy of the gastrointestinal area, thus suppressing appetite and improving weight loss and metabolic status (Table 2.2) (Kissler & Settmacher, 2013; Piché et al., 2015; Wolfe, Kvach & Eckel, 2016). Despite the beneficial effects of bariatric surgery, these surgical procedures are expensive and are associated with post-surgery complications such as the malabsorption of essential vitamins, minerals and pharmacological drugs (Kassir et al., 2016).

2.6 Natural products as anti-obesity agents

Plant-derived natural products are attracting increasing interest as therapeutic agents due to the perception that they are safer and more cost-effective than synthetic drugs (Mopuri & Islam, 2017; Jack et al., 2019). Natural products from different sources, especially from plants, have been used as remedies for human diseases for centuries and offer potential as a source for the development of new drugs (Veeresham, 2012; Mushtaq et al., 2018). Polyphenols are secondary plant metabolites with a variety of beneficial health effects (Pandey & Rizvi, 2009). They are found in a variety of dietary sources including fruits, vegetables and beverages such as tea or wine and are widely explored as an alternative or as an adjunct to conventional obesity treatment (Manach et al., 2004; Pandey & Rizvi, 2009; Meydani & Hasan, 2010; Wang et al., 2014). *Aspalathus linearis*

(rooibos) and *Cyclopia* ssp. (honeybush) are endemic South African plants consumed as herbal teas globally. These teas are caffeine-free and have a low tannin content (Joubert et al., 2008; Stander, Joubert & De Beer, 2019). Over the last few years, the global demand for these teas has increased and is partly attributed to their perceived beneficial health properties (Muller et al., 2018; Joubert et al., 2019). Likewise, studies have reported that the major phenolic compounds present in rooibos and honeybush possess anti-obesity effects (Fomenko & Chi, 2016; Johnson et al., 2018; Jack et al., 2019).

2.6.1 *Aspalathus linearis*

Aspalathus linearis (Brum.f) Dahlg. (Fabaceae), commonly known as rooibos, is a shrub-like leguminous member of the fynbos biome indigenous to the Western and Northern Cape region of South Africa (Joubert et al., 2008; Joubert & de Beer, 2011). Rooibos is consumed as a “fermented” (oxidised) or “unfermented” (green) rooibos tea (Joubert & de Beer, 2011). During fermentation, the leaves and stems of the rooibos plant material are bruised and soaked to enhance the natural oxidation process, which gives rise to a rooibos infusion with a distinctive reddish-brown colour and a pleasant, slightly sweet flavour. Unfermented rooibos tea maintains its green colour due to limited oxidation (Joubert et al., 2008; Joubert & de Beer, 2011).

Unlike the fermented rooibos, which has reduced anti-oxidant content as a result of oxidation, the unfermented rooibos product preserves the quality of anti-oxidants and polyphenols such as Aspalathin (Marnewick et al., 2005; Villaño et al., 2010; Joubert & de Beer, 2011). Unfermented rooibos tea displays a 28% higher *in vitro* anti-oxidant capacity than fermented rooibos tea (Villaño et al., 2010). Aspalathin, a C-glucosyl dihydrochalcone unique to rooibos (Figure 2.3), is considered the major biological active polyphenol in rooibos (Joubert & de Beer, 2011). Other major bioactive compounds found in rooibos include the dihydrochalcone, Nothofagin, flavones (Orientin, Isoorientin, Luteolin, and Apigenin) and the flavonols (Quercetin and Rutin) (Joubert & de Beer, 2011). Phenylpyruvic acid-2-O- β -D-glucoside (PPAG) is one of the major constituents of fermented rooibos infusions (Muller et al., 2013).

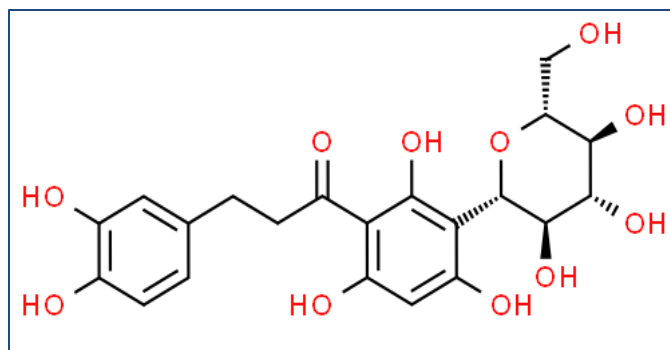


Figure 2.3 Chemical structure of Aspalathin

Chemical structure obtained from ChemSpider database (<http://www.chemspider.com>, 2019a).

In addition to its widely reported anti-oxidant properties (Joubert et al., 2005; Villaño et al., 2010), many studies have reported that rooibos tea has anti-mutagenic (Marnewick, Gelderblom & Joubert, 2000; Standley et al., 2001), anti-cancer (Marnewick et al., 2005), anti-inflammatory (Baba et al., 2009), cardioprotective (Pantsi et al., 2011; Dlodla et al., 2014), anti-diabetic (Muller et al., 2012; Mazibuko et al., 2013; Kamakura et al., 2015; Sasaki, Nishida & Shimada, 2018), and anti-obesity (Beltrán-Debón et al., 2011; Sanderson et al., 2014) properties. Sanderson et al. showed that rooibos inhibits adipogenesis and intracellular lipid accumulation in 3T3-L1 adipocytes, accompanied by decreased expression of adipogenesis and lipid accumulation genes and proteins (Sanderson et al., 2014). Although the anti-obesity effects of Aspalathin have not been reported yet, this compound was shown to improve glucose and lipid metabolism in insulin resistant 3T3-L1 adipocytes (Mazibuko et al., 2015). Recently, a green rooibos extract (GRT) was manufactured by Afriplex (Paarl, Western Cape, SA) according to standardised conditions. The polyphenol content is enriched as the rooibos is not fermented (Figure 2.4). GRT was shown to have beneficial health effects against hyperglycaemia, oxidative stress and dyslipidaemia in high-fat diet-induced diabetic vervet monkeys (Orlando et al., 2019).

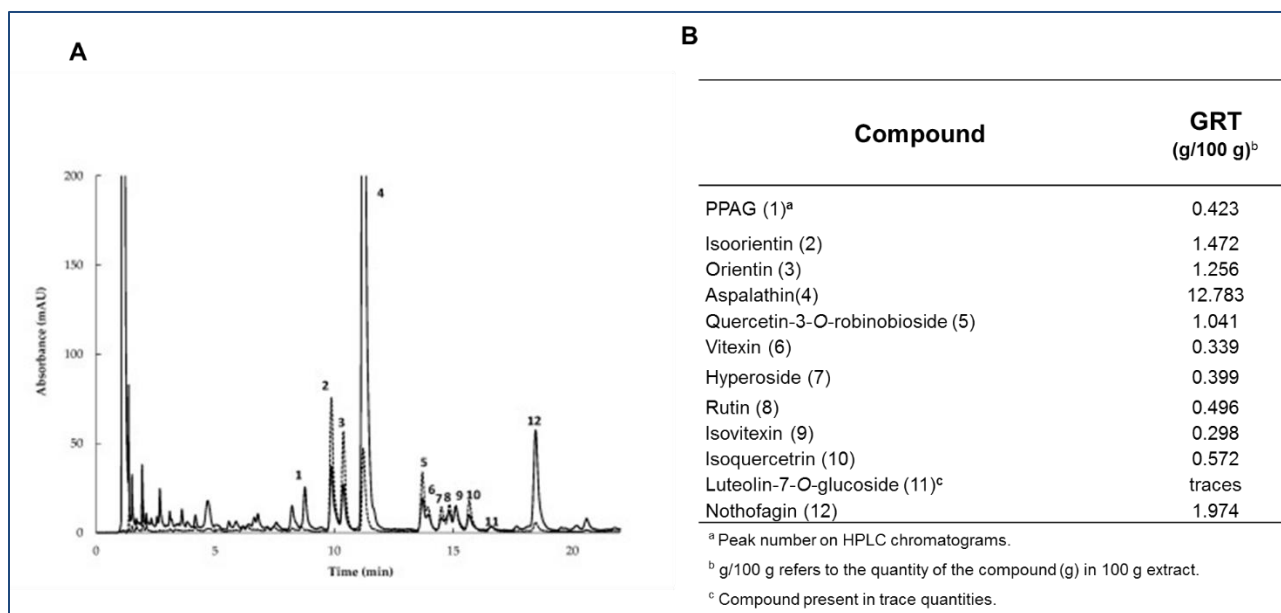


Figure 2.4 Chemical composition of *Aspalathus linearis* (Afriflex GRT)

Figure shows high performance liquid chromatography (HPLC) chromatograms of the GRT extract (A) with compound content values presented in g/100g extract (B). Adapted and modified from (Patel et al., 2016).

2.6.2 *Cyclopia* spp.

Cyclopia spp. (Genus: *Cyclopia* Vent.; Family: *Fabaceae*; Tribe: *Podalrieae*) are indigenous South African plants that are used to produce honeybush tea (Joubert et al., 2011, 2019). Twenty-three species of *Cyclopia* have been described thus far, with six species (*C. subternata*, *C. genistoides*, *C. intermedia*, *C. maculata*, *C. longifolia* and *C. sessiliflora*) used for commercial tea production (Joubert et al., 2011). Over the past 20 years, the honeybush tea industry has gained increased popularity, mainly due to its distinctively sweet flavour and aroma (Joubert et al., 2019). Plant material is fermented or oxidised at a high temperature to give the distinctive characteristics of honeybush tea. In recent years, unfermented or green honeybush has attracted interest due to its higher polyphenol content and perceived increased health effects (Joubert et al., 2011).

Cyclopia spp. are a rich source of complex bioactive phenolic compounds, and high quantities of the xanthenes, Mangiferin (Figure 2.5) and its isomer, Isomangiferin, the flavanone, Hesperidin, the benzophenone glucosides (3- β -D-glucopyranosyliriflophenone, 3- β -D-glucopyranosyl-4- β -D-glucopyranosyloxyiriflophenone and 3- β -D-glucopyranosylmaclurin), as well as dihydrochalcone glycosides (Phloretin-3',5'-di-C- β -D-glucoside and 3-hydroxy-phloretin-3',5'-di-C-hexoside) have been detected in extracts of several *Cyclopia* plants (Jack et al., 2019; Joubert et al., 2019). Other phenolic compounds found in *Cyclopia* spp. include the flavanones (Hesperitin, Naringenin, Eriocitrin, Neoponcirin and Eriodictyol) and flavones (Luteolin, Scolymoside and Vicenin-2), which have been detected in relatively small amounts in extracts of several *Cyclopia* plants (Jack et al., 2019; Joubert et al., 2019).

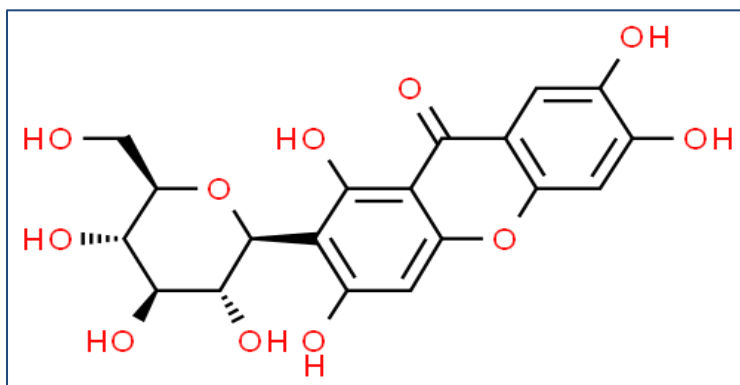


Figure 2.5 Chemical structure of Mangiferin

Chemical structure obtained from ChemSpider database (<http://www.chemspider.com>, 2019b).

Cyclopia spp. exhibit potential anti-obesity (Dudhia et al., 2013; Pfeiffer et al., 2013; Jack et al., 2017, 2018), anti-diabetic (Muller et al., 2011; Chellan et al., 2014), anti-oxidant (Joubert et al., 2008; Lawal, Davids & Marnewick, 2019), anti-mutagenic (van der Merwe et al., 2006), anti-cancer (Marnewick et al., 2005), phytoestrogenic (Mortimer et al., 2015), anti-osteoclastogenic (Visagie et al., 2015), anti-allergic (Murakami et al., 2018) and anti-inflammatory (Lawal, Davids & Marnewick, 2019) activities. Recently, Jack et al. demonstrated that a crude polyphenol-

enriched organic fraction of *C. intermedia* (CPEF) possesses anti-obesity effects *in vitro* and *in vivo* (Jack et al., 2017). The polyphenolic profile and compounds within CPEF are shown in Figure 2.6. Several studies have reported that Mangiferin, the major polyphenol detected within *Cyclopia* spp. (Figures 2.5 and 2.6), possesses anti-obesity properties *in vitro* in adipocyte models (Yoshikawa et al., 2002; Subash-Babu & Alshatwi, 2015; Yang et al., 2017). *In vivo* studies revealed that Mangiferin can reduce body weight and ameliorate obesity-associated metabolic conditions (Guo et al., 2011; Niu et al., 2012; Apontes et al., 2014; Lim et al., 2014; Acevedo et al., 2017; Wang et al., 2017).

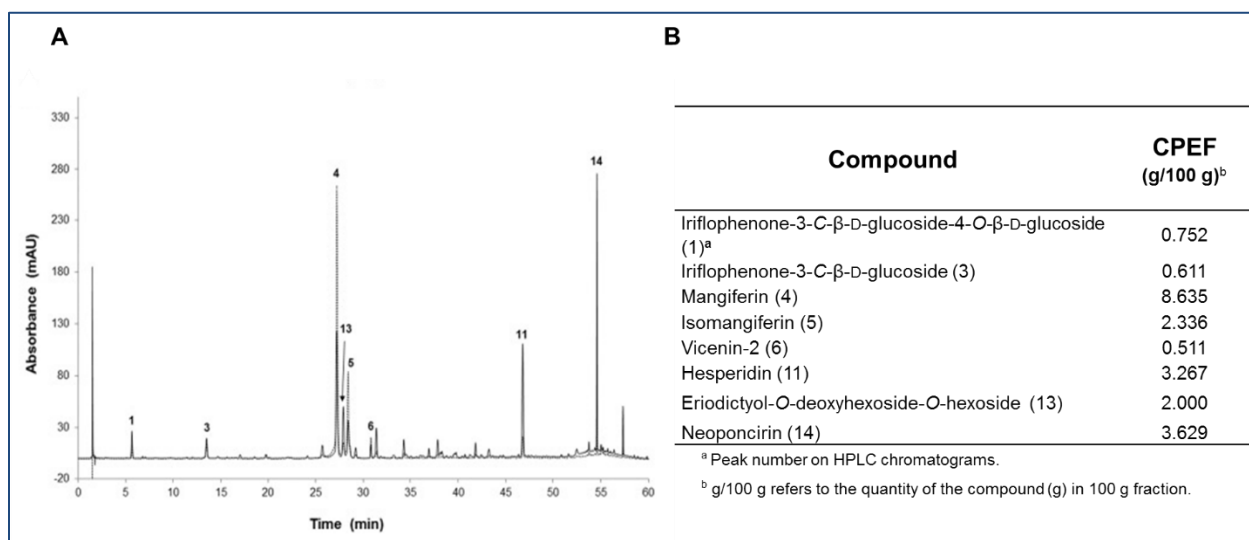


Figure 2.6 Chemical composition of *Cyclopia intermedia* (CPEF)

Figure shows a HPLC chromatogram of CPEF (A) with compound content values presented in g/100g fraction (B). Adapted and modified from (Jack et al., 2017).

2.7 Experimental models

Development of anti-obesity therapeutics require extensive preclinical screening which makes use of *in vivo* animal models and *in vitro* cell culture models.

2.7.1 *In vivo* models

Animal models have played a key role in elucidating the aetiology of obesity, including the physiological processes and genetic mechanisms that regulate energy homeostasis, appetite and adipose tissue metabolism (Agahi & Murphy, 2014; Barrett, Mercer & Morgan, 2016). *In vivo* models such as rodents and non-human primates have been used to better elucidate the efficacy, safety, pharmacology and pharmacokinetic potential of anti-obesity drug candidates before testing in humans (Agahi & Murphy, 2014). The currently used animal models of obesity include diet-induced obese (DIO) animal models and genetic models (Barrett, Mercer & Morgan, 2016). The DIO animal model involves feeding animals a diet that is high in fat, sucrose or fructose (or the combination) to induce obesity and several glucose and lipid metabolic abnormalities. As such, DIO models have been used to develop anti-obesity drugs because they provide a better understanding of the pathophysiology of obesity, especially the gene–environment interactions underlying the major causes of human obesity (Barrett, Mercer & Morgan, 2016; Ohta, Murai & Yamada, 2017). Genetic models have a spontaneous mutation or are genetically engineered to express certain physiological traits such as extreme obesity. They have been used to provide valuable insight into the pathophysiological contribution of particular genes to obesity (Agahi & Murphy, 2014; Barrett, Mercer & Morgan, 2016). The use of animal models for screening anti-obesity drugs is restricted due to ethical concerns and legislations including the “Three Rs” (reduction, refinement, and replacement) (Sharma et al., 2011; Pasupuleti, Molahally & Salwaji, 2016). As a result, *in vitro* models are commonly used as an alternative first line screening tool.

2.7.2 *In vitro* models

In vitro models such as immortalized cell lines are used as an alternative to *in vivo* animal testing in biomedical research (Chacon et al., 1996, Romero et al., 2014). These *in vitro* models are commonly used for the initial high throughput screening of anti-obesity compounds in order to

understand their effects on cellular physiology and metabolism, dose response and toxicity effects (Astashkina, Mann & Grainger, 2012; Ruiz-Ojeda et al., 2016). In addition, *in vitro* models are useful for rapid and inexpensive screening of bioactive compounds in a controlled environment (temperature, pH, hormone and nutrient concentrations, etc.), thus reducing experimental variation. Cell lines provide homogeneous, genetically identical cellular populations and cell types which are at the same differentiation stage, therefore, allowing a homogeneous response to treatments and providing consistent and reproducible results (Carter & Shieh 2010). However, cell lines have altered characteristics and functions compared to their *in vivo* counterparts.

In vitro models such as 3T3-L1 and 3T3F442A cells are the most commonly used adipocyte models for obesity studies (Ruiz-Ojeda et al., 2016). In this study we used the 3T3-L1 cell line, a well-established pre-adipocyte cell line derived from murine swiss 3T3 mouse embryos (Green & Meuth, 1974). 3T3-L1 cells exhibit a fibroblast-like morphology and upon stimulation with adipocyte differentiation inducers (insulin, dexamethasone and 3-isobutyl 1-methylxanthine (IBMX)), are converted to mature adipocytes (Green & Meuth, 1974; Green & Kehinde, 1975). Although mature 3T3-L1 adipocytes exhibit the physiological characteristics and molecular mechanisms of adipocytes *in vivo*, there have been concerns about how closely they mimic the pathophysiology of obesity and its associated morbidities (oxidative stress, mitochondrial dysfunction, inflammation, etc.) *in vivo*. Therefore, it is imperative to develop a 3T3-L1 adipocyte model that closely mimics the pathophysiology of obesity in order to allow the screening and implementation of safe and effective therapeutics to curb the burgeoning obesity epidemic.

Chapter 3

3. Materials and methods

3.1 Study design

The experimental overview is illustrated in Figure 3.1. Firstly, to develop a model of increased lipid accumulation, basal lipolysis, oxidative stress and inflammation, 3T3-L1 pre-adipocytes were differentiated in 5.5 mM, 25 mM or 33 mM glucose concentrations for 7 or 14 days. Lipid accumulation, basal lipolysis, oxidative stress and inflammation were assessed using Oil Red O (ORO) staining, glycerol release, cytokine secretion (tumour necrosis factor- α (TNF α), MCP1 and interleukin-6 (IL6)) and quantifying ROS using the 2',7'-dichlorofluorescein-diacetate (DCFH-DA) fluorescent dye, respectively. In addition, mitochondrial dehydrogenase activity was assessed using the 3- [4, 5-Dimethylthiazol-2-yl]-2, 5 diphenyltetrazolium bromide (MTT) assay, and the expression of genes associated with lipid accumulation, basal lipolysis, inflammation and oxidative stress were measured using quantitative real-time polymerase chain reaction (qRT-PCR).

Secondly, the anti-obesity effects of two plant extracts and their major polyphenols were assessed by investigating their ameliorative properties against lipid accumulation, basal lipolysis, oxidative stress and inflammation in the optimised experimental model developed previously. Briefly, 3T3-L1 adipocytes were treated with a standardised green rooibos extract of *Aspalathus linearis* (GRT), a crude polyphenol enriched fraction of *Cyclopia intermedia* (CPEF) and their major compound Aspalathin and Mangiferin, respectively. The treatment was divided into acute and chronic treatment, whereby mature adipocytes were treated for 24 hrs or 7 days, respectively.

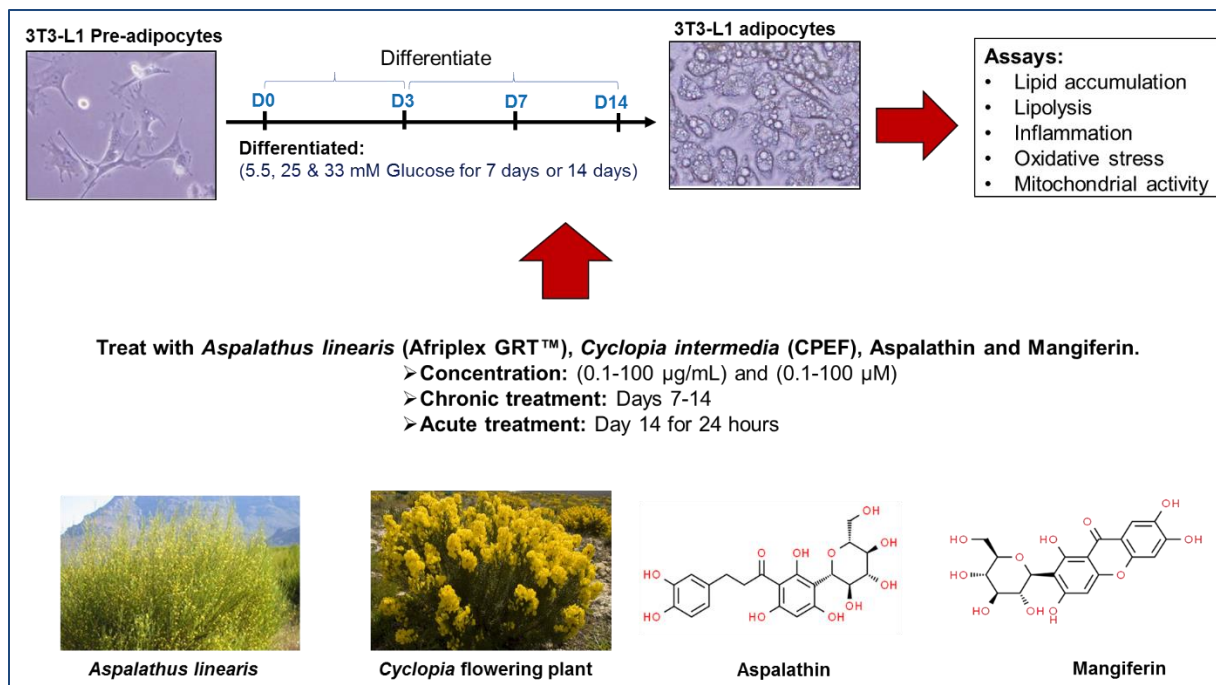


Figure 3.1 Experimental overview

3.2 Materials

The murine 3T3-L1 pre-adipocyte cell line (ATCC® CL-173™) was purchased from the American Type Culture Collection (ATCC), Manassas, VA, USA. GRT, a standardised, commercial extract of *Aspalathus linearis* containing 12.8% of Aspalathin was obtained from Afriplex (Pty) Ltd., Paarl, Western Cape, SA. The CPEF was supplied by Babalwa Jack (Jack et al., 2017). Aspalathin (ca. 98% purity) was purchased from High Force Research Ltd., Durham, UK. Mangiferin (≥ 98% purity) was purchased from Sigma-Aldrich, St Louis, MO, USA and Isoproterenol was purchased from Merck (Sigma-Aldrich, St Louis, MO, USA). All other chemicals were purchased from Sigma-Aldrich, St Louis, MO, USA, unless otherwise stated. All materials, suppliers and product numbers are listed in the Appendix.

3.3 Cell culture

Cell culture was conducted adhering to aseptic technique (Appendix). The 3T3-L1 pre-adipocytes were cultured and maintained in Dulbecco's modified eagle media (DMEM, Gibco, Thermo Fisher Scientific, Waltham, MA, USA) supplemented with 25 mM glucose and 10% fetal bovine serum (FBS, Gibco, Thermo Fisher Scientific, Waltham, MA, USA) (standard conditions for 3T3-L1 culture recommended by the ATCC) (ATCC, 2013), or in 5.5 mM, 25 mM, or 33 mM glucose and 10% FBS for experimental conditions. Cell culture procedures were conducted in a biohazard safety cabinet, class II (Airvolution lab, Johannesburg, Gauteng, SA) and cells were maintained in an incubator (Galaxy R CO₂ incubator, RS Biotech, West Lothian, UK) at 37°C in humidified air with 5% carbon dioxide (CO₂) (Air Products, Bellville, Western Cape, SA).

3.3.1 Thawing and culturing of 3T3-L1 cells

A cryogenic vial containing 3T3-L1 cells (1×10^6 cells/ml) in cryopreserving medium containing DMEM, 10% FBS and 7% (v/v) dimethyl sulfoxide (DMSO) (Sigma-Aldrich, St Louis, MO, USA) was removed from liquid nitrogen storage and thawed in a 37°C water bath. Immediately after thawing, the cells were transferred into a 15 ml centrifuge tube containing 9 ml of 37°C pre-warmed, pre-adipocyte growth medium (DMEM supplemented with 10% FBS) and centrifuged at $800 \times g$ for 5 min (Eppendorf 5810 Centrifuge, Eppendorf, Hamburg, Germany). Thereafter, the supernatant was aspirated, and the cell pellet was resuspended in 5 ml of pre-warmed, pre-adipocyte growth medium. Following this, 1 ml of cell suspension was transferred to a 75 cm² tissue culture flask (T75) (Nest Scientific, Rahway, NJ, USA) containing 17 ml of pre-warmed, pre-adipocyte growth medium. The cells were incubated under standard cell culture conditions (37°C in humidified air with 5% CO₂) for 24 hrs, where after the pre-adipocyte growth medium was refreshed. Cells were kept under standard cell culture conditions until they reached 70-80% confluency and subsequently sub-cultured using a split ratio of 1:5 (section 3.3.2). Passage number was kept to below 20 in order to prevent the depletion of specific cell phenotypes such as the ability of these cells to differentiate due to excessive passage and to maintain consistency between experiments.

3.3.2 Sub-culture of 3T3-L1 cells

3.3.2.1 Trypsin treatment

Upon confluency, pre-adipocyte growth medium was aspirated from the T75 flask, (Nest Scientific, Rahway, NJ, USA) and cells were rinsed with pre-warmed Dulbecco's phosphate buffered saline (DPBS) (Lonza, Walkersville, MD, USA). Thereafter, the adherent cells were dislodged by incubating with 2 ml of trypsin (Lonza, Walkersville, MD, USA) under standard cell culture conditions for 5 - 7 min. Cells were viewed under an Olympus inverted light microscope (CKX 41, Olympus; Melville, NY, USA) to confirm whether they had dislodged from the flask. Trypsinisation was stopped by adding 8 ml of pre-warmed pre-adipocyte growth medium directly to the cells, where after the cell suspension was thoroughly mixed by gently pipetting up and down at least 8 times to disaggregate cell clumps and ensure a single cell suspension. Thereafter, the cell suspension was transferred to a 15 ml centrifuge tube and centrifuged for 5 min at $800 \times g$ (Eppendorf 5810 Centrifuge, Eppendorf, Hamburg, Germany). The supernatant was aspirated, and the cell pellet was resuspended in pre-warmed, pre-adipocyte growth medium, subsequently sub-cultured in T75 flasks and incubated under standard cell culture conditions. Cell density and viability were determined (section 3.3.2.2) prior to freezing cells for storage (section 3.3.2.3) or seeding cells in their appropriate multi-well plates for subsequent *in vitro* bioassays (section 3.3.2.4).

3.3.2.2 Cell counting

Following trypsinisation, the number of viable cells were quantified using a haemocytometer and trypan blue dye (Invitrogen, Carlsbad, CA, USA). Briefly, a 10 μ l volume containing the cell suspension and trypan blue in a 1:1 ratio was loaded onto one of the haemocytometer chambers (Figure 3.2B) and viewed under an inverted microscope where both viable (clear/unstained) and non-viable (stained blue) cells were counted in four of the nine quadrants of the haemocytometer (Figure 3.2C). The percentage of viable cells was calculated using the formula in Figure 3.2A. If the viability of cells was 70% or above, they were used for making stocks for freezing or seeded into multi-well plates for subsequent *in vitro* bioassays.

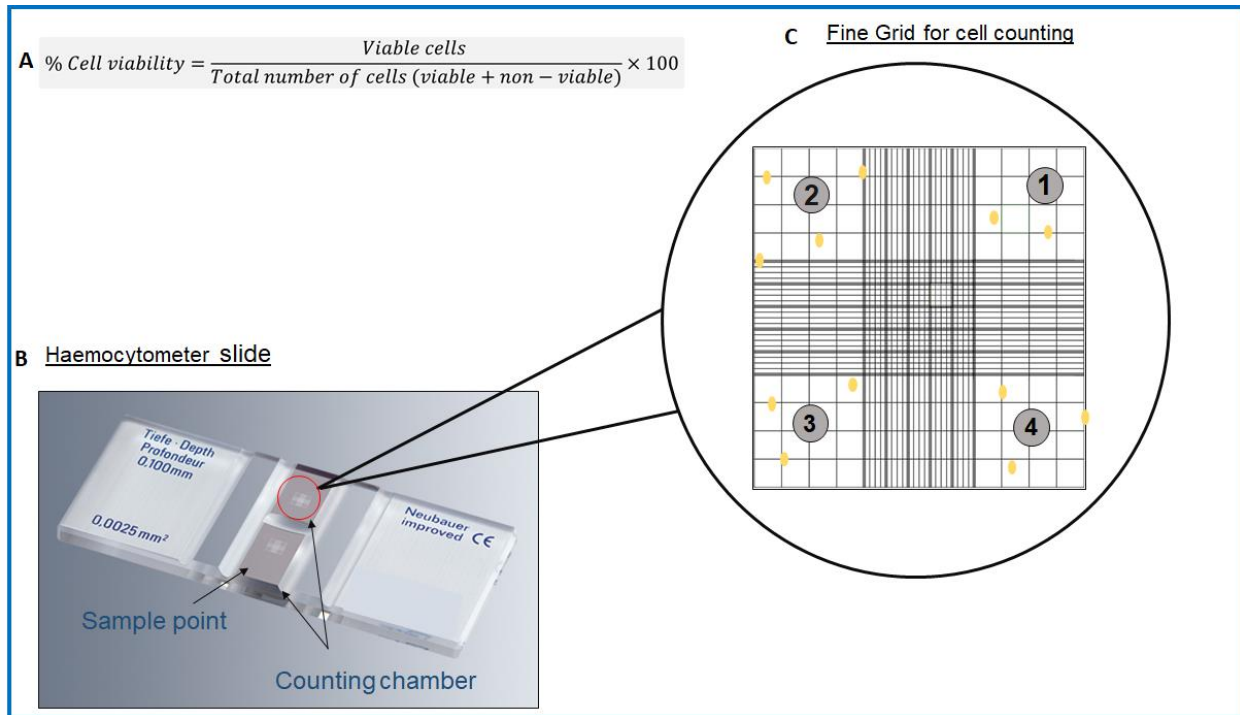


Figure 3.2 Cell counting

Equation for determining cell viability (A), an illustration showing the haemocytometer slide with two counting chambers (B) and the number of squares used for cell counting (indicated by grey circled numbers) to obtain number of cells/ml (C). Cells on the bottom and right lines of the quadrant were not counted.

3.3.2.3 Freezing 3T3-L1 pre-adipocytes

Subsequent to cell counting, cells were centrifuged at $800 \times g$ for 5 min. The supernatant was carefully discarded without disturbing the pellet, and the pellet was resuspended in sterile cold freezing medium containing DMEM, 10% FBS and 7% (v/v) DMSO at a volume required to achieve 1×10^6 cells/ml. The resuspended cell suspension was aliquoted into cryotubes (1 ml) and placed on ice. Each cryovial was labelled with the cell line, passage number, cell concentration and date. Cells were stored overnight at -80°C and thereafter transferred to liquid nitrogen for long term storage.

3.3.2.4 Seeding of 3T3-L1 pre-adipocytes

After quantifying the number of viable cells, 3T3-L1 pre-adipocytes were seeded at relative seeding densities into their respective multi-well plates (Table 3.1). The seeding cell concentration for 3T3-L1 pre-adipocytes is 2×10^4 cells/ml. Thereafter, the cells were incubated under standard cell culture conditions in pre-adipocyte growth medium, until they reached 100% confluency (~4 days) and the medium was refreshed every 48 hrs.

Table 3.1 Cell densities used for seeding 3T3-L1 pre-adipocytes

Cell culture plates	Seeding Concentration (cells/ml)	Cell density (cells/well)	Volume (ml)
96-well	2×10^4	4×10^3	0.2 ml
24-well	2×10^4	2×10^4	1 ml
6-well	2×10^4	6×10^4	3 ml

3.3.3 3T3-L1 pre-adipocyte differentiation

Adipocyte differentiation was conducted in accordance with the ATCC protocol (ATCC, 2013), with slight modifications in order to develop an *in vitro* 3T3-L1 adipocyte model with increased lipid accumulation, basal, oxidative stress and inflammation. Briefly, fully confluent 3T3-L1 pre-adipocytes (100% confluent at day 4 post seeding) were induced to differentiate into adipocytes by incubating the cells (day 0) in adipocyte differentiation medium (ADM) consisting of DMEM, at various concentrations of glucose (5.5 mM, 25 mM and 33 mM) each supplemented with 10% FBS, 0.5 mM IBMX (Sigma-Aldrich, St Louis, MO, USA), 1 μ g/ml insulin (Sigma-Aldrich, St Louis, MO, USA) and 1 μ M dexamethasone (Sigma-Aldrich, St Louis, MO, USA) under standard cell culture conditions until day 3 of differentiation (Figure 3.3). After 72 hrs (day 3), the ADM was changed to adipocyte maintenance medium (AMM) consisting of DMEM, at various concentrations of glucose (5.5 mM, 25 mM and 33 mM) each supplemented with 10% FBS and 1 μ g/ml of insulin for a further two days (Figure 3.3). On day 5, adipocytes were incubated in DMEM

(5.5 mM, 25 mM or 33 mM glucose concentrations) supplemented with 10% FBS under standard cell culture conditions until day 7 or day 14 of differentiation, with medium refreshed every 48 hrs (Figure 3.3). The cells and the cell culture media were collected at days 0, 7 and 14 of differentiation, and used for bioassays and gene expression analysis as shown in Figure 3.3.

3.3.4 Cell culture media collection

After the 3T3-L1 cells were differentiated or treated as described in sections 3.3.3 and 3.3.5, cell culture media were collected into 15 ml centrifuge tubes (Nest Scientific, Rahway, NJ, USA). The collected media were centrifuged (SL 16R Thermo Fisher Scientific, Waltham, MA, USA) at $3500 \times g$ for 15 min at 4°C to remove cell debris. Thereafter, the media were aliquoted and stored at -80°C , for subsequent measurement of basal lipolysis (section 3.6) and inflammation (section 3.8).

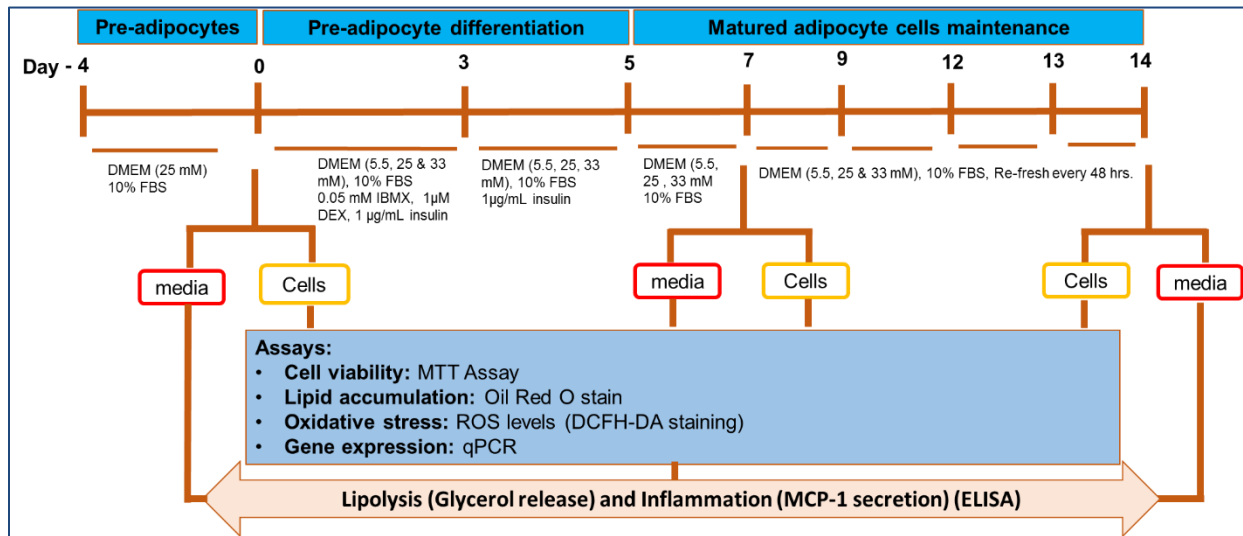


Figure 3.3 Experimental protocol for model development

3.3.5 Treatment with GRT, CPEF, Aspalathin and Mangiferin

3.3.5.1 Preparation of extracts and compounds

The GRT and CPEF extracts were each weighed and prepared fresh daily by dissolving in 10% DMSO to yield a stock concentration of 10 mg/ml. The compounds, Aspalathin (452.13 g/mol) and Mangiferin (422.34 g/mol) were both weighed (20 mg) and dissolved in 2 ml of 100% DMSO to yield stock solutions of 22.1 mM and 23.6 mM, respectively. Stock solutions of compounds were aliquoted into 2 ml Eppendorf tubes and stored at -80°C until required. Thereafter, stock solutions of 1 mg/ml GRT, 1 mg/ml CPEF, 22.1 mM Aspalathin and 23.6 mM Mangiferin were prepared in treatment medium (either DMEM supplemented with 33 mM glucose and 10% FBS or DMEM without phenol red supplemented with 33 mM glucose, 0.1% bovine serum albumin (BSA) and 3.7 g/l sodium bicarbonate (NaHCO_3) (Sigma-Aldrich, St Louis, MO, USA)). Stock solutions were serially diluted 10-fold to prepare 0.1, 1, 10 and 100 $\mu\text{g/ml}$ or 0.1, 1, 10 and 100 μM working solutions in their respective treatment media. The highest working solution (100 $\mu\text{g/ml}$ or 100 μM) was filter sterilised using a 0.22 μm pore-size Millex-GP Polyethersulfone membrane syringe filter before subsequent dilutions were prepared. The final concentration of DMSO in the working solutions was 0.01% (v/v) DMSO, thus 0.01% (v/v) DMSO prepared in treatment medium was used as a vehicle control since it was previously shown not to affect cell viability and lipid content in 3T3-L1 adipocytes (Dludla et al., 2018). A 10 μM concentration of Isoproterenol, a selective β -adrenergic receptor agonist that induces lipolysis (Schott et al., 2017), was added to the cells as a positive control. Cells were treated as described below (sections 3.3.5.2 and 3.3.5.3).

3.3.5.2 Chronic treatment

For chronic treatment, 3T3-L1 pre-adipocytes were seeded into 24-well plates and differentiated in 33 mM glucose media until day 7, as described in section 3.3.3. At day 7, 3T3-L1 adipocytes were treated with 33 mM glucose media, a vehicle control (0.01% DMSO), GRT, CPEF, Aspalathin, Mangiferin or Isoproterenol for 6 days, and treatment media was refreshed every 48 hrs. At day 13, the treatment media was replaced with DMEM without phenol red media and treated for a further 24 hrs.

3.3.5.3 Acute treatment

For acute treatment, 3T3-L1 pre-adipocytes were seeded in 24-well plates and differentiated in 33 mM glucose for 14 days as described in section 3.3.3. On day 14, differentiated 3T3-L1 adipocytes were treated for 24 hrs with 33 mM glucose medium, a vehicle control, the GRT, CPEF, Aspalathin and Mangiferin or Isoproterenol prepared in DMEM without phenol red as described in Section 3.3.5.1.

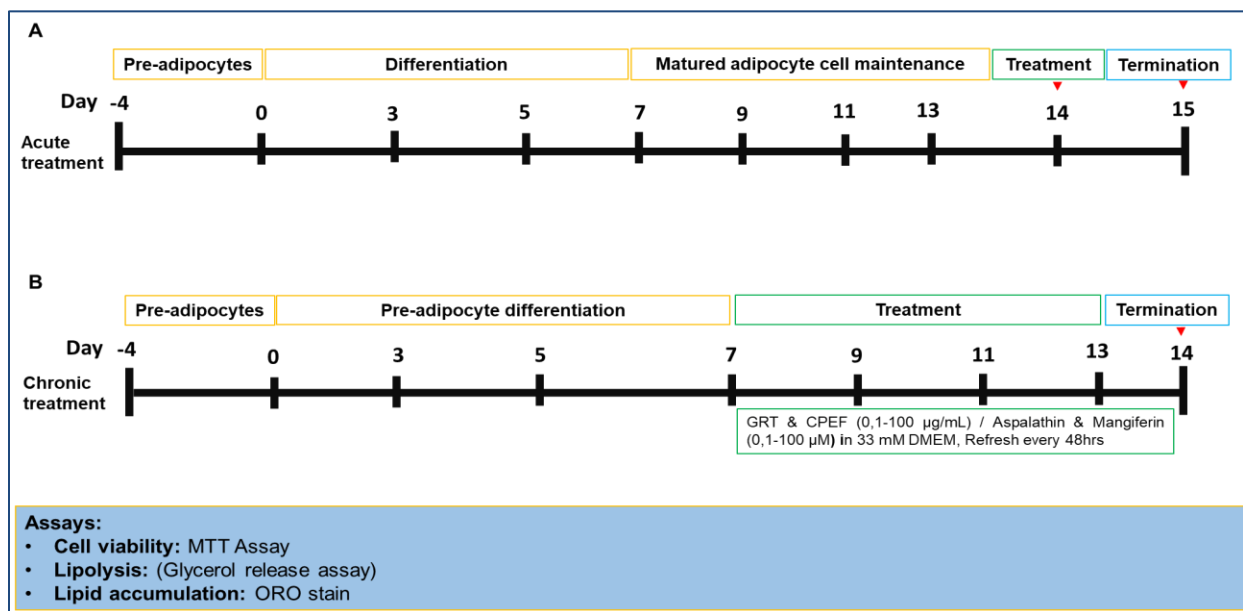


Figure 3.4 Treatment experimental outline

Timeline for acute (A) and chronic (B) treatment.

3.4 The 3- [4, 5-dimethylthiazol-2-yl]-2, 5 diphenyltetrazolium bromide assay

Cell viability was assessed using the MTT assay, a quantitative colorimetric assay that measures cell survival and proliferation. The MTT assay measures the reduction of the yellow tetrazolium salt (MTT) to a purple formazan product by mitochondrial succinate dehydrogenase activity (Mosmann, 1983; Weyermann, Lochmann & Zimmer, 2005), a process which indicates metabolically viable cells. After the 3T3-L1 cells were differentiated or treated as described previously (sections 3.3.3 and 3.3.5), the medium was aspirated, and cells were washed with pre-warmed DPBS. Afterwards, 50 µl of pre-warmed MTT (Sigma-Aldrich, St Louis, MO, USA) solution (2 mg/ml prepared in DPBS) was added to the cells and incubated at 37°C under standard cell culture conditions for 30 min. After incubation, the MTT solution was aspirated, 200 µl of DMSO and 25 µl of Sorenson's glycine buffer (0.1 M Glycine and 0.1 M Sodium chloride, pH 10.5) were added to each well, and the plate was gently shaken to dissolve the purple formazan crystals. Absorbance was measured at 570 nm using the BioTek® ELx800 plate reader and the Gen 5 software (BioTek Instruments Inc., Winooski, VA, USA). Absorbance values were used to quantify MTT content and results were expressed as a percentage relative to the control at 100%.

3.5 Oil red o assay

The accumulation of lipid droplets was measured using ORO staining. ORO is a hydrophobic fat-soluble dye that stains and quantifies neutral intracellular lipids red (Escorcia et al., 2018). After the 3T3-L1 cells were differentiated or treated as described previously (sections 3.3.3 and 3.3.5), the medium was aspirated, cells were washed with pre-warmed DPBS and thereafter fixed with 10% (v/v) neutral buffered formalin for 15 min at room temperature. Cells were rinsed with DPBS and stained with 0.7% (v/v) ORO (Sigma-Aldrich, St Louis, MO, USA) working solution (prepared by diluting a 1% stock (w/v) in 100% Isopropanol (Sigma-Aldrich, St Louis, MO, USA) with distilled water) for 30 min at room temperature. Subsequently, ORO stain was removed, and cells were rinsed with distilled water at least three times to remove the unbound stain. Thereafter, the amount of lipid accumulation in cells was quantified by dissolving the dye that was retained in the cells with 200 µl of 100% Isopropanol, after which absorbance was read at 490 nm using a BioTek® ELx800 plate reader equipped with Gen 5® software (BioTek Instruments Inc., Winooski, USA) for data acquisition.

Lipid content was normalised to cell density using crystal violet (CV) staining that stains live cells (Chiba, Kawakami & Tohyama, 1998). Briefly, after extraction of the ORO stain, cells were washed with 70% (v/v) ethanol (Sigma-Aldrich, St Louis, MO, USA), and thereafter stained with CV solution (0.5% v/v) prepared by diluting a 1% (w/v) stock with distilled water. Following 5 min of incubation at room temperature, the CV dye was removed, cells were washed three times with DPBS, and cell density was quantified by eluting the CV dye retained in the cells with 70% (v/v) ethanol. Absorbance was measured at 570 nm using a BioTek® ELx800 plate reader equipped with Gen 5® software (BioTek Instruments Inc., Winooski, USA) for data acquisition. The ORO/CV values were calculated and expressed as a percentage relative to the control.

3.6 Glycerol release assay

Lipolysis was assessed by measuring the glycerol secreted in the cell culture media. Lipolysis is the process whereby triglycerides are broken down to FAs and glycerol, and the dysregulation of lipolysis is associated with adipose tissue dysfunction and obesity (Gaidhu et al., 2010). Thus, the quantification of glycerol is used as a marker for lipolysis. After 3T3-L1 cells were differentiated or treated as described previously (sections 3.3.3 and 3.3.5), glycerol secreted into cell culture media was quantified using the Lipolysis Colorimetric Assay Kit (Sigma-Aldrich, St Louis, MO, USA) according to the manufacturer's instructions. Briefly, a glycerol standard curve was prepared by pipetting 0, 2, 4, 6, 8, and 10 µl (in duplicate) of a 1 mM glycerol standard into a clear 96-well plate, where after glycerol assay buffer was added into each well to a final volume of 50 µl. For each sample, 50 µl of the undiluted cell culture medium was added to the 96 well plate, in duplicate, and thereafter, 50 µl of a reaction mix consisting of 46 µl of glycerol assay buffer, 2 µl of glycerol probe and 2 µl of glycerol enzyme mix was added to both sample and standard wells. The plate was incubated for 30 min at room temperature, protected from light. After incubation, absorbance was measured at 570 nm using a SpectraMax® i3x Multi-Mode Microplate reader and the SoftMax Pro 7 Software (Molecular Devices, Sunnyvale, CA, USA). The glycerol concentration for each sample was calculated from the standard curve and represented as a percentage relative to the control.

3.7 The 2',7'-dichlorofluorescein-diacetate (DCFH-DA) fluorescent assay

Intracellular production of ROS, a marker of oxidative stress, was measured using the 2',7'-dichlorofluorescein-diacetate (DCFH-DA) fluorescent dye as previously described (Dludla et al., 2018). The method is based on the oxidation of the non-fluorescent fluorescein derivative (DCFH-DA) by ROS to yield a highly fluorescent product, 2',7'-dichlorofluorescein (DCF). After 3T3-L1 cells were differentiated as described in section 3.3.3, cells were rinsed with Hank's Balanced Salt Solution (HBSS, Lonza, Walkersville, MD, USA) followed by incubation with 1 μ M of DCFH-DA (Biolabs, Inc., San Diego, CA, USA) (prepared in HBSS) for 30 min, under standard cell culture conditions. The cells were washed once with 100 μ l of HBSS, thereafter, the same volume of HBSS was added in each well to measure DCF fluorescence signal at an excitation/emission spectrum of 485 ± 20 and 528 ± 20 nm using a BioTek[®] FLx800 plate reader and Gen 5 software (BioTek Instruments Inc., Winooski, USA).

3.8 Enzyme-linked immunosorbent assay (ELISA)

Inflammation was quantified by measuring the amount of MCP1 secretion. MCP1 is a potent chemoattractant for macrophage infiltration and activation in adipose tissue and induces inflammation in adipocytes (Kanda et al., 2006). After 3T3-L1 cells were differentiated or treated as described previously (sections 3.3.3), MCP1 secretion was quantified in cell culture supernatants using the mouse MCP1 DuoSet ELISA Kit (R&D Systems, Minneapolis, MN, USA), according to the manufacturer's instructions. Briefly, a 96-well microplate was coated with 100 μ l per well of capture antibody diluted with phosphate buffered saline (PBS) and incubated at room temperature overnight (~16 hrs). The following day, each well was aspirated and washed 3 times by filling with wash buffer (400 μ l) using a squirt bottle. For good performance, after the last wash the plate was blotted against clean paper towel to completely remove wash buffer residue. The plate was blocked by adding 300 μ l of reagent diluent to each well, sealed and incubated at room temperature for a minimum of 1 hr. Thereafter, each well was aspirated and washed 3 times as previously described. Hereafter, 100 μ l of samples or standards (250, 125, 62.5, 31.3, 15.6, 7.8, 3.9 pg/ml) were added to the plate in duplicate. The plate was sealed with an adhesive strip and incubated for 2 hrs at room temperature. The wells were aspirated and washed with wash buffer as previously described. Subsequently, 100 μ l of the detection antibody diluted in reagent diluent

was added into each well and the plate was sealed with a new adhesive strip and incubated for 2 hrs at room temperature. Each well was aspirated and washed with wash buffer as previously described. After adding 100 µl of streptavidin horseradish peroxidase (HRP) working dilution to each well, the plate was sealed and incubated away from light for 20 min at room temperature. The wells were aspirated and washed 3 times with wash buffer as previously described. Thereafter, 100 µl of substrate solution was added to each well and incubated for 20 min at room temperature avoiding direct light. The reaction was stopped by adding 50 µl of stop solution to each well. The plate was mixed by tapping it gently. Finally, absorbance was measured at 450 nm on a SpectraMax® i3x Multi-Mode Microplate reader using the SoftMax Pro 7 Software (Molecular Devices, Sunnyvale, CA, USA). The readings at 540 nm were subtracted from the readings at 450 nm to correct for optical imperfections in the plate.

3.9 Gene expression analysis

Quantitative real-time polymerase chain reaction (qRT-PCR) was used to assess the expression of genes involved in lipid metabolism, glucose homeostasis, inflammation and oxidative stress in the experimental model (Table 3.4). This is one of the most sensitive and specific techniques commonly used to study gene expression (Bustin & Mueller, 2005).

3.9.1 RNA extraction

The 3T3-L1 cells were seeded into 6 well plates and differentiated as described in section 3.3.3. Thereafter, media was aspirated, cells were washed with pre-warmed DPBS and 300 µl of QIAzol lysis reagent (Qiagen, Hilden, Germany) was added per well and incubated for 5 min at room temperature. After incubation, cells were scraped from the plates and triplicate wells were pooled into a sterile 2 ml Eppendorf tube and stored at -80°C. For RNA extraction, cells were homogenised using stainless steel beads (Qiagen, Hilden, Germany), altering between 2 min at 25 Hz in the TissueLyser (Qiagen, Hilden, Germany) using pre-cooled adapters and 1 minute on ice. Homogenisation was repeated 4 times. Homogenates were centrifuged at 15 000 × g for 10 min at 4°C (Eppendorf 5415R Centrifuge, Eppendorf, Hamburg, Germany). The supernatant was carefully transferred to a new 1.5 ml Eppendorf tube, 200 µl of chloroform (Sigma-Aldrich, St

Louis, MO, USA) was added and mixed by shaking the tube for 3 min, followed by centrifugation at $15\ 000 \times g$ for 15 min at 4°C . The upper aqueous phase containing the RNA was transferred to a new 1.5 ml Eppendorf tube (this was done carefully without disturbing the white interphase or organic phase), 0.5 ml of Isopropanol was added, and the samples were incubated overnight at -20°C to precipitate the RNA. The next day, samples were centrifuged at $15\ 000 \times g$ for 30 min at 4°C to pellet the RNA. The supernatant was discarded, and the pellet was washed with 70% (v/v) ethanol and centrifuged at $15\ 000 \times g$ for 15 min at 4°C . The wash step was repeated twice. After the final wash, the Eppendorf tubes were blotted against paper towel to drain out ethanol and the pellet was allowed to air dry. After drying, the RNA pellet was redissolved in 100 μl of RNase-free water, mixed by pipetting up and down several times, and then incubated at 55°C for 10 min to aid resuspension. RNA purification was done using the RNeasy Mini kit (Qiagen, Hilden, Germany) according to the manufacturer's instructions. Briefly, 350 μl of RLT lysis buffer was added to each RNA sample and mixed by pipetting up and down numerous times, followed by the addition of 250 μl of 100% ethanol and mixed as before. The samples were then transferred to RNeasy spin columns in 2 ml collection tubes. Spin columns were centrifuged at $13\ 000 \times g$ for 15 sec at room temperature to allow RNA to bind, and the flow through was discarded. RPE wash buffer (500 μl) was added to the column and centrifuged at $13\ 000 \times g$ for 15 sec at room temperature, and the flow through was discarded. This step was repeated and thereafter, the column was transferred to a new 2 ml collection tube and centrifuged at $16\ 000 \times g$ for 1 min at room temperature, to completely dry the column. RNA was eluted by placing the spin column into a sterile 1.5 ml collection tube, 50 μl of RNase-free water was added directly to the column membrane, and the column was centrifuged for 1 min at $16\ 000 \times g$. The elution step was repeated as described above in a separate 1.5 ml collection tube to ensure that all the RNA in the membrane column was retrieved. The eluted RNA samples were used for RNA quantification and subsequently stored at -80°C for future use.

3.9.2 RNA quantification

RNA concentration and purity were assessed by measuring absorbance at 260 nm (A_{260}) and 280 nm (A_{280}) using the NanoDrop™ One/OneC microvolume UV-Vis Spectrophotometer (Thermo Fisher Scientific, Waltham, MA, USA). A 260 nm wavelength measures nucleic acids such as

RNA and DNA, while proteins are absorbed at a wavelength of 280 nm. Therefore, the ratio of 260 nm to 280 nm ($A_{260/280}$) is used to assess the purity of a sample (Die & Román, 2012). For RNA samples, a ratio between 1.8-2.0 is generally accepted as being sufficiently pure. The ratio of 260 nm to 230 nm ($A_{260/230}$) is used as a secondary measure of purity and shows contaminants that absorb at or near 230 nm (Die & Román, 2012). For RNA quantification, the pedestal of the nanodrop was wiped with a tissue paper and further cleaned with 1 μ l of RNase-free water. The spectrophotometer was blanked by pipetting 1 μ l of RNase-free water onto the pedestal. Thereafter, 1 μ l of each RNA sample was pipetted onto the pedestal and the absorbance and concentration of each sample was read in duplicate and the mean value of the two readings was used.

3.9.3 RNA integrity

High quality RNA is crucial for accurate gene expression results (Imbeaud et al., 2005; Fleige & Pfaffl, 2006). The integrity of RNA is assessed by visualisation of the 28S and 18S ribosomal RNA bands; a 28S:18S ratio of 2 indicates intact RNA, whereas lower ratios indicate RNA degradation. RNA quality and integrity can be assessed using either traditional methods such as gel electrophoresis or automated methods such as the Agilent bioanalyser. The Agilent bioanalyser is more convenient, sensitive and uses small quantities of RNA samples compared to gel electrophoresis (Schroeder et al., 2006). Furthermore, the software calculates the RNA Integrity number (RIN) which is based on a numbering system of 1 to 10, with 1 indicating a degraded RNA and a RIN number between 7-10 indicating good and intact RNA quality (Schroeder et al., 2006). RNA integrity was assessed by the Central Analytical Facilities (CAF), Stellenbosch University, Western Cape, SA using the Agilent 2100 bioanalyzer (Agilent Technologies Inc. Waldbronn, Germany) and the Agilent RNA 6000 Nano kit. Control RNA (100 ng/ μ l was included as an internal reference), Agilent RNA Nano Ladder and RNA samples were heat denatured for 2 min at 70°C, briefly centrifuged and immediately placed on ice. The chip was primed on the priming station with Agilent RNA Nano gel-dye mix and 5 μ l of Agilent RNA Nano Marker was added to all wells including the RNA ladder well. Thereafter, 1 μ l of RNA ladder, control or sample was added to respective wells. The chip was mixed for 1 minute at 2 400 \times g using the IKA vortex mixer, then immediately loaded and analysed on an Agilent 2100 Bioanalyser.

3.9.4 Reverse transcription

Total RNA was reverse transcribed into complementary DNA (cDNA) using the High Capacity cDNA kit (Applied Biosystems, Foster City, CA, USA) according to the manufacturer's instructions. Briefly, 1 µg of RNA was added to RNase-free water to a final volume of 10 µl and placed on ice. A reverse transcription (RT) reaction mix consisting of nuclease-free water (Ambion Inc., Austin, TX, USA), reaction buffer, random primers, dNTPs and reverse transcriptase was prepared into separate 2 ml Eppendorf tubes and designated as RT plus. A second reverse transcriptase-free reaction mix was made using the same reaction mix with the reverse transcription enzyme replaced by water (Table 3.2) and designated as RT minus. RT plus and RT minus reaction mixes were mixed by pipetting and the tubes were briefly centrifuged. Thereafter, 10 µl of RT plus or RT minus reaction mixes were added to 0.2 ml tubes containing 1 µg of each of the RNA samples. After brief centrifugation the tubes were placed in a 2720 thermal cycler. Reactions were incubated at 25°C for 10 min, 37°C for 3 hrs, and 85°C for 5 sec to inactivate the reverse transcriptase enzyme. Samples were stored at -20°C until gene expression analyses by qRT-PCR. The amount of genomic DNA contamination was calculated by subtracting RT plus from RT minus tube (negative control).

Table 3.2 Reaction components used for reverse transcription

Component	RT plus (µl)	RT minus (µl)
1 µg RNA (in RNase free H ₂ O)	10	10
10 x RT buffer	2	2
25 x dNTP mix	0.8	0.8
10 x random primers	2	2
Nuclease-free water	3.2	4.2
Reverse Transcriptase	1	0
Total volume	20	20

3.9.5 Quantitative real-time PCR

TaqMan[®] Gene Expression Assays from Applied Biosystems (Table 3.4) were used to assess the expression of genes associated with lipid accumulation, basal lipolysis, inflammation and oxidative stress. We used the TaqMan[®] Gene Expression Assays that span an exon junction to avoid the interference of genomic DNA contamination in the PCR (Bustin, 2000; Bustin & Nolan, 2004), therefore DNase treatment of RNA was not required. TaqMan[®] Gene Expression assays consist of primers and a TaqMan[®] probe with a FAM[™] fluorescent reporter dye on the 5' end and a non-fluorescent quencher dye (NFQ) on the 3' end of the probe. TaqMan[®] probes do not fluoresce when the reporter and quencher dyes are in close proximity. During a PCR reaction, following primer and probe binding, the Taq polymerase cleaves the probe to release the fluorescent reporter from the quencher dye, thereby allowing the detection of the reporter dye fluorescence (Arya et al., 2005).

A reaction mixture (final volume of 9 µl) containing 5 µl of TaqMan[®] universal PCR master mix II (Applied Biosystems, Foster City, CA, USA), 0.5 µl of TaqMan[®] Gene Expression Assay (Table 3.4) and 3.5 µl of nuclease-free water was prepared (Table 3.3) and scaled up based on the number of samples to be analysed. Thereafter, the reaction mix was transferred into the wells of the PCR plate, followed by 1 µl of the cDNA samples or the standard curve, which was prepared by making a 10-fold dilution series of pooled cDNA (5 µl of each cDNA sample) (Table 3.3). A no template control sample i.e. no cDNA and substituted with 1 µl of nuclease-free water was used as a negative control in all PCR reactions. The PCR plates were covered with adhesive film, centrifuged briefly at 3 000 × g, mixed by shaking the plate for 5 min on an IKA plate shaker, followed by another brief centrifugation at 3 000 × g. Thereafter, the PCR plate was run on an ABI 7500 sequence detection system instrument (Applied Biosystems, Foster City, CA, USA) using the following universal cycling conditions; 50°C for 2 min and 95°C for 10 min, followed by 40 cycles of 95°C for 15 sec and 60°C for 1 min. Data was analysed using the ABI standard quantification (AQ) software (SDS V1.4) using automatic Ct threshold and baseline settings.

Table 3.3 Reaction components for qRT-PCR reactions

Component	Volume (µl)
2 × Master mix	5
TaqMan Gene Expression Assay	0.5
Water	3.5
cDNA	1
Total volume	10

Table 3.4 Taqman probes

Probe	Function	Assay ID
Tumour necrosis factor alpha (<i>TNFα</i>)	Pro-inflammatory	Mm00443258_m1
Adiponectin (<i>ADIPOQ</i>)	Anti-inflammatory	Mm00456425_m1
Peroxisome proliferator-activated receptor gamma (<i>PPARγ</i>)	Promotes adipogenesis	Mm00440940_m1
Acetyl-CoA Carboxylase Alpha (<i>ACACA</i>)	Fatty acid synthesis	Mm01304257_m1
Sterol Regulatory Element Binding Transcription Factor 1 (<i>SREBF1</i>)	Promotes adipogenesis	Mm00550338_m1
GATA Binding Protein 2 (<i>GATA2</i>)	Inhibits adipogenesis	Mm00492301_m1
Hormone sensitive lipase (<i>HSL</i>)	Lipolysis	Mm00495359_m1
Nuclear respiratory factor 1 (<i>NRF1</i>)	Anti-oxidant	Mm01135606-m1
NADPH oxidase 4 (<i>NOX4</i>)	Pro-oxidant	Mm00479246-m1
Beta-2-Microglobulin (<i>B2M</i>)	Housekeeping genes	Mm00437762_m1
Ribosomal protein L13a (<i>RPL13</i>)	Housekeeping genes	Mm01612986_gH

3.10 Data and statistical analysis

Data was analysed in Microsoft Excel[®] (Microsoft Office, version 2016, Microsoft Corporation, Washington, DC, USA) and GraphPad Prism version 7 (GraphPad Software, La Jolla, CA, USA). Tissue culture data was expressed as the average of three independent experiments, assayed in triplicate or more, and represented as the mean \pm standard deviation (SD) or as a percentage relative to 5.5 mM glucose on day 7 or day 14, which was set as 100%. For treatment, the mean values were normalised to the DMSO vehicle control set as 100%. Statistical differences between groups were determined one-way analysis of variance (ANOVA) and the Kruskal-Wallis test as appropriate with the Tukey or Dunn's posthoc tests, respectively. A p value of < 0.05 was considered to be statistically significant.

Chapter 4

4. Results

4.1 Development of the *in vitro* model

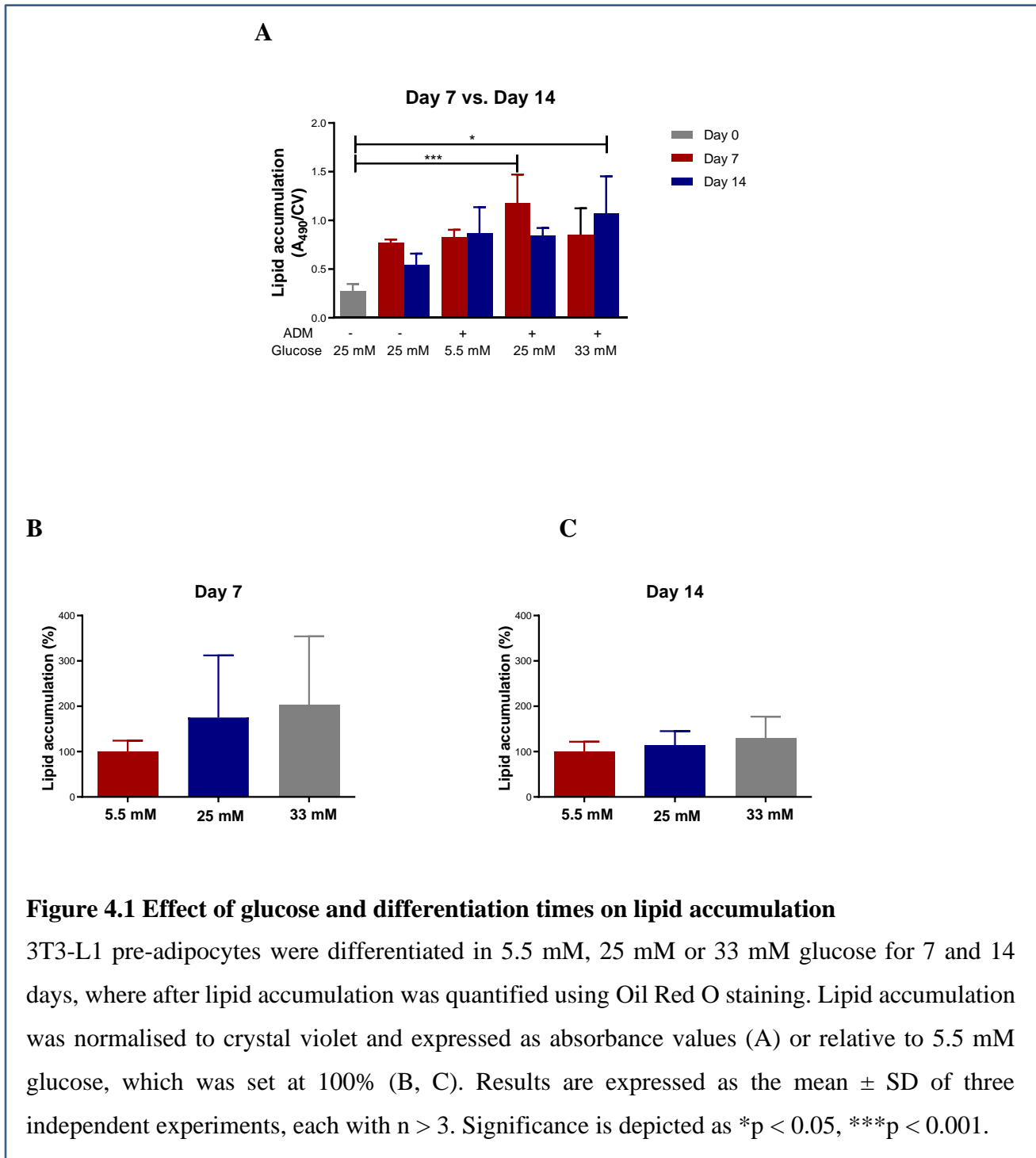
4.1.1 Lipid accumulation

To investigate the effect of different glucose concentrations and differentiation times on intracellular lipid accumulation, 3T3-L1 pre-adipocytes were differentiated in 5.5 mM, 25 mM or 33 mM glucose, and lipid content quantified at day 0 (pre-adipocytes) and after 7 and 14 days using ORO staining. Lipid accumulation increased with time in pre-adipocytes cultured with or without ADM. Lipid content was significantly higher in adipocytes exposed to 25 mM glucose for 7 days (1.17 ± 0.30 vs. 0.27 ± 0.07 OD₄₉₀/CV, $p < 0.001$) and 33 mM glucose for 14 days (1.07 ± 0.38 vs. 0.27 ± 0.07 OD₄₉₀/CV, $p = 0.012$) compared to pre-adipocytes (Figure 4.1A). At day 7, lipid accumulation appeared to be higher with increasing glucose concentrations (Figure 4.1B), although differences were not statistically significant. Glucose concentrations did not exhibit any significant difference on lipid accumulation at day 14 (Figure 4.1C). The results further show that, the long-term exposure of the cells to high glucose (25 mM) in the induced adipogenesis in the absence of differentiation cocktail, suggesting that high glucose and incubation time have a positive effect on adipogenesis.

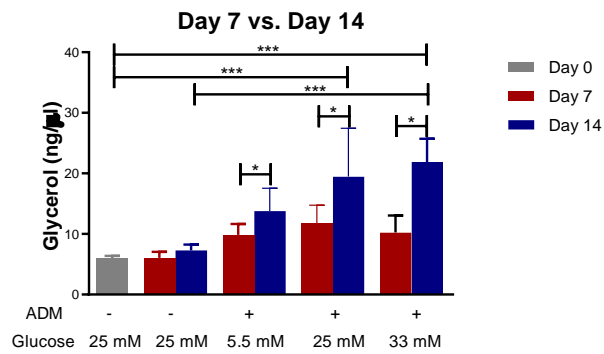
4.1.2 Basal lipolysis

The effect of different glucose concentrations on basal lipolysis was investigated by differentiation of 3T3-L1 pre-adipocytes in 5.5 mM, 25 mM or 33 mM glucose and quantification of glycerol release, a marker of lipolysis after 0, 7 and 14 days. As expected, glycerol secretion in pre-adipocytes was lower than in differentiated adipocytes, with statistical significance reached for 25 mM (6.00 ± 0.37 vs. 19.50 ± 7.90 ng/ μ l, $p < 0.001$) and 33 mM (6.00 ± 0.37 vs. 21.88 ± 3.83 ng/ μ l, $p < 0.001$) glucose at 14 days (Figure 4.2A). After 14 days of culture, adipocytes exposed to 5.5 mM (13.78 ± 3.76 vs. 9.84 ± 1.81 ng/ μ l, $p = 0.022$), 25 mM (19.50 ± 7.94 vs. 11.75 ± 2.99 ng/ μ l, $p = 0.015$) and 33 mM (21.88 ± 3.83 vs. 10.24 ± 2.80 ng/ μ l, $p < 0.001$) glucose exhibited higher glycerol secretion than adipocytes exposed to those concentrations for 7 days. Comparison of adipocytes at 14 days, showed that culture in ADM and 33 mM glucose significantly increased basal lipolysis compared to controls (21.88 ± 3.83 vs. 7.28 ± 0.98 ng/ μ l, $p = 0.009$). Although

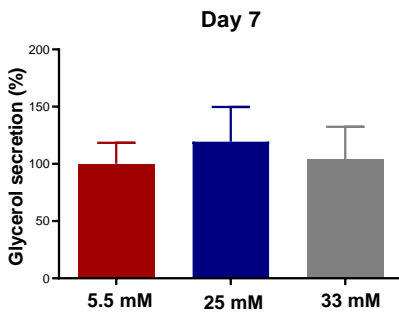
glycerol release increased with higher glucose concentrations, the results were not statistically significant (Figure 4.2B, C).



A



B



C

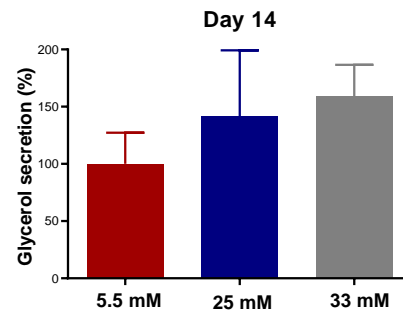


Figure 4.2 Effect of glucose and differentiation times on basal lipolysis

3T3-L1 pre-adipocytes were differentiated in 5.5 mM, 25 mM or 33 mM glucose for 7 and 14 days, where after glycerol release, a marker of lipolysis was quantified using the Glycerol Assay Kit. Glycerol concentration is represented in A, while B and C represents the percentage secretion at day 7 (A) and day 14 (B) relative to 5.5 mM glucose, which was set at 100%. Results are expressed as the mean \pm SD of three independent experiments, each with $n > 3$. Significance is depicted as * $p < 0.05$, *** $p < 0.001$.

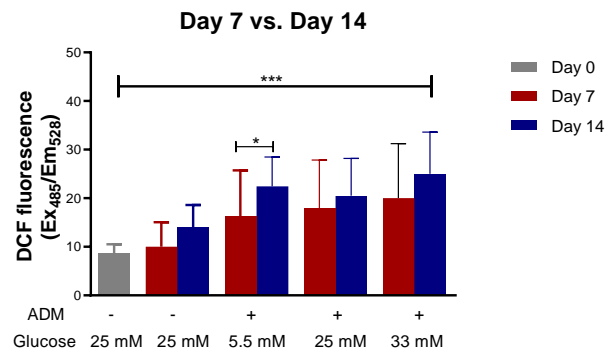
4.1.3 Oxidative stress

To assess the effect of different glucose concentrations and differentiation times on oxidative status, intracellular ROS production was quantified using DCF fluorescence. DCF fluorescence was higher in differentiated compared to undifferentiated adipocytes (Figure 4.3A) and at day 14 compared to day 7. Adipocytes differentiated in 5.5 mM glucose for 14 days had higher levels of ROS compared to adipocytes differentiated for 7 days (22.44 ± 6.06 vs. 16.29 ± 9.46 DCF units, $p = 0.032$). ROS production increased with increasing glucose concentrations (100.00 ± 6.7 vs. 114.4 ± 12.5 vs. 125.20 ± 17.1 % for 5.5 mM, 25 mM and 33 mM respectively; $p < 0.01$) at day 7 (Figure 4.3B) and at day 14 DCF fluorescence was higher at 33 mM compared to 5.5 mM (108.50 ± 17.00 vs. 100.0 ± 17.4 %, $p = 0.015$) and 25 mM (108.50 ± 17.00 vs. 89.50 ± 21.7 %, $p < 0.001$) at day 14 (Figure 4.3C).

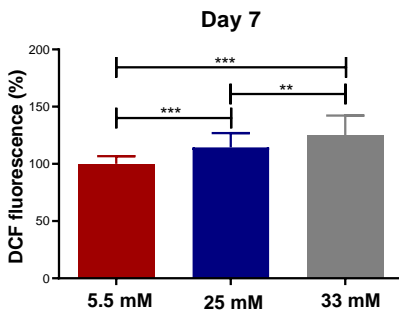
4.1.4 Inflammation

To assess the effect of different glucose concentrations and differentiation times on inflammation, 3T3-L1 pre-adipocytes were differentiated in 5.5 mM, 25 mM or 33 mM glucose and MCP1, IL6 and TNF α secretion quantified after 7 and 14 days. MCP1 secretion was significantly higher in adipocytes cultured in 33 mM glucose compared to pre-adipocytes (2219.00 ± 178.10 vs. 1800.00 ± 205.20 pg/ml, $p=0.005$) (Figure 4.4A). Differentiation with varying glucose concentrations for 7 days did not affect MCP1 secretion (Figure 4.4B). However, after 14 days, differentiation in 33 mM compared to 5.5 mM (120.20 ± 9.60 vs. 100.00 ± 7.60 %, $p=0.007$) and 25 mM (120.20 ± 9.60 vs. 105.20 ± 7.30 %, $p=0.034$) glucose increased MCP1 secretion (Figure 4.4C). TNF α and IL6 expression could not be detected. The kit used to detect TNF α and IL6 was not sensitive enough to detect the expression of these inflammation parameters.

A



B



C

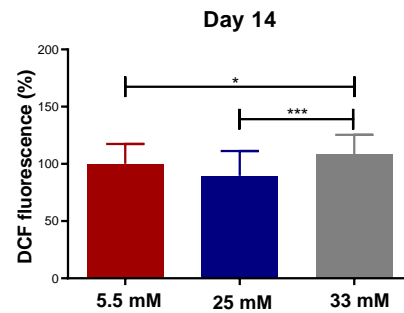
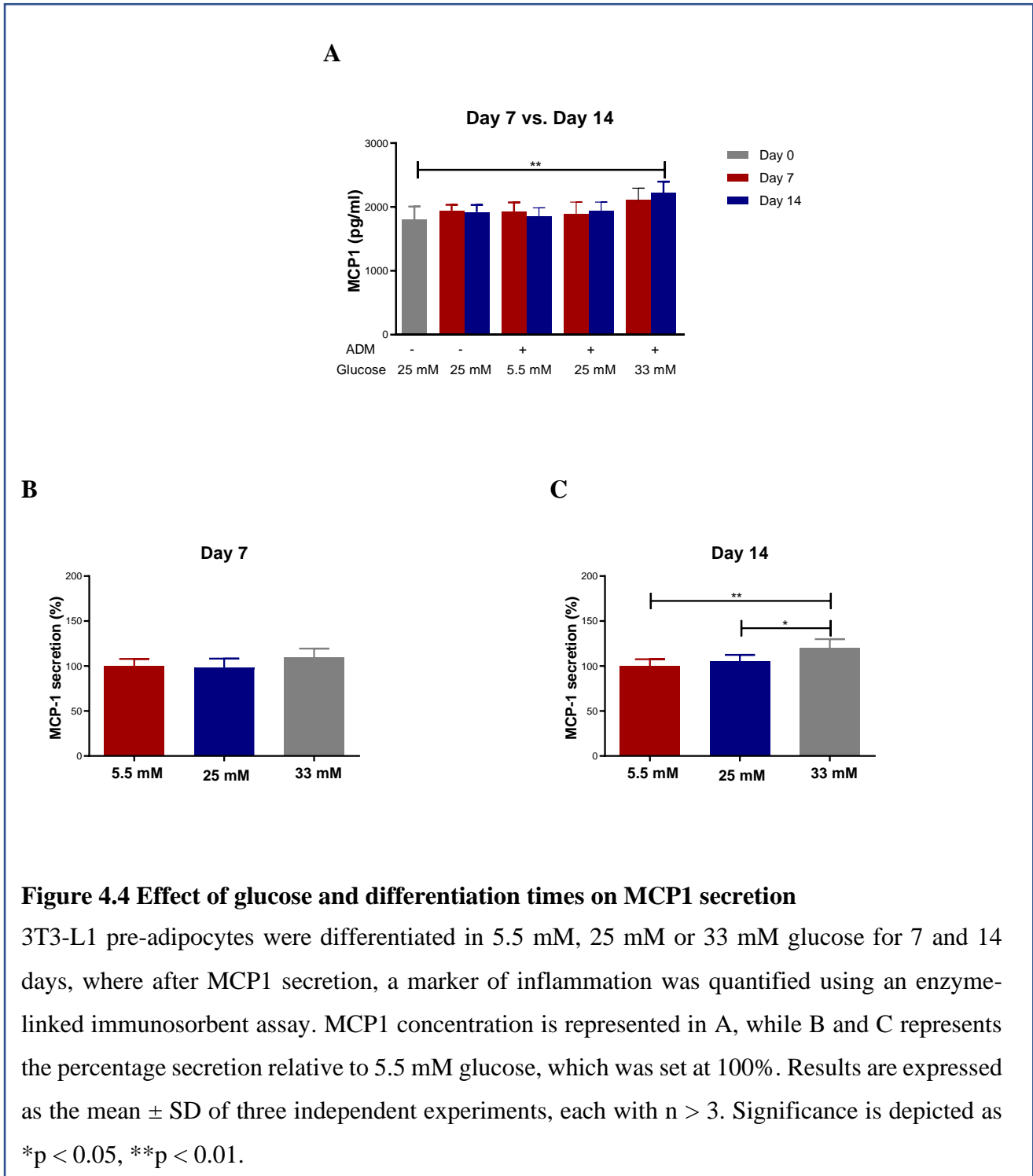


Figure 4.3 Effect of glucose and differentiation times on oxidative stress

3T3-L1 pre-adipocytes were differentiated in 5.5 mM, 25 mM or 33 mM glucose for 7 and 14 days, where after oxidative stress was measured by quantification of DCF fluorescence. A represents fluorescence values, while the percentage fluorescence at day 7 (B) and day 14 (C) are expressed relative to 5.5 mM glucose, which was set at 100%. Results are expressed as the mean \pm SD of three independent experiments, each with $n > 3$. Significance is depicted as * $p < 0.05$, ** $p < 0.01$, *** $p < 0.001$.



4.1.5 Mitochondrial activity

The effect of glucose concentration and differentiation times on mitochondrial activity was quantified with the MTT assay. Adipocytes cultured with or without ADM and glucose has significantly higher mitochondrial activity compared to pre-adipocytes (all $p < 0.001$) (Figure 4.5A). Adipocytes differentiated in 33 mM glucose for 14 days had lower MTT activity than those cultured for 7 days (2.00 ± 0.15 vs. 2.57 ± 0.16 A_{570} , $p < 0.001$). Increased glucose concentration increased MTT activity ($p < 0.001$) after 7 (Figure 4.5B) and 14 (Figure 4.5C) days.

4.1.6 Gene expression

The quality and purity (Table 4.1) and integrity (Table 4.2) of RNA were within the acceptable range. To assess whether genomic DNA was present and could interfere with qRT-PCR results, reverse transcription reactions with (plus RT) or without (minus RT) the reverse transcription enzyme was subjected to qRT-PCR using primers spanning a single exon. Taq polymerase only amplifies double stranded DNA, therefore RNA must be reverse transcribed before it is used as a template in PCR. Amplification in the minus RT reactions represent genomic DNA contamination. As shown in Table 4.3, a Ct difference of more than 8 was observed between the plus and minus RT reactions indicating negligible genomic DNA contamination. The quality of most RNA samples was at acceptable range as shown in Table 4.1. Thus, RNA was acceptable to use for qRT-PCR without DNase treatment. The slope and R^2 (correlation co-efficient) values obtained for the Taqman[®] Gene Expression Assays used in this study were calculated using the standard curve (Table 4.4). All slopes (between -3.1 and -3.6) and R^2 were within the acceptable range.

Neither differentiation in different glucose concentrations nor time affected the expression of genes involved in adipogenesis, basal lipolysis nor lipid metabolism (Figure 4.6). Adiponectin expression appeared to be lower with increasing glucose concentrations and after longer culture, but differences were not statistically significant (Figure 4.6). The expression of NOX, a marker of oxidative stress, was higher in adipocytes cultured for 14 compared to 7 days, with differences at 25 mM glucose reaching statistical significance (2.6-fold \uparrow , $p = 0.013$) (Figure 4.7).

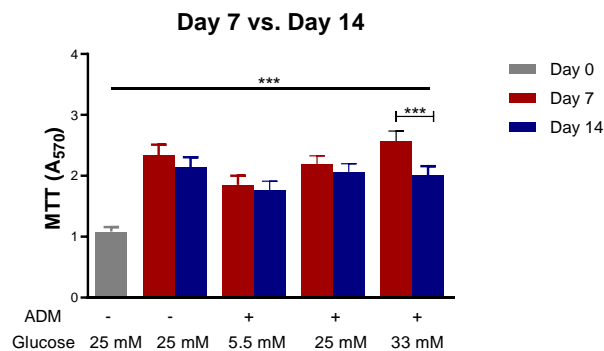
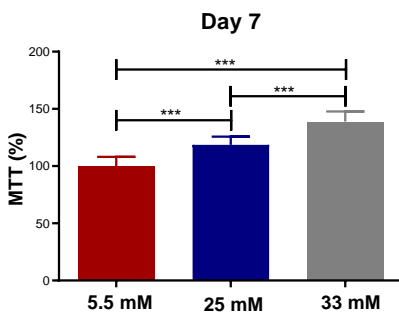
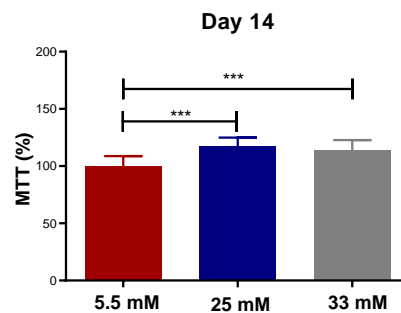
A**B****C**

Figure 4.5 Effect of glucose and differentiation times on mitochondrial activity

3T3-L1 pre-adipocytes were differentiated in 5.5 mM, 25 mM or 33 mM glucose for 7 and 14 days, where after mitochondrial dehydrogenase activity was measured using the MTT assay. A represents absorbance values. All concentrations and differentiation time were significantly different to pre-adipocytes. B and C represent the percentage MTT activity expressed relative to 5.5 mM glucose, which was set at 100%. Results are expressed as the mean \pm SD of three independent experiments, each with $n > 3$. Significance is depicted as *** $p < 0.001$.

Table 4.1 RNA concentrations, total yield and purity

Sample	ng/ μ l [#]	Total yield (μ g) [†]	A ₂₆₀ /A ₂₈₀	A ₂₆₀ /A ₂₃₀
Day 7				
Undifferentiated				
Experiment 1	496.52	24.83	2.08	1.06
Experiment 2	841.41	42.07	2.09	1.37
Experiment 3	809.63	40.48	2.10	0.92
5.5 mM Glucose				
Experiment 1	701.51	35.08	2.09	1.50
Experiment 2	970.86	48.54	2.08	0.80
Experiment 3	157.02	7.85	1.65	2.14
25 mM Glucose				
Experiment 1	1232.75	61.64	2.07	1.89
Experiment 2	982.26	49.11	2.08	1.93
Experiment 3	504.32	25.22	2.07	0.78
33 mM Glucose				
Experiment 1	793.44	39.67	2.10	0.78
Experiment 2	1102.17	55.11	2.08	2.11
Experiment 3	538.40	26.92	2.06	1.52
Day 14				
Undifferentiated				
Experiment 1	841.41	42.07	2.10	1.06
Experiment 2	-	-	-	-
Experiment 3	809.63	40.48	2.08	1.37
5.5 mM Glucose				
Experiment 1	1169.10	58.45	2.09	1.66
Experiment 2	157.02	7.85	1.65	0.80
Experiment 3	970.86	48.54	2.08	1.50
25 mM Glucose				
Experiment 1	1232.75	61.64	2.07	2.14
Experiment 2	982.26	49.11	2.08	1.89
Experiment 3	504.32	25.22	2.07	1.93
33 mM Glucose				
Experiment 1	793.44	39.67	2.10	0.78
Experiment 2	1102.17	55.11	2.08	2.11
Experiment 3	538.40	26.92	2.06	1.52

[#]ng/ μ l was calculated using the average of two independent Nanodrop measurements

[†]Total yield was calculated by multiplying ng/ μ l by the total volume of RNA obtained

Table 4.2 RNA integrity

Sample	RIN number		
	Experiment 1	Experiment 2	Experiment 3
Day 7			
Undifferentiated	8.9	9.3	9.5
5.5 mM Glucose	8.5	8.4	6.8
25 mM Glucose	8.7	8.9	8.7
33 mM Glucose	8.9	9.5	9.5
Day 14			
Undifferentiated	8.8	9.5	9.0
5.5 mM Glucose	9.2	8.3	8.4
25 mM Glucose	9.2	9.3	8.1
33 mM Glucose	9.3	9.1	9.4

RIN number represents the RNA integrity as calculated using the Agilent bioanalyser

Table 4.3 Assessment of genomic DNA contamination

Sample	Ct (minus RT)	Ct (plus RT)	Ct difference
Day 0			
Pre-adipocytes	29.58	17.27	12.30
Day 7			
Undifferentiated	27.97	17.59	10.38
5.5 mM Glucose	25.88	17.04	8.84
25 mM Glucose	25.61	16.72	8.89
33 mM Glucose	25.70	16.97	8.73
Day 14			
Undifferentiated	27.28	17.39	9.90
5.5 mM Glucose	27.63	> 40	>12
25 mM Glucose	27.18	16.93	10.25
33 mM Glucose	27.07	16.43	10.64
No template		> 40	

Ct: Threshold cycle for qRT-PCR

> 40 represents samples where amplification was undetected after 40 cycles of PCR

Table 4.4 Amplification efficiency

Gene	Slope	R ²
<i>PPARγ</i>	-3.53	0.99
<i>GATA2</i>	-3.723	1.00
<i>SREBF1</i>	-3.58	1.00
<i>HSL</i>	-3.30	1.00
<i>ACACA</i>	-3.26	1.00
<i>ADIPOQ</i>	-3.51	1.00
<i>NRF1</i>	-3.41	0.98
<i>NOX4</i>	-3.43	1.00

Abbreviations: *ACACA*, Acetyl-CoA Carboxylase Alpha; *ADIPOQ*, Adiponectin; *GATA2*, GATA Binding Protein 2; *HSL*, Hormone sensitive lipase; *NOX4*, NADPH oxidase 4; *NRF1*, Nuclear respiratory factor 1; *PPAR γ* , Peroxisome proliferator-activated receptor gamma; *SREBF1*, Sterol Regulatory Element Binding Transcription Factor 1.

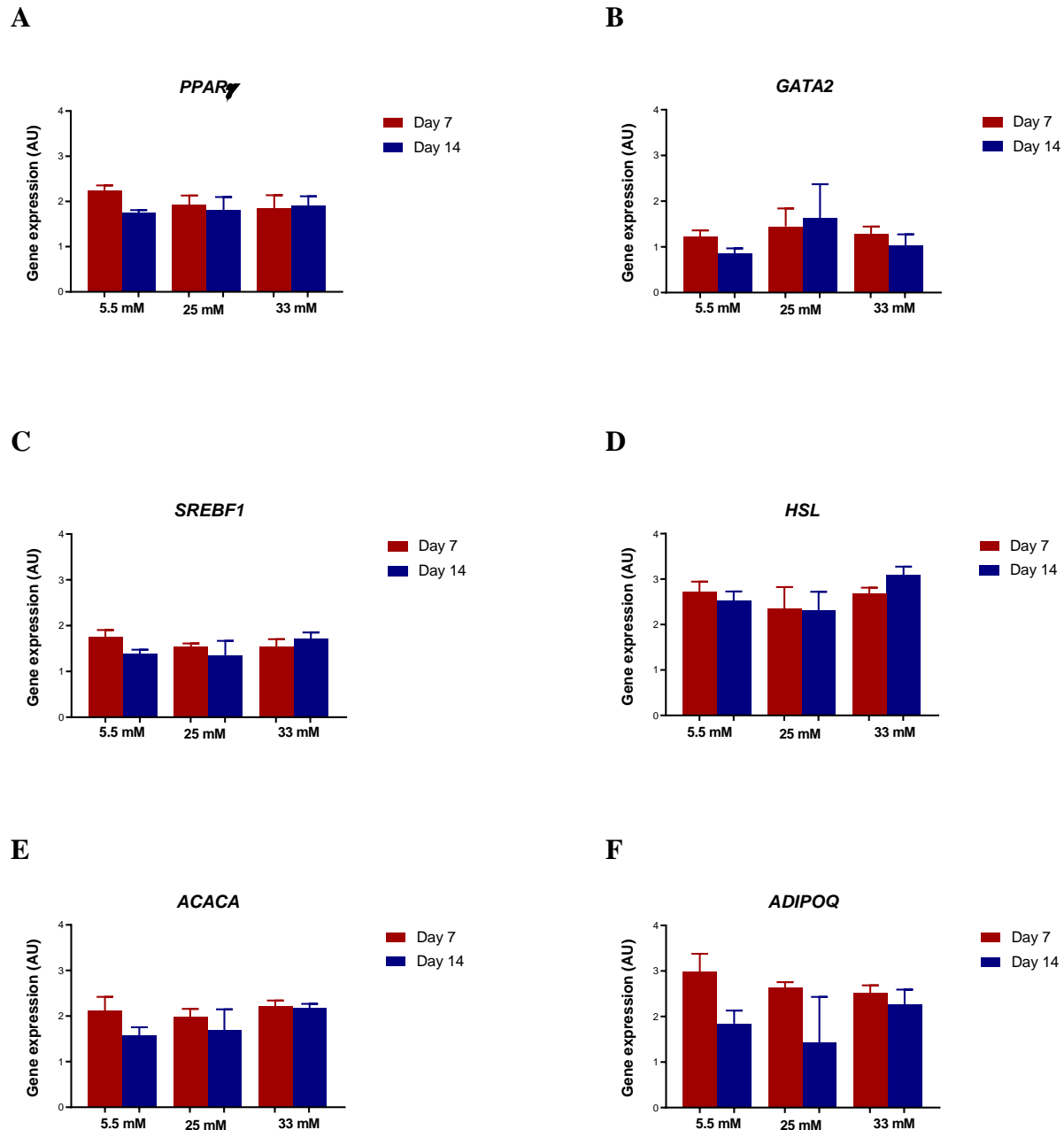
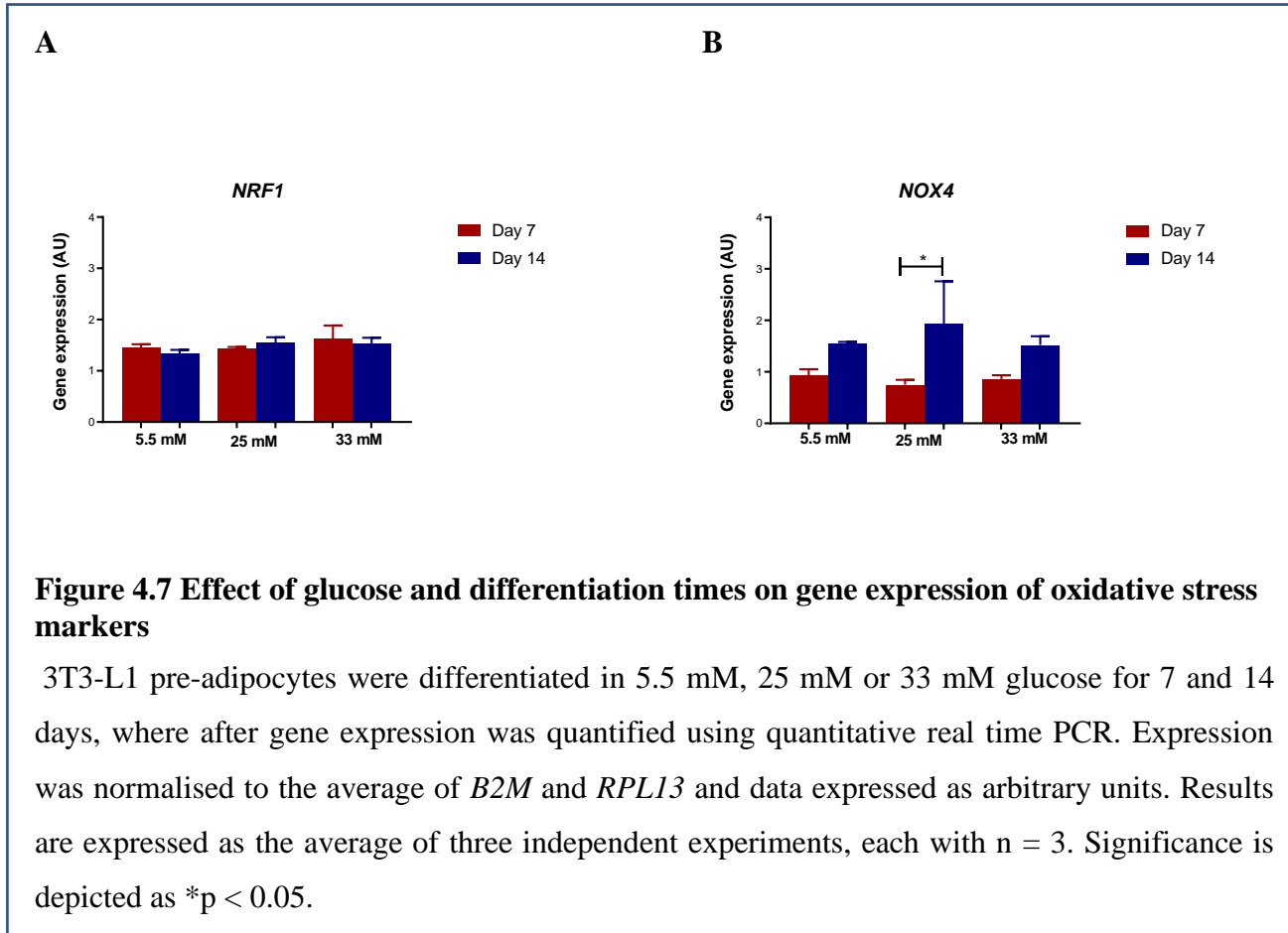


Figure 4.6 Effect of glucose and differentiation times on adipogenesis, lipid metabolism and adipokine genes

3T3-L1 pre-adipocytes were differentiated in 5.5 mM, 25 mM or 33 mM glucose for 7 and 14 days, where after gene expression was quantified using quantitative real time PCR. Expression was normalised to the average of *B2M* and *RPL13* and data expressed as arbitrary units. Results are expressed as the average of three independent experiments, each with $n = 3$.



4.2 Treatment with GRT, CPEF, Aspalathin and Mangiferin

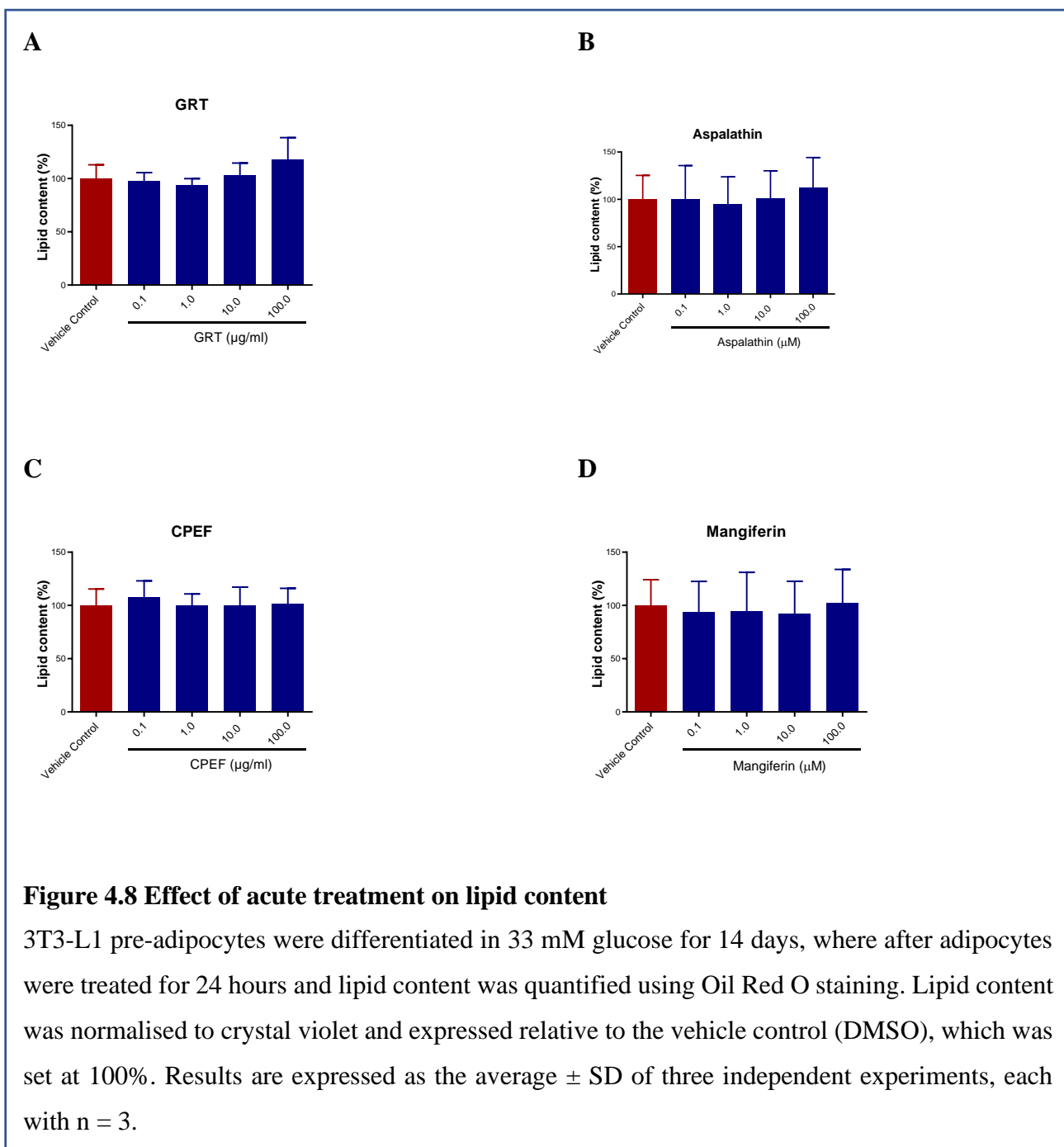
3T3-L1 adipocytes differentiated in 33 mM glucose for 14 days were either treated with GRT, CPEF, Aspalathin or Mangiferin acutely for 24 hrs to investigate whether treatment could ameliorate or reverse lipid accumulation and basal lipolysis, or chronically in the last 7 days of differentiation to investigate the preventative effects of these compounds.

4.2.1 Acute treatment

To investigate the ameliorative properties of GRT, CPEF, Aspalathin and Mangiferin, 3T3-L1 pre-adipocytes were differentiated in 33 mM glucose for 14 days (selected from 4.1), where after they were treated for 24 hrs. None of the treatments decreased lipid content (Figure 4.8). As expected, Isoproterenol, the positive control increased glycerol release. All treatments decreased glycerol release, varying between 82-92% (Figure 4.9) and increased mitochondrial activity (Figure 4.10).

4.2.2 Chronic treatment

To investigate the preventative properties of GRT, CPEF, Aspalathin and Mangiferin, 3T3-L1 pre-adipocytes were differentiated in 33 mM glucose for 14 days and treated from day 7 to day 14 (last 7 days of differentiation). As observed for acute treatment, none of the treatments significantly decreased lipid content (Figure 4.11). All treatments decreased glycerol release, although this was not statistically significant (Figure 4.12). Similarly, as with acute treatment, all treatments increased mitochondrial activity (Figure 4.13).



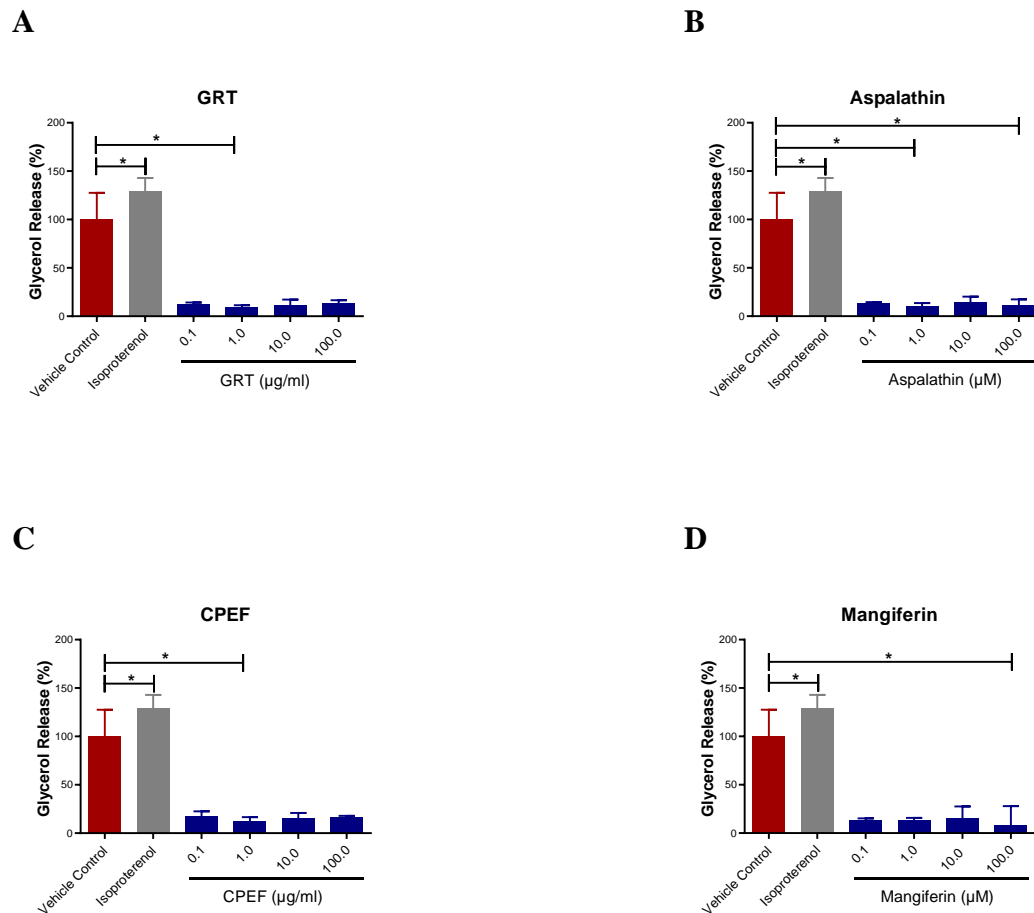


Figure 4.9 Effect of acute treatment on glycerol release

3T3-L1 pre-adipocytes were differentiated in 33 mM glucose for 14 days, where after glycerol release, a marker of lipolysis was quantified. Glycerol release was expressed relative to the vehicle control (DMSO), which was set at 100%. Isoproterenol was used a positive control. Results are expressed as the mean \pm SD of three independent experiments, each with $n=3$. Significance is depicted as $*p < 0.05$.

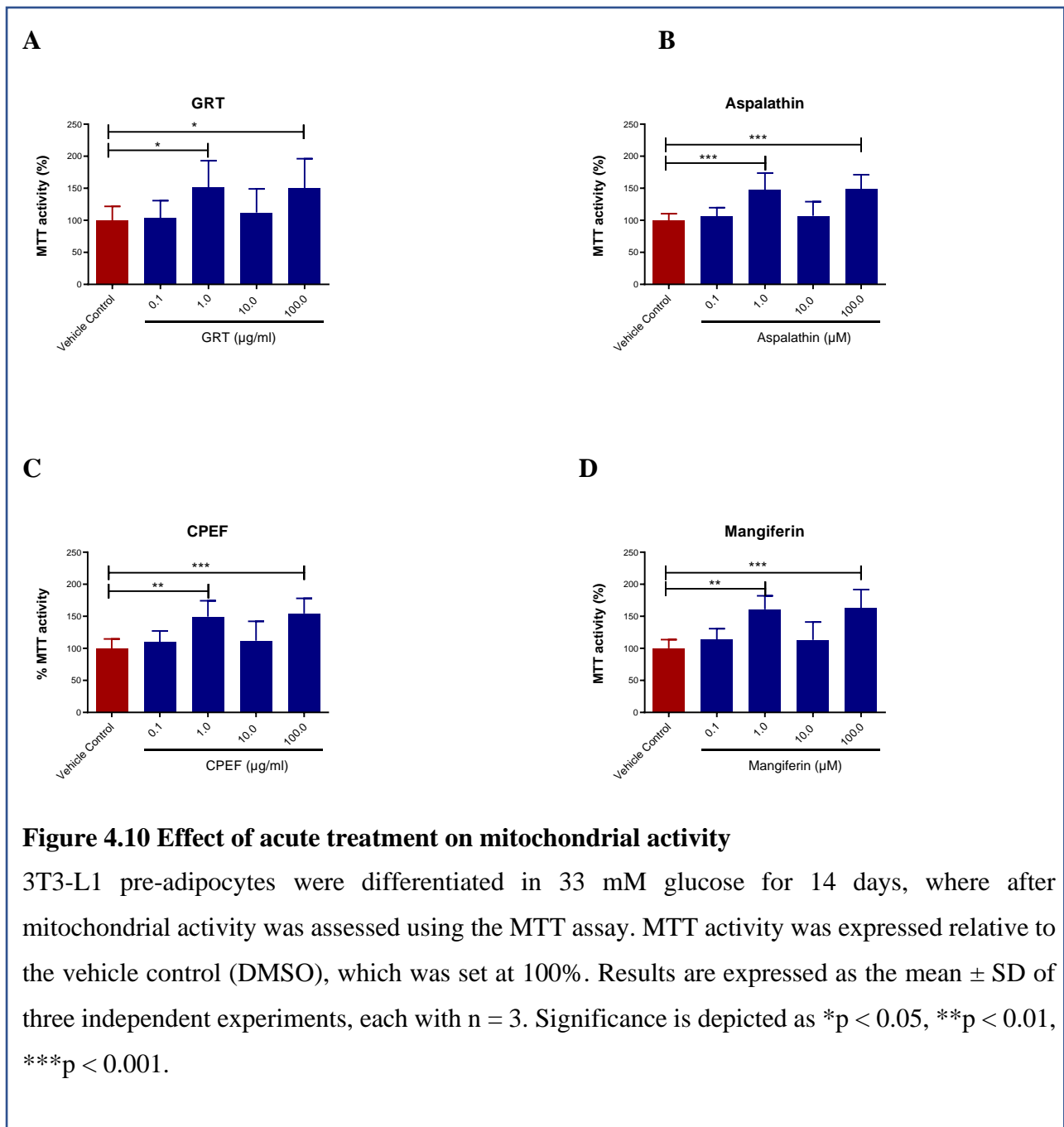
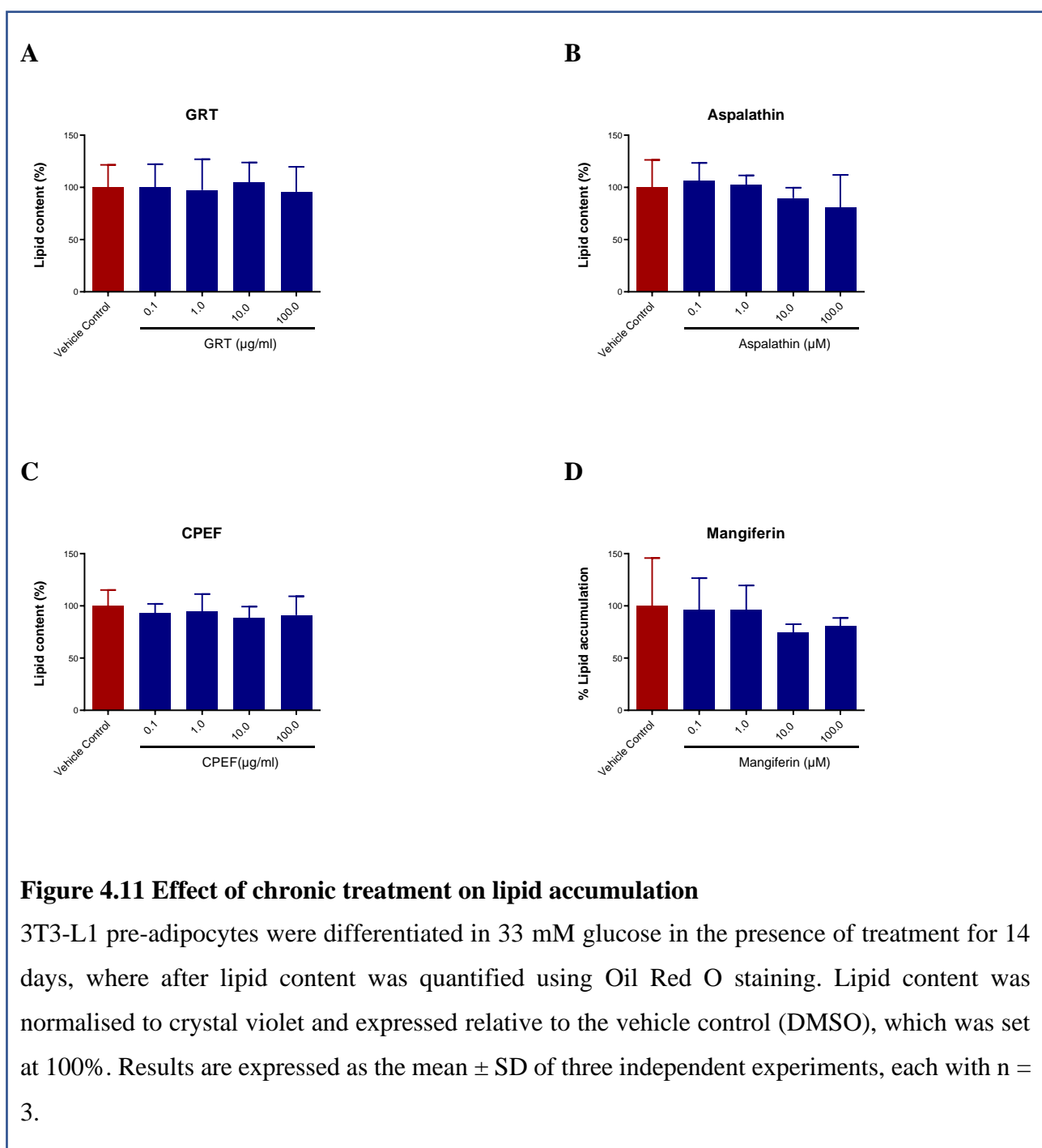


Figure 4.10 Effect of acute treatment on mitochondrial activity

3T3-L1 pre-adipocytes were differentiated in 33 mM glucose for 14 days, where after mitochondrial activity was assessed using the MTT assay. MTT activity was expressed relative to the vehicle control (DMSO), which was set at 100%. Results are expressed as the mean \pm SD of three independent experiments, each with $n = 3$. Significance is depicted as * $p < 0.05$, ** $p < 0.01$, *** $p < 0.001$.



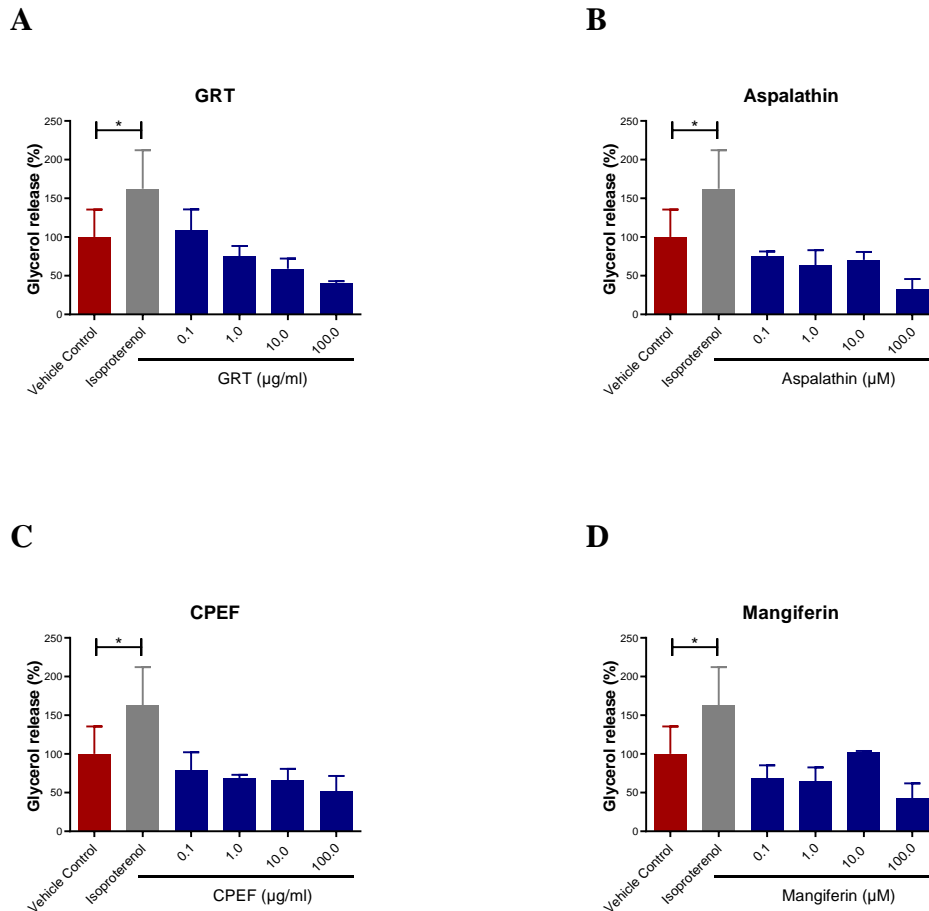


Figure 4.12 Effect of chronic treatment on glycerol release

3T3-L1 pre-adipocytes were differentiated in 33 mM glucose in the presence of treatment for 14 days, where after glycerol release, a marker of lipolysis was quantified. Glycerol release was expressed relative to the vehicle control (DMSO), which was set at 100%. Results are expressed as the mean \pm SD of three independent experiments, each with n=3. Significance is depicted as *p < 0.05.

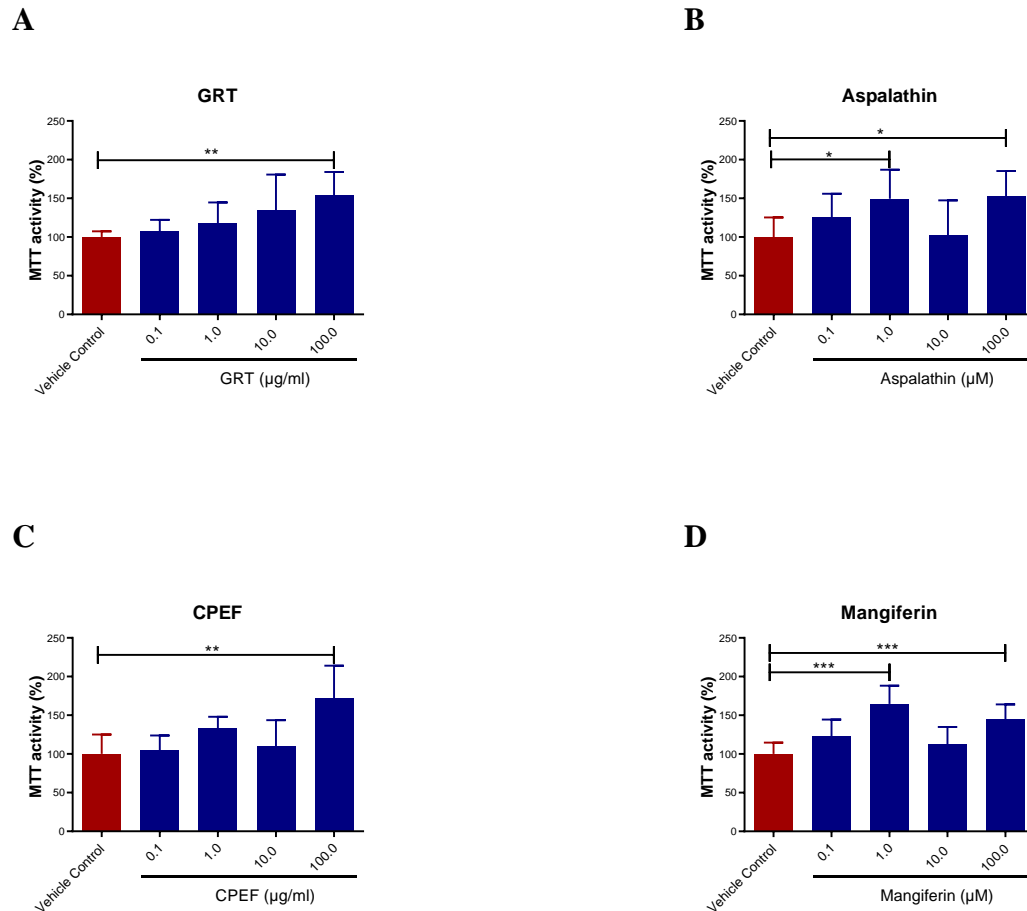


Figure 4.13 Effect of chronic treatment on mitochondrial activity

3T3-L1 pre-adipocytes were differentiated in 33 mM glucose in the presence of treatment for 14 days, where after mitochondrial activity was assessed using the MTT assay. MTT activity was expressed relative to the vehicle control (DMSO), which was set at 100%. Results are expressed as the mean \pm SD of three independent experiments, each with $n=3$. Significance is depicted as * $p < 0.05$, ** $p < 0.01$, *** $p < 0.001$.

4.3 Summary of results

A summary of the results is presented in Table 4.5 and Table 4.6.

Table 4.5 Results for model development

Assay	Day 7			Day 14			Day 14 vs. Day 7		
	5.5 mM	25 mM	33 mM	5.5 mM	25 mM	33 mM	5.5 mM	25 mM	33 mM
Oil Red O	Ref	↑	↑	Ref	↔	↔	↔	↔	↔
Basal lipolysis	Ref	↔	↔	Ref	↑	↑	↑*	↑*	↑*
Oxidative stress	Ref	↑***	↑↑***	Ref	↔	↑***	↑*	↔	↔
Inflammation	Ref	↔	↔	Ref	↔	↑*	↔	↔	↔
Mitochondrial activity	Ref	↑***	↑↑***	Ref	↑***	↑***	↔	↔	↓***
Gene expression									
<i>PPARγ</i>	Ref	↔	↔	Ref	↔	↔	↔	↔	↔
<i>GATA2</i>	Ref	↔	↔	Ref	↔	↔	↔	↔	↔
<i>SREBF1</i>	Ref	↔	↔	Ref	↔	↔	↔	↔	↔
<i>HSL</i>	Ref	↔	↔	Ref	↔	↔	↔	↔	↔
<i>ACACA</i>	Ref	↔	↔	Ref	↔	↔	↔	↔	↔
<i>ADIPOQ</i>	Ref	↔	↔	Ref	↔	↔	↔	↔	↔
<i>NRF1</i>	Ref	↔	↔	Ref	↔	↔	↔	↔	↔
<i>NOX4</i>	Ref	↔	↔	Ref	↔	↔	↑	↑*	↑

* $p < 0.05$, ** $p < 0.01$ and *** $p < 0.001$ compared to 5.5 mM (Day 7 or Day 14) or Day 14 vs. Day 7.

↑ increased; ↓ decreased; ↔ no difference.

Abbreviations: *ACACA*, Acetyl-CoA Carboxylase Alpha; *ADIPOQ*, Adiponectin; *GATA2*, GATA Binding Protein 2; *HSL*, Hormone sensitive lipase; *NOX4*, NADPH oxidase 4; *NRF1*, Nuclear respiratory factor 1; *PPAR γ* , Peroxisome proliferator-activated receptor gamma; Ref, Reference; *SREBF1*, Sterol Regulatory Element Binding Transcription Factor 1.

Table 4.6 Results of treatment

Treatment	Lipid accumulation		Basal lipolysis		Mitochondrial activity	
	Acute	Chronic	Acute	Chronic	Acute	Chronic
GRT						
0.1 µg/ml	↔	↔	↓	↓	↔	↑
1 µg/ml	↔	↔	↓*	↓	↑*	↑
10 µg/ml	↔	↔	↓	↓	↔	↑
100 µg/ml	↔	↔	↓	↓	↑*	↑**
Aspalathin						
0.1 µM	↔	↔	↓	↓	↔	↑
1 µM	↔	↔	↓*	↓	↑***	↑*
10 µM	↔	↔	↓	↓	↔	↑
100 µM	↔	↔	↓*	↓	↑***	↑*
CPEF						
0.1 µg/ml	↔	↔	↓	↓	↔	↑
1 µg/ml	↔	↔	↓*	↓	↑**	↑
10 µg/ml	↔	↔	↓	↓	↔	↑
100 µg/ml	↔	↔	↓	↓	↑***	↑**
Mangiferin						
0.1 µM	↔	↔	↓	↓	↔	↑
1 µM	↔	↔	↓	↓	↑**	↑***
10 µM	↔	↔	↓	↓	↔	↑
100 µM	↔	↔	↓*	↓	↑***	↑***

*p < 0.05, **p < 0.01 and ***p < 0.001 compared to 5.5 mM (Day 7 and Day 14) or Day 14 vs. Day 7

↑ increased; ↓ decreased; ↔ no difference.

Abbreviations: CPEF, crude polyphenol enriched *Cyclopia intermedia*; GRT, *Aspalathus linearis* GRTTM.

Chapter 5

5. Discussion

Obesity is considered one of the greatest health challenges of the 21st century, despite the availability of several anti-obesity strategies. In recent years, plant polyphenols have attracted increasing interest as more effective and potentially safer anti-obesity therapeutics. However, the first-line screening of these compounds is hampered by the shortage of *in vitro* experimental models that mimic the complex pathophysiology of obesity *in vivo*. This study, firstly, examined the effects of glucose concentration and differentiation times on lipid accumulation, basal lipolysis, oxidative stress and inflammation, and secondly, investigated the ameliorative effects of *Aspalathus linearis*, *Cyclopia intermedia* and their major polyphenols, Aspalathin and Mangiferin, against these conditions.

5.1 Model development

5.1.1 Lipid accumulation

Exposure to high glucose concentrations increased lipid accumulation after 7 days, however, this effect was not observed after long-term culturing (14 days). The role of glucose in accelerating adipocyte differentiation and promoting the formation of lipid droplets is widely reported. Aguiari et al. reported that culturing adipocyte derived stem cells (ADSCs) in 25 mM glucose is sufficient to induce adipogenesis and adipocyte maturation (Aguiari et al., 2008). Adipogenesis is a multi-step process, encompassing a cascade of cell-cycle proteins and nuclear transcription factors such as PPAR γ that regulate gene expression, leading to morphological changes, cell arrest, mitosis, lipid accumulation and metabolic function (Gustafson et al., 2009). The effect of varying glucose concentrations in combination with the standard adipogenesis inducing cocktail, as used in this study, has been reported previously. Differentiation of 3T3-L1 adipocytes (Lin et al., 2005; Han et al., 2007) and MSCs (Chuang et al., 2007) in 25 mM compared to either 4, 5 or 5.5 mM glucose increased lipid accumulation and adipocyte hypertrophy. Palacios-Ortega et al. reported that lipid accumulation increased in 3T3-L1 pre-adipocytes differentiated in 25 mM compared to 5 mM glucose (Palacios-Ortega et al., 2016). Shilpa and co-authors reported that exposure to 25, 45, 65, 85, and 105 mM increased lipid accumulation by approximately 45.7%, 170.4%, 237.8%, 139.8% and 23.4%, respectively, in comparison to pre-adipocytes (Shilpa, Dinesh & Lakshmi, 2013). We

similarly showed increased lipid accumulation compared to pre-adipocytes and modest effects were observed with increasing glucose concentrations, acknowledging that our concentrations were much lower than that used by Shilpa et al. (Shilpa, Dinesh & Lakshmi, 2013). Consistent with our findings, the high glucose-induced lipid accumulation reported by (Palacios-Ortega et al., 2016) was evident at 7 days, but not after long-term culturing (21 days), suggesting that adipocytes have probably saturated their lipid storage capacity after 7 days. Alternatively, continuous exposure to high glucose until day 14, possibly induced glucotoxicity stress, thus inhibiting the differentiation of 3T3-L1 pre-adipocytes into functional adipocytes with lipid storage capacity (Rharass & Lucas, 2019). No changes in adipogenic and lipogenic gene expression (*PPAR γ* , *SREBF1*, *ACACA* and *GATA2*) was observed. *PPAR γ* is essential during the early stages of adipocyte differentiation, however, is not required or has lesser importance for the maintenance of differentiated adipocytes, which could explain the lack of significant differences between days 7 and 14 (Liao et al., 2007; Kolodziej et al., 2019). In concurrence to our findings, Kolodziej et al., reported that a prolong incubation of fat with high glucose concentration intensifies the degree of differentiation in mature adipocytes, however, have no effect on *PPAR- γ* expression (Kolodziej et al., 2019). Functional studies by Liao and colleagues provided the evidence that a *PPAR- γ* knockdown inhibited adipocyte differentiation however, *PPAR- γ* was not required for maintenance of the adipocyte differentiation state post adipogenesis in 3T3-L1 (Liao et al., 2007).

5.1.2 Basal lipolysis

Exposure to different glucose concentrations had a modest effect on basal lipolysis, which appeared to be induced by extended differentiation times at all glucose concentrations tested. Increased basal lipolysis at day 14 compared to 7 was statistically significant when adipocytes were differentiated in 33 mM glucose, and accompanied by a small, although not statistically significant increase in *HSL* gene expression. Lipolysis is a normal physiological function of adipocytes in response to energy demands, such as fasting or physical exercise, allowing adipocytes to mobilise their fat stores for use by other organs (Morigny et al., 2016). During lipolysis, triacylglycerols are hydrolysed into FAs and glycerol through a sequential process catalysed by three major lipases, of which *HSL* is key. During obesity however, lipolysis is increased leading to insulin resistance. Several mechanisms that link increased lipolysis with

insulin resistance have been proposed. First, increased FA secretion from adipocytes may lead to lipid accumulation in insulin-sensitive tissues such as the liver and muscle, thus impairing insulin sensitivity (Samuel & Shulman, 2016). Second, increased lipolysis may dysregulate adipokine secretion and affect insulin sensitivity (Ertunc et al., 2015). Third, higher levels of circulatory FAs may lead to inflammation through their pro-inflammatory stimulating effects on macrophages (Suganami, Nishida & Ogawa, 2005). Green et al. reported that high glucose concentrations markedly increased the lipolytic action of TNF α (Green et al., 2004). Furthermore, these authors report that glucose alone did not cause a substantial increase in lipolysis, however, the addition of TNF α to the culture medium enhanced the lipolytic effect of glucose. These findings suggest that future experiments should investigate whether the addition of TNF α will further induce lipolysis in our model. The activity of HSL is regulated by protein phosphorylation (Krintel et al., 2009; McDonough et al., 2011), thus future studies should quantify protein levels.

White adipocytes are capable of producing large amounts of lactate and glycerol from glucose (Rotondo et al., 2017). Thus, the increased glycerol concentration observed on day 14 compared to day 7 could be due to prolonged exposure to excess glucose concentrations, which result in the synthesis and secretion of glycerol via glycerogenesis (Del Mar Romero et al., 2015; Rotondo et al., 2017). Other markers of lipolysis such as FA secretion need to be quantified to ascertain whether the increase in glycerol levels are due to triacylglycerol breakdown to FA and glycerol via lipolysis.

5.1.3 Oxidative stress

Differentiation in higher glucose concentrations increased oxidative stress at day 7, with modest effects and increased *NOX4* expression observed at day 14. Obesity is associated with increased ROS production and oxidative stress in adipose tissue (Dludla et al., 2019). Oxidative stress induces cellular damage by oxidising cellular constituents such as proteins, lipids and DNA. NOX is the main source of ROS production in adipocytes (Bedard & Krause, 2007), catalysing the transfer of electrons from NADPH to oxygen, thus generating superoxide anion (O²⁻), which is further converted to hydrogen peroxide (H₂O₂) by superoxide dismutase. Several studies have

reported that high glucose concentrations increase ROS production in adipocytes, which could be due to the excess glucose influx to the glycolytic pathway resulting in NADH production, an electron carrier of the mitochondrial electron transport chain (Yan, 2014). Lin et al. showed increased ROS production in 3T3-L1 adipocytes differentiated in 25 mM compared to 4 mM glucose, and in adipocytes isolated from hyperglycaemic mice compared to controls (Lin et al., 2005). Aguiari et al. reported that ADSCs differentiate into adipocytes when cultured in 25 mM glucose, with a concomitant increase in ROS production compared to ADSCs cultured in 5 mM glucose (Aguiari et al., 2008). Furukawa et al. demonstrated increased ROS production in adipocytes from obese mice and in 3T3-L1 adipocytes cultured with FAs (Furukawa et al., 2004). In both instances, higher ROS levels was accompanied by increased *NOX4* expression, consistent with our findings after 14 days of culture. Several studies have reported that intracellular ROS are regulated by NOX expression (Lee et al., 2009; Kanda et al., 2011; Castro, Grune & Speckmann, 2016).

5.1.4 Inflammation

Exposure to different glucose concentrations had a modest effect on MCP1 secretion at day 14, but not at day 7. Adipocytes differentiated in 33 mM glucose had the highest levels of MCP1 secretion. Obesity is associated with chronic low-grade inflammation, partly attributed to the infiltration of pro-inflammatory macrophages into adipose tissue (Boutens & Stienstra, 2016). Increased expression of MCP1 has been demonstrated in adipose tissues and plasma of obese individuals. Mice knockout studies showed that the secretion of MCP1 from adipocytes directly trigger the recruitment of macrophages into adipose tissue, which in turn secrete a variety of chemokines and cytokines that further promote a local inflammatory response and systemic insulin resistance (Kanda et al., 2006). Consistent with our findings at day 14, Han et al., (2007) reported increased expression of MCP1 and serum amyloid A, another protein involved in macrophage recruitment, in adipocytes cultured in 25 mM compared to 5 mM glucose. Furthermore, our findings are similar to (Han et al., 2007) who reported that exposure of 3T3-L1 adipocytes to high glucose concentrations (25 mM) increased MCP1 secretion but had no effect on TNF α secretion. Similarly, He et al. also did not observe increased TNF α secretion in human adipose tissue exposed to high glucose concentrations (He et al., 2003). We were not able to detect TNF α and IL6

secretion in this study, suggesting that pro-inflammatory cytokine secretion in adipose tissue is mainly driven by infiltrated macrophages rather than by adipocytes. Future experiments should focus on co-culturing adipocytes and macrophages to explore this hypothesis. It is possible that TNF α and IL6 values may have been below the detection range of the kit, or alternatively the assay did not work and the inclusion of a positive control (such as lipopolysaccharide) may have shed light on the reason for our failure to detect these cytokines. Although the differences were not statistically significant, the expression of *ADIPOQ* was lower with increasing glucose concentrations and after day 14. Adiponectin is an adipokine mainly produced and secreted by adipose tissue that regulates insulin sensitivity and anti-inflammatory response (Lihn, Pedersen & Richelsen, 2005; Ouchi & Walsh, 2007). The expression of adiponectin is reduced during obesity and intermittent exposure of 3T3-L1 adipocytes to high glucose (alternating between 5 and 20 mM) exacerbated the suppression of *ADIPOQ* expression and secretion compared to culture at constant high glucose (20 mM) (Sun et al., 2010).

5.1.5 Mitochondrial activity

Exposure to higher glucose concentrations increased mitochondrial dehydrogenase activity in 3T3-L1 adipocytes after 7 and 14 days. Mitochondria play a critical role in metabolic disease (Johannsen & Ravussin, 2009), with conflicting reports on whether increased or decreased mitochondrial activity is associated with disease. Tanis et al. showed differences in mitochondrial bioenergetics (increased respiration) between 3T3-L1 adipocytes cultured in 5 mM and 30 mM glucose (Tanis et al., 2015). Palacios-Ortega et al. reported no change in mitochondrial activity after long-term glucose exposure, however high glucose concentrations decreased cell viability compared to short-term culture (Palacios-Ortega et al., 2016). Low glucose (5.5 mM) had decreased MTT activity compared to 25 mM and 33 mM glucose at both day 7 and 14, suggesting that deficiency in glucose induces stress or glucose starvation in these cells hence the mitochondrial activity is low.

5.2 Treatment

The second aim of the study was to investigate the ameliorative effects of *Aspalathus linearis* (GRT), *Cyclopia intermedia* (CPEF), Aspalathin and Mangiferin against lipid accumulation and basal lipolysis. These effects were assessed using both an acute and chronic treatment protocol. Acute treatment assessed whether GRT, CPEF, Aspalathin and Mangiferin treatments exhibit therapeutic effects in reversing adipocyte dysfunction induced by high glucose (33 mM) exposure for 14 days. Chronic treatment assessed whether GRT, CPEF, Aspalathin and Mangiferin treatments have preventative effects on adipocyte dysfunction induced by high glucose (33 mM) exposure for 14 days. Acute and chronic treatments showed similar effects on lipid accumulation, basal lipolysis and mitochondrial dehydrogenase activity. Both acute and chronic treatments did not reduce lipid accumulation and mitochondrial dehydrogenase activity, while they both decreased basal lipolysis. This suggests that length of exposure to GRT, CPEF, Aspalathin and Mangiferin treatment was not a contributing factor to the lack of bioactivity observed in response to treatment with GRT, CPEF, Aspalathin and Mangiferin.

5.2.1 Lipid accumulation

Neither acute nor chronic treatment with GRT, CPEF, Aspalathin or Mangiferin affected lipid accumulation, in contrast to previous studies that reported their ability to decrease lipid content through inhibition of adipocyte differentiation and expression of adipogenic genes such as *PPAR γ* and *SREBF1* (Dudhia et al., 2013; Pheiffer et al., 2013; Zhang et al., 2013; Sanderson et al., 2014; Mazibuko et al., 2015; Jack et al., 2017). Dudhia et al. assessed the effect of an aqueous extract of “fermented” *C. maculata* and aqueous extracts of “unfermented” *C. maculata* and *C. subternata* on obesity in differentiating 3T3-L1 pre-adipocytes and demonstrated that these extracts dose-dependently inhibited adipogenesis, lipid accumulation, triglyceride content and peroxisome proliferator-activated receptor gamma (*PPAR γ*) expression (Dudhia et al., 2013). The aqueous extract of “fermented” *C. maculata* also stimulated lipolysis and increased hormone sensitive lipase (HSL) and perilipin expression in mature 3T3-L1 adipocytes (Pheiffer et al., 2013). More recently, Jack et al. reported that a crude polyphenol-enriched fraction of *Cyclopia intermedia* (CPEF) decreased lipid content, and increased *Hsl* and uncoupling protein 3 (*Ucp3*) gene expression in 3T3-L1 adipocytes, while inhibiting body weight gain in obese leptin receptor

deficient (*Lepr^{db/db}*) mice (Jack et al., 2017). Sanderson et al. showed that rooibos inhibits adipogenesis and intracellular lipid accumulation in 3T3-L1 adipocytes, accompanied by decreased expression of adipogenesis and lipid accumulation genes and proteins (Sanderson et al., 2014). Similarly, Mangiferin decreases triglycerides and FAs in 3T3-L1 adipocytes through the decreased expression of SREBP and HSL (Zhang et al., 2013). The disparities could be due to the differences in culture conditions. For example, Jack et al. differentiated 3T3-L1s in 25 mM glucose for 7 days, whereas we exposed cells to 33 mM for 7 day or 14 days (Jack et al., 2017). We recommend that treatment conditions be standardised across studies to prevent the conflicting results that are widely reported. Interestingly, studies conducted in Vervet monkeys, similarly reported that treatment with GRT did not decrease triglyceride content in diabetic and non-diabetic monkeys (Orlando et al., 2019). Thus, our findings suggest that these compounds may not decrease lipid content, but rather may have ameliorative properties against oxidative stress, as reported by (Orlando et al., 2019).

5.2.2 Basal lipolysis

Treatment with GRT, CPEF, Aspalathin and Mangiferin (both acute and chronic) reversed the basal lipolysis induced by differentiating 3T3-L1 adipocytes in 33 mM glucose for 14 days. Studies on polyphenols and lipolysis have reported conflicting results. Jack et al. reported that CPEF increases lipolysis in 3T3-L1 adipocytes (Jack et al., 2017), while Pheiffer et al. reported that *Cyclopia maculata* increases lipolysis, which is accompanied by an increase in the expression of HSL (Pheiffer et al., 2013). Similar results were reported for Mangiferin in obese rats (Yoshikawa et al., 2002). However, antilipolytic effects have also been reported. Zhang et al. reported that Mangiferin exerts its anti-obesity effects by decreasing both lipid content and lipolysis (Zhang et al., 2013). While Sanderson et al. demonstrated that a fermented rooibos extract inhibits adipogenesis, lipolysis and improves glucose uptake (Sanderson et al., 2014). Once again, the discrepant results between studies could be due to different culture conditions and varying polyphenol content of plant extracts. Furthermore, results are affected by several factors including treatment time and dose, extraction procedure and the stressors used to induce the experimental model (Beltrán-Debón et al., 2011). Surprisingly, we did not observe a decrease in lipid content, suggesting that the ORO method may not have been sensitive enough to detect modest differences

in lipid content, thus future work should measure intracellular triglyceride levels. Decreased lipolysis and FAs in the circulation improves insulin sensitivity in peripheral organs such as the liver and muscle (Girousse et al., 2013). Our results suggest that the antilipolytic activity of these treatments may be a promising therapeutic agent for treating insulin resistance and metabolic disease.

5.2.3 Mitochondrial activity

Acute and chronic treatment with GRT, CPEF, Aspalathin and Mangiferin did not decrease mitochondrial dehydrogenase activity, with slight increases observed at specific concentrations. The MTT assay is widely used to assess the cytotoxicity of extracts or compounds. None of the treatments induced toxic effects, suggesting that the decrease in lipolysis is not due to cell death, but rather the effect of the treatment. A study by Mazibuko et al. similarly showed that GRT and Aspalathin increases MTT activity and basal intracellular ATP content (Mazibuko et al., 2015).

5.3 Strengths and limitations

The study is a comprehensive analysis of the effects of varying glucose concentration and maturation time on various obesity associated conditions and may lead to the development of a more relevant *in vitro* model. Furthermore, we provide new information about the therapeutic potential of GRT, CPEF, Aspalathin and Mangiferin against these conditions. However, the study also has several limitations. First, due to technical challenges with our microscope, we were not able to capture ORO images, thus could not visualise lipid content and adipocyte hypertrophy. Second, we did not correct for osmolarity, which can lead to oxidative stress. High glucose concentrations increase osmotic pressure and induces glucotoxicity, thus controlling for osmolarity using mannitol is recommended. Glucose concentrations in this study were lower than used in other studies and did not induce cytotoxicity, as assessed with the MTT assay. However, the effect of osmolarity should be acknowledged and future studies should control for osmotic pressure. Third, ROS was assessed using DCF, which is a rapid and cost-effective method of quantification. However, it is not as sensitive as flow cytometry, and presents another weakness of our study. Furthermore, oxidative stress occurs due to the imbalance between pro-oxidants

(ROS) and antioxidants, thus assays measuring the total redox (both ROS and total anti-oxidant capacity) may be better indicators of oxidative stress that should be considered for future. *NOX4* gene expression, however, supported the increased oxidative stress observed with DCF. Fourth, protein expression was not assessed. Gene expression does not necessarily correlate with protein levels due to post-translational and translational modifications such as phosphorylation (Tokmakov et al., 2012). Fifth, due to time and resource constraints, we did not investigate the effect of treatments against oxidative stress and inflammation. The MTT assay offers challenges when using polyphenols. The colour emitted by polyphenols may interfere with the assay and underestimate the results obtained, thus the use of controls consisting of polyphenols, without cells should be used (Wisman et al., 2008). Treatment with GRT, CPEF, Aspalathin and Mangiferin unexpectedly showed similar effects on lipolysis (i.e. all four treatments decreased lipolysis to the same levels), which could be due to polyphenols in the samples interfering with the assay by inhibiting enzymes in the glycerol assay kit. Future studies using diluted samples are recommended to minimize enzyme inhibition. Lipolysis, oxidative stress and inflammation assays were not normalized in this study. Normalization to total protein content or cell viability are essential to reduce experimental variability and improve data comparisons and statistical significance. Lastly, it is important to include positive controls such as rosiglitazone and hydrogen peroxide for lipid accumulation and oxidative stress assays, respectively to ensure that the assays were worked.

5.4 Conclusion

Both glucose concentration and differentiation times affect lipid accumulation, basal lipolysis, oxidative stress and inflammation, although these vary according to the parameter measured. Differentiation of adipocytes in 33 mM glucose for 14 days represents an *in vitro* model that may more closely mimic the *in vivo* situation. GRT, CPEF, Mangiferin and Aspalathin decreased basal lipolysis, supporting the therapeutic potential of *Aspalathus linearis* and *Cyclopia intermedia* against metabolic disturbances induced by obesity. Obesity is associated with an increase in basal lipolysis and FAs, which leads to insulin resistance in peripheral tissues such as the skeletal muscle and liver (Girousse et al., 2013). Thus, future studies involving co-culture of adipocytes with cells

from other tissues are required to gain insight into the mechanisms and relationship between lipolysis and insulin sensitivity.

5.5 Future work

The limitations of the study should be addressed in future work:

- Microscopy to measure adipocyte hypertrophy;
- Measure intracellular triglycerides;
- Use mannitol to correct for osmotic pressure;
- Quantify oxidative stress in our model using a more sensitive approach such as flow cytometry;
- Measure the effects of GRT, CPEF, Aspalathin and Mangiferin against oxidative stress and inflammation; and
- Assess protein expression.

In addition, future work should consider including TNF α as an inducer to exacerbate the effect of glucose concentration in our model. Furthermore, it is important to examine the relationship between the antilipolytic effects of GRT, CPEF, Aspalathin and Mangiferin, and insulin resistance.

6. Bibliography

- Acevedo, L.M., Raya, A.I., Martõãnez-Moreno, J.M., Aguilera-Tejero, E. & Rivero, J.L.L. 2017. Mangiferin protects against adverse skeletal muscle changes and enhances muscle oxidative capacity in obese rats. *PLoS ONE*. 12(3):e0173028. DOI: 10.1371/journal.pone.0173028.
- Adan, R.A.H. 2013. Mechanisms underlying current and future anti-obesity drugs. *Trends in Neurosciences*. 36(2):133–140. DOI: 10.1016/j.tins.2012.12.001.
- Agahi, A. & Murphy, K.G. 2014. Models and Strategies in the Development of Antiobesity Drugs. *Veterinary Pathology*. 51(3):695–706. DOI: 10.1177/0300985813492801.
- Aguiari, P., Leo, S., Zavan, B., Vindigni, V., Rimessi, A., Bianchi, K., Franzin, C., Cortivo, R., et al. 2008. High glucose induces adipogenic differentiation of muscle-derived stem cells. *Proceedings of the National Academy of Sciences of the United States of America*. 105(4):1226–1231. DOI: 10.1073/pnas.0711402105.
- Alexopoulos, N., Katritsis, D. & Raggi, P. 2014. Visceral adipose tissue as a source of inflammation and promoter of atherosclerosis. *Atherosclerosis*. 233(1):104–112. DOI: 10.1016/j.atherosclerosis.2013.12.023.
- Anderson, J.W., Luan, J. & Høie, L.H. 2004. Structured weight-loss programs: Meta-analysis of weight loss at 24 weeks and assessment of effects of intervention intensity. *Advances in Therapy*. 21(2):61–75. DOI: 10.1007/BF02850334.
- Apontes, P., Liu, Z., Su, K., Benard, O., Youn, D.Y., Li, X., Li, W., Mirza, R.H., et al. 2014. Mangiferin stimulates carbohydrate oxidation and protects against metabolic disorders induced by high-fat diets. *Diabetes*. 63(11):3626–3636. DOI: 10.2337/db14-0006.
- Arya, M., Shergill, I.S., Williamson, M., Gommersall, L., Arya, N. & Patel, H.R.H. 2005. Basic principles of real-time quantitative PCR. *Expert Review of Molecular Diagnostics*. 5(2):209–219. DOI: 10.1586/14737159.5.2.209.
- Astashkina, A., Mann, B. & Grainger, D.W. 2012. A critical evaluation of *in vitro* cell culture models for high-throughput drug screening and toxicity. *Pharmacology and Therapeutics*. 134(1):82–106. DOI: 10.1016/j.pharmthera.2012.01.001.
- ATCC. 2013. *3T3-L1 (ATCC® CL-173™)*. Available: https://www.lgcstandards-atcc.org/products/all/CL-173.aspx?geo_country=za#culturemethod [2019, November 28].
- Baba, H., Ohtsuka, Y., Haruna, H., Lee, T., Nagata, S., Maeda, M., Yamashiro, Y. & Shimizu, T. 2009. Studies of anti-inflammatory effects of Rooibos tea in rats. *Pediatrics International*. 51(5):700–704. DOI: 10.1111/j.1442-200X.2009.02835.x.
- Barja-Fenández, S., Leis, R., Casanueva, F.F. & Seoane, L. 2014. Drug development strategies for the treatment of obesity: how to ensure efficacy, safety, and sustainable weight loss. *Drug Design, Development and Therapy*. 8:2391. DOI: 10.2147/DDDT.S53129.

- Barrett, P., Mercer, J.G. & Morgan, P.J. 2016. Preclinical models for obesity research. *Disease Models & Mechanisms*. 9(11):1245–1255. DOI: 10.1242/dmm.026443.
- Bedard, K. & Krause, K.H. 2007. The NOX family of ROS-generating NADPH oxidases: Physiology and pathophysiology. *Physiological Reviews*. 87(1):245–313. DOI: 10.1152/physrev.00044.2005.
- Beltrán-Debón, R., Rull, A., Rodríguez-Sanabria, F., Iswaldi, I., Herranz-López, M., Aragonès, G., Camps, J., Alonso-Villaverde, C., et al. 2011. Continuous administration of polyphenols from aqueous rooibos (*Aspalathus linearis*) extract ameliorates dietary-induced metabolic disturbances in hyperlipidemic mice. *Phytomedicine*. 18(5):414–424. DOI: 10.1016/j.phymed.2010.11.008.
- Blüher, M. 2010. The distinction of metabolically ‘healthy’ from ‘unhealthy’ obese individuals. *Current Opinion in Lipidology*. 21(1):38–43. DOI: 10.1097/MOL.0b013e3283346ccc.
- Blüher, M. 2019. Obesity: global epidemiology and pathogenesis. *Nature Reviews Endocrinology*. 15(5):288–298. DOI: 10.1038/s41574-019-0176-8.
- Boden, G. 2011. Obesity, insulin resistance and free fatty acids. *Current Opinion in Endocrinology, Diabetes and Obesity*. 18(2):139–143. DOI: 10.1097/MED.0b013e3283444b09.
- Booth, A., Magnuson, A., Fouts, J. & Foster, M.T. 2016. Adipose tissue: an endocrine organ playing a role in metabolic regulation. *Hormone Molecular Biology and Clinical Investigation*. 26(1):25–42. DOI: 10.1515/hmbci-2015-0073.
- Borga, M., West, J., Bell, J.D., Harvey, N.C., Romu, T., Heymsfield, S.B. & Dahlqvist Leinhard, O. 2018. Advanced body composition assessment: from body mass index to body composition profiling. *Journal of Investigative Medicine*. 66(5):1.10-9. DOI: 10.1136/jim-2018-000722.
- Boutens, L. & Stienstra, R. 2016. Adipose tissue macrophages: going off track during obesity. *Diabetologia*. 59(5):879–94. DOI: 10.1007/s00125-016-3904-9.
- Bray, M.S. 2008. Implications of gene-behavior interactions: Prevention and intervention for obesity. *Obesity*. 16(SUPPL. 3):S72–S78. DOI: 10.1038/oby.2008.522.
- Bustin, S.A. 2000. Absolute quantification of mrna using real-time reverse transcription polymerase chain reaction assays. *Journal of Molecular Endocrinology*. 25(2):169–193. DOI: 10.1677/jme.0.0250169.
- Bustin, S.A. & Mueller, R. 2005. Real-time reverse transcription PCR (qRT-PCR) and its potential use in clinical diagnosis. *Clinical Science*. 109(4):365–379. DOI: 10.1042/CS20050086.
- Bustin, S.A. & Nolan, T. 2004. Pitfalls of quantitative real-time reverse-transcription polymerase chain reaction. *Journal of Biomolecular Techniques*. 15(3):155-166.
- Castro, J.P., Grune, T. & Speckmann, B. 2016. The two faces of reactive oxygen species (ROS) in adipocyte function and dysfunction. *Biological Chemistry*. 397(8):709–724. DOI: 10.1515/hsz-2015-0305

- Carter, M. & Shieh, J. 2015. Guide to Research Techniques in Neuroscience (Second Edition), Chapter 6 - visualizing neural structure. *Academic Press, San Diego*, 145-166. DOI: 10.1016/B978-0-12-800511-8.00006-X
- Chellan, N., Joubert, E., Strijdom, H., Roux, C., Louw, J. & Muller, C.J.F. 2014. Aqueous extract of unfermented honeybush (*Cyclopia maculata*) attenuates stz-induced diabetes and β -cell cytotoxicity. *Planta Medica*. 80(8–9):622–629. DOI: 10.1055/s-0034-1368457.
- Chiba, K., Kawakami, K. & Tohyama, K. 1998. Simultaneous evaluation of cell viability by neutral red, MTT and crystal violet staining assays of the same cells. *Toxicology in Vitro*. 12(3):251–258. DOI: 10.1016/S0887-2333(97)00107-0.
- Choe, S.S., Huh, J.Y., Hwang, I.J., Kim, J.I. & Kim, J.B. 2016. Adipose Tissue Remodeling: Its Role in Energy Metabolism and Metabolic Disorders. *Frontiers in Endocrinology*. 7(APR):30. DOI: 10.3389/fendo.2016.00030.
- Chooi, Y.C., Ding, C. & Magkos, F. 2019. The epidemiology of obesity. *Metabolism*. 92:6–10. DOI: 10.1016/j.metabol.2018.09.005.
- Chuang, C.C., Yang, R. Sen, Tsai, K.S., Ho, F.M. & Liu, S.H. 2007. Hyperglycemia enhances adipogenic induction of lipid accumulation: Involvement of extracellular signal-regulated protein kinase 1/2, phosphoinositide 3-kinase/Akt, and peroxisome proliferator-activated receptor γ signaling. *Endocrinology*. 148(9):4267–4275. DOI: 10.1210/en.2007-0179.
- Church, C., Horowitz, M. & Rodeheffer, M. 2012. WAT is a functional adipocyte? *Adipocyte*. 1(1):38–45. DOI: 10.4161/adip.19132.
- Cinti, S. 2005. The adipose organ. *Prostaglandins Leukotrienes and Essential Fatty Acids*. 73(1 SPEC. ISS.):9–15. DOI: 10.1016/j.plefa.2005.04.010.
- Coelho, M., Oliveira, T. & Fernandes, R. 2013. State of the art paper Biochemistry of adipose tissue: an endocrine organ. *Archives of Medical Science*. 2(2):191–200. DOI: 10.5114/aoms.2013.33181.
- Cornier, M.-A., Després, J.-P., Davis, N., Grossniklaus, D.A., Klein, S., Lamarche, B., Lopez-Jimenez, F., Rao, G., et al. 2011. Assessing Adiposity. *Circulation*. 124(18):1996–2019. DOI: 10.1161/CIR.0b013e318233bc6a.
- Del Mar Romero, M., Sabater, D., Fernández-López, J.A., Remesar, X. & Alemany, M. 2015. Glycerol production from glucose and fructose by 3T3-L1 Cells: A mechanism of Adipocyte defense from excess substrate. *PLoS ONE*. 10(10):e0139502. DOI: 10.1371/journal.pone.0139502.
- Denayer, T., Stöhrn, T. & Van Roy, M. 2014. Animal models in translational medicine: Validation and prediction. *New Horizons in Translational Medicine*. 2(1):5–11. DOI: 10.1016/j.nhtm.2014.08.001.
- Denis, G. V. & Obin, M.S. 2013. “Metabolically healthy obesity”: Origins and implications. *Molecular Aspects of Medicine*. 34(1):59–70. DOI: 10.1016/j.mam.2012.10.004.

- Die, J. V. & Román, B. 2012. RNA quality assessment: A view from plant qPCR studies. *Journal of Experimental Botany*. 63(17):6069–6077. DOI: 10.1093/jxb/ers276.
- Dludla, P. V., Muller, C.J.F., Louw, J., Joubert, E., Salie, R., Opoku, A.R. & Johnson, R. 2014. The cardioprotective effect of an aqueous extract of fermented rooibos (*Aspalathus linearis*) on cultured cardiomyocytes derived from diabetic rats. *Phytomedicine: international journal of phytotherapy and phytopharmacology*. 21(5):595–601. DOI: 10.1016/j.phymed.2013.10.029.
- Dludla, P. V., Jack, B., Viraragavan, A., Pheiffer, C., Johnson, R., Louw, J. & Muller, C.J.F. 2018. A dose-dependent effect of dimethyl sulfoxide on lipid content, cell viability and oxidative stress in 3T3-L1 adipocytes. *Toxicology Reports*. 5:1014–1020. DOI: 10.1016/j.toxrep.2018.10.002.
- Dludla, P. V., Nkambule, B.B., Jack, B., Mkandla, Z., Mutize, T., Silvestri, S., Orlando, P., Tiano, L., et al. 2019. Inflammation and oxidative stress in an obese state and the protective effects of gallic acid. *Nutrients*. 11(1):23. DOI: 10.3390/nu11010023.
- Dudhia, Z., Louw, J., Muller, C., Joubert, E., de Beer, D., Kinnear, C. & Pheiffer, C. 2013. *Cyclopia maculata* and *Cyclopia subternata* (honeybush tea) inhibits adipogenesis in 3T3-L1 pre-adipocytes. *Phytomedicine: international journal of phytotherapy and phytopharmacology*. 20(5):401–8. DOI: 10.1016/j.phymed.2012.12.002.
- Eghan, B.A., Agyemang-Yeboah, F., Togbe, E., Annani-Akollor, M.E., Donkor, S. & Afranie, B.O. 2019. Waist circumference and hip circumference as potential predictors of visceral fat estimate among type 2 diabetic patients at the Komfo Anokye Teaching Hospital (KATH), Kumasi-Ghana. *Alexandria Journal of Medicine*. 55(1):49–56. DOI: 10.1080/20905068.2019.1658340.
- Ertunc, M.E., Sikkeland, J., Fenaroli, F., Griffiths, G., Daniels, M.P., Cao, H., Saatcioglu, F. & Hotamisligil, G.S. 2015. Secretion of fatty acid binding protein aP2 from adipocytes through a nonclassical pathway in response to adipocyte lipase activity. *Journal of Lipid Research*. 56(2):423–434. DOI: 10.1194/jlr.M055798.
- Escorcia, W., Ruter, D.L., Nhan, J. & Curran, S.P. 2018. Quantification of lipid abundance and evaluation of lipid distribution in *Caenorhabditis elegans* by Nile red and oil red O staining. *Journal of Visualized Experiments*. 2018(133). DOI: 10.3791/57352.
- Esteve Ràfols, M. 2014. Tejido adiposo: heterogeneidad celular y diversidad funcional. *Endocrinología y Nutrición*. 61(2):100–112. DOI: 10.1016/j.endonu.2013.03.011.
- Fleige, S. & Pfaffl, M.W. 2006. RNA integrity and the effect on the real-time qRT-PCR performance. *Molecular Aspects of Medicine*. 27(2–3):126–139. DOI: 10.1016/j.mam.2005.12.003.
- Fock, K.M. & Khoo, J. 2013. Diet and exercise in management of obesity and overweight. *Journal of Gastroenterology and Hepatology (Australia)*. 28(S4):59–63. DOI: 10.1111/jgh.12407.
- Fomenko, E.V. & Chi, Y. 2016. Mangiferin modulation of metabolism and metabolic syndrome. *BioFactors*. 42(5):492–503. DOI: 10.1002/biof.1309.
- Ford, N.D., Patel, S.A. & Narayan, K.M.V. 2017. Obesity in Low- and Middle-Income Countries:

- Burden, Drivers, and Emerging Challenges. *Annual Review of Public Health*. 38(1):145–164. DOI: 10.1146/annurev-publhealth-031816-044604.
- Fox, A., Feng, W. & Asal, V. 2019. What is driving global obesity trends? Globalization or “modernization”? *Globalization and Health*. 15(1):32. DOI: 10.1186/s12992-019-0457-y.
- Frühbeck, G., Toplak, H., Woodward, E., Yumuk, V., Maislos, M. & Oppert, J.-M. 2013. Obesity: The Gateway to Ill Health - an EASO Position Statement on a Rising Public Health, Clinical and Scientific Challenge in Europe. *Obesity Facts*. 6(2):117–120. DOI: 10.1159/000350627.
- Furukawa, S., Fujita, T., Shimabukuro, M., Iwaki, M., Yamada, Y., Nakajima, Y., Nakayama, O., Makishima, M., et al. 2004. Increased oxidative stress in obesity and its impact on metabolic syndrome. *Journal of Clinical Investigation*. 114(12):1752–1761. DOI: 10.1172/JCI21625.
- Gaidhu, M.P., Anthony, N.M., Patel, P., Hawke, T.J. & Ceddia, R.B. 2010. Dysregulation of lipolysis and lipid metabolism in visceral and subcutaneous adipocytes by high-fat diet: role of ATGL, HSL, and AMPK. *American Journal of Physiology-Cell Physiology*. 298(4):C961–C971. DOI: 10.1152/ajpcell.00547.2009.
- Gallagher, D., Heymsfield, S.B., Heo, M., Jebb, S.A., Murgatroyd, P.R. & Sakamoto, Y. 2000. Healthy percentage body fat ranges: an approach for developing guidelines based on body mass index. *The American Journal of Clinical Nutrition*. 72(3):694–701. DOI: 10.1093/ajcn/72.3.694.
- Gambero, A. & Ribeiro, M. 2015. The Positive Effects of Yerba Maté (*Ilex paraguariensis*) in Obesity. *Nutrients*. 7(2):730–750. DOI: 10.3390/nu7020730.
- Girousse, A., Tavernier, G., Valle, C., Moro, C., Mejhert, N., Dinel, A.L., Houssier, M., Roussel, B., et al. 2013. Partial Inhibition of Adipose Tissue Lipolysis Improves Glucose Metabolism and Insulin Sensitivity Without Alteration of Fat Mass. *PLoS Biology*. 11(2):e1001485. DOI: 10.1371/journal.pbio.1001485.
- Gonçalves, L.F., Machado, T.Q., Castro-Pinheiro, C., de Souza, N.G., Oliveira, K.J. & Fernandes-Santos, C. 2017. Ageing is associated with brown adipose tissue remodelling and loss of white fat browning in female C57BL/6 mice. *International Journal of Experimental Pathology*. 98(2):100–108. DOI: 10.1111/iep.12228.
- Goossens, G.H. 2017. The Metabolic Phenotype in Obesity: Fat Mass, Body Fat Distribution, and Adipose Tissue Function. *Obesity Facts*. 10(3):207–215. DOI: 10.1159/000471488.
- Green, H. & Kehinde, O. 1975. An established preadipose cell line and its differentiation in culture II. Factors affecting the adipose conversion. *Cell*. 5(1):19–27. DOI: 10.1016/0092-8674(75)90087-2.
- Green, H. & Meuth, M. 1974. An established pre-adipose cell line and its differentiation in culture. *Cell*. 3(2):127–133. DOI: 10.1016/0092-8674(74)90116-0.
- Green, A., Rumberger, J.M., Stuart, C.A. & Ruhoff, M.S. 2004. Stimulation of Lipolysis by Tumor Necrosis Factor- α in 3T3-L1 Adipocytes Is Glucose Dependent: Implications for Long-Term

- Regulation of Lipolysis. *Diabetes*. 53(1):74–81. DOI: 10.2337/diabetes.53.1.74.
- Gregoire, F.M., Smas, C.M. & Sul, H.S., 1998. Understanding adipocyte differentiation. *Physiological Reviews*. 78(3), 783-809. DOI: 10.1152/physrev.1998.78.3.783
- Grundy, A., Cotterchio, M., Kirsh, V.A. & Kreiger, N. 2014. Associations between anxiety, depression, antidepressant medication, obesity and weight gain among Canadian women. *PLoS ONE*. 9(6):e99780. DOI: 10.1371/journal.pone.0099780.
- Grundy, S.M., Williams, C. & Vega, G.L. 2018. Upper body fat predicts metabolic syndrome similarly in men and women. *European Journal of Clinical Investigation*. 48(7):e12941. DOI: 10.1111/eci.12941.
- Guo, F., Huang, C., Liao, X., Wang, Y., He, Y., Feng, R., Li, Y. & Sun, C. 2011. Beneficial effects of mangiferin on hyperlipidemia in high-fat-fed hamsters. *Molecular nutrition & food research*. 55(12):1809–18. DOI: 10.1002/mnfr.201100392.
- Gustafson, B., Gogg, S., Hedjazifar, S., Jenndahl, L., Hammarstedt, A. & Smith, U. 2009. Inflammation and impaired adipogenesis in hypertrophic obesity in man. *American Journal of Physiology - Endocrinology and Metabolism*. 297(5): E999-E1003. DOI: 10.1152/ajpendo.00377.2009.
- Han, Y.C., Subramanian, S., Chan, C.K., Omer, M., Chiba, T., Wight, T.N. & Chait, A. 2007. Adipocyte-derived serum amyloid A3 and hyaluronan play a role in monocyte recruitment and adhesion. *Diabetes*. 56(9):2260–2273. DOI: 10.2337/db07-0218.
- Haslam, D.W. & James, W.P.T. 2005. Obesity. *The Lancet*. 366(9492):1197–1209. DOI: 10.1016/S0140-6736(05)67483-1.
- He, G., Bruun, J.M., Lihn, A.S., Pedersen, S.B. & Richelsen, B. 2003. Stimulation of PAI-1 and adipokines by glucose in human adipose tissue *in vitro*. *Biochemical and Biophysical Research Communications*. 310(3):878–883. DOI: 10.1016/j.bbrc.2003.09.091.
- Hill, J.O., Wyatt, H.R. & Peters, J.C. 2012. Energy Balance and Obesity. *Circulation*. 126(1):126–132. DOI: 10.1161/CIRCULATIONAHA.111.087213.
- Hruby, A. & Hu, F.B. 2015. The Epidemiology of Obesity: A Big Picture. *Pharmacoeconomics*. 33(7):673–89. DOI: 10.1007/s40273-014-0243-x.
- <http://www.chemspider.com>. 2019a. *Aspalathin*. Available: <http://www.chemspider.com/Chemical-Structure.9457391.html?rid=61c71bcb-4287-4f2a-b5d1-820d11ad5778> [2019, December 03].
- <http://www.chemspider.com>. 2019b. *Mangiferin*. Available: <http://www.chemspider.com/Chemical-Structure.4444966.html?rid=1a18e95b-811d-41e1-af5c-05887057c338> [2019, December 03].
- Hvizdos, K.M. & Markham, A. 1999. Orlistat. A review of its use in the management of obesity. *Drugs*. 58(4):743–760. DOI: 10.2165/00003495-199958040-00015.

- Ibrahim, M.M. 2010. Subcutaneous and visceral adipose tissue: structural and functional differences. *Obesity Reviews*. 11(1):11–18. DOI: 10.1111/j.1467-789X.2009.00623.x.
- Imbeaud, S., Graudens, E., Boulanger, V., Barlet, X., Zaborski, P., Eveno, E., Mueller, O., Schroeder, A., et al. 2005. Towards standardization of RNA quality assessment using user-independent classifiers of microcapillary electrophoresis traces. *Nucleic Acids Research*. 33(6):1–12. DOI: 10.1093/nar/gni054.
- Jack, B.U., Malherbe, C.J., Huisamen, B., Gabuza, K., Mazibuko-Mbeje, S., Schulze, A.E., Joubert, E., Muller, C.J.F., et al. 2017. A polyphenol-enriched fraction of *Cyclopia intermedia* decreases lipid content in 3T3-L1 adipocytes and reduces body weight gain of obese db/db mice. *South African Journal of Botany*. 110:216–229. DOI: 10.1016/j.sajb.2016.08.007.
- Jack, B.U., Malherbe, C.J., Willenburg, E.L., de Beer, D., Huisamen, B., Joubert, E., Muller, C.J.F., Louw, J., et al. 2018. Polyphenol-Enriched Fractions of *Cyclopia intermedia* Selectively Affect Lipogenesis and Lipolysis in 3T3-L1 Adipocytes. *Planta medica*. 84(2):100–110. DOI: 10.1055/s-0043-119463.
- Jack, B.U., Malherbe, C.J., Mamushi, M., Muller, C.J.F., Joubert, E., Louw, J. & Pheiffer, C. 2019. Adipose tissue as a possible therapeutic target for polyphenols: A case for *Cyclopia* extracts as anti-obesity nutraceuticals. *Biomedicine & Pharmacotherapy*. 120:109439. DOI: 10.1016/j.biopha.2019.109439.
- Janochova, K., Haluzik, M. & Buzga, M. 2019. Visceral fat and insulin resistance - what we know? *Biomedical Papers*. 163(1):19–27. DOI: 10.5507/bp.2018.062.
- Jastroch, M., Oelkrug, R. & Keipert, S. 2018. Insights into brown adipose tissue evolution and function from non-model organisms. *Journal of Experimental Biology*. 121(Suppl 1):jeb169425. DOI: 10.1242/jeb.169425.
- Jo, J., Gavrilova, O., Pack, S., Jou, W., Mullen, S., Sumner, A.E., Cushman, S.W. & Periwai, V. 2009. Hypertrophy and/or hyperplasia: Dynamics of adipose tissue growth. *PLoS Computational Biology*. 5(3):e1000324. DOI: 10.1371/journal.pcbi.1000324.
- Johannsen, D.L. & Ravussin, E. 2009. The role of mitochondria in health and disease. *Current Opinion in Pharmacology*. 9(6):780–786. DOI: 10.1016/j.coph.2009.09.002.
- Johnson, R., Beer, D. De, Dlodla, P., Ferreira, D., Muller, C. & Joubert, E. 2018. Aspalathin from Rooibos (*Aspalathus linearis*): A Bioactive C-glucosyl Dihydrochalcone with Potential to Target the Metabolic Syndrome. *Planta Medica*. 84(09/10):568–583. DOI: 10.1055/s-0044-100622.
- Joubert, E. & de Beer, D. 2011. Rooibos (*Aspalathus linearis*) beyond the farm gate: From herbal tea to potential phytopharmaceutical. *South African Journal of Botany*. 77(4):869–886. DOI: 10.1016/j.sajb.2011.07.004.
- Joubert, E., Winterton, P., Britz, T.J. & Gelderblom, W.C.A. 2005. Antioxidant and pro-oxidant activities of aqueous extracts and crude polyphenolic fractions of rooibos (*Aspalathus linearis*). *Journal of Agricultural and Food Chemistry*. 53(26):10260–10267. DOI: 10.1021/jf051355a.

- Joubert, E., Gelderblom, W.C.A., Louw, A. & de Beer, D. 2008. South African herbal teas: *Aspalathus linearis*, *Cyclopia* spp. and *Athrixia phylicoides*—A review. *Journal of Ethnopharmacology*. 119(3):376–412. DOI: 10.1016/j.jep.2008.06.014.
- Joubert, E., Joubert, M.E., Bester, C., de Beer, D. & De Lange, J.H. 2011. Honeybush (*Cyclopia* spp.): From local cottage industry to global markets — The catalytic and supporting role of research. *South African Journal of Botany*. 77(4):887–907. DOI: 10.1016/j.sajb.2011.05.014.
- Joubert, E., de Beer, D., Malherbe, C.J., Muller, M., Louw, A. & Gelderblom, W.C.A. 2019. Formal honeybush tea industry reaches 20-year milestone – progress of product research targeting phenolic composition, quality and bioactivity. *South African Journal of Botany*. 127:58–79. DOI: 10.1016/j.sajb.2019.08.027.
- Jung, U. & Choi, M.-S. 2014. Obesity and Its Metabolic Complications: The Role of Adipokines and the Relationship between Obesity, Inflammation, Insulin Resistance, Dyslipidemia and Nonalcoholic Fatty Liver Disease. *International Journal of Molecular Sciences*. 15(4):6184–6223. DOI: 10.3390/ijms15046184.
- Kahn, C.R., Wang, G. & Lee, K.Y. 2019. Altered adipose tissue and adipocyte function in the pathogenesis of metabolic syndrome. *Journal of Clinical Investigation*. 129(10):3990–4000. DOI: 10.1172/JCI129187.
- Kakkar, A.K. & Dahiya, N. 2015. Drug treatment of obesity: Current status and future prospects. *European Journal of Internal Medicine*. 26(2):89–94. DOI: 10.1016/j.ejim.2015.01.005.
- Kamakura, R., Son, M.J., de Beer, D., Joubert, E., Miura, Y. & Yagasaki, K. 2015. Antidiabetic effect of green rooibos (*Aspalathus linearis*) extract in cultured cells and type 2 diabetic model KK-Ay mice. *Cytotechnology*. 67(4):699–710. DOI: 10.1007/s10616-014-9816-y.
- Kanda, H., Tateya, S., Tamori, Y., Kotani, K., Hiasa, K.I., Kitazawa, R., Kitazawa, S., Miyachi, H., et al. 2006. MCP-1 contributes to macrophage infiltration into adipose tissue, insulin resistance, and hepatic steatosis in obesity. *Journal of Clinical Investigation*. 116(6):1494–1505. DOI: 10.1172/JCI26498.
- Kanda, Y., Hinata, T., Kang, S.W. & Watanabe, Y. 2011. Reactive oxygen species mediate adipocyte differentiation in mesenchymal stem cells. *Life Sciences*. 89(7–8):250–258. DOI: 10.1016/j.lfs.2011.06.007.
- Kassir, R., Debs, T., Blanc, P., Gugenheim, J., Ben Amor, I., Boutet, C. & Tiffet, O. 2016. Complications of bariatric surgery: Presentation and emergency management. *International Journal of Surgery*. 27:77–81. DOI: 10.1016/j.ijssu.2016.01.067.
- Keipert, S. & Jastroch, M. 2014. Brite/beige fat and UCP1 — is it thermogenesis? *Biochimica et Biophysica Acta (BBA) - Bioenergetics*. 1837(7):1075–1082. DOI: 10.1016/j.bbabi.2014.02.008.
- Kershaw, E.E. & Flier, J.S. 2004. Adipose Tissue as an Endocrine Organ. *The Journal of Clinical Endocrinology & Metabolism*. 89(6):2548–2556. DOI: 10.1210/jc.2004-0395.

- Kissler, H.J. & Settmacher, U. 2013. Bariatric Surgery to Treat Obesity. *Seminars in Nephrology*. 33(1):75–89. DOI: 10.1016/j.semnephrol.2012.12.004.
- Kolodziej, M., Strauss, S., Lazaridis, A., Bucan, V., Kuhbier, J.W., Vogt, P.M. & Könneker, S. 2019. Influence of glucose and insulin in human adipogenic differentiation models with adipose-derived stem cells. *Adipocyte*. 8(1):254–264. DOI: 10.1080/21623945.2019.1636626.
- Krintel, C., Mörgelin, M., Logan, D.T. & Holm, C. 2009. Phosphorylation of hormone-sensitive lipase by protein kinase A *in vitro* promotes an increase in its hydrophobic surface area. *FEBS Journal*. 276(17):4752–4762. DOI: 10.1111/j.1742-4658.2009.07172.x.
- Kuriyan, R. 2018. Body composition techniques. *Indian Journal of Medical Research*. 148(5):648. DOI: 10.4103/ijmr.IJMR_1777_18.
- Kwon, H., Kim, D. & Kim, J.S. 2017. Body Fat Distribution and the Risk of Incident Metabolic Syndrome: A Longitudinal Cohort Study. *Scientific Reports*. 7(1):10955. DOI: 10.1038/s41598-017-09723-y.
- Lagerros, Y.T. & Rössner, S. 2013. Obesity management: What brings success? *Therapeutic Advances in Gastroenterology*. 6(1):77–88. DOI: 10.1177/1756283X12459413.
- Langhans, S.A. 2018. Three-dimensional *in vitro* cell culture models in drug discovery and drug repositioning. *Frontiers in Pharmacology*. 9:6. DOI: 10.3389/fphar.2018.00006.
- Lawal, A.O., Davids, L.M. & Marnewick, J.L. 2019. Rooibos (*Aspalathus linearis*) and honeybush (*Cyclopia* species) modulate the oxidative stress associated injury of diesel exhaust particles in human umbilical vein endothelial cells. *Phytomedicine*. 59:152898. DOI: 10.1016/j.phymed.2019.152898.
- Lee, H., Lee, Y.J., Choi, H., Ko, E.H. & Kim, J.-W. 2009. Reactive oxygen species facilitate adipocyte differentiation by accelerating mitotic clonal expansion. *The Journal of biological chemistry*. 284(16):10601–9. DOI: 10.1074/jbc.M808742200.
- Lee, M.-J., Wu, Y. & Fried, S.K. 2010. Adipose tissue remodeling in pathophysiology of obesity. *Current Opinion in Clinical Nutrition and Metabolic Care*. 13(4):371–376. DOI: 10.1097/MCO.0b013e32833aabef.
- Lee, S., Ahn, S., Kim, Y., Ji, M., Kim, K., Choi, S., Jang, H. & Lim, S. 2018. Comparison between Dual-Energy X-ray Absorptiometry and Bioelectrical Impedance Analyses for Accuracy in Measuring Whole Body Muscle Mass and Appendicular Skeletal Muscle Mass. *Nutrients*. 10(6):738. DOI: 10.3390/nu10060738.
- Lee, Y.-H., Mottillo, E.P. & Granneman, J.G. 2014. Adipose tissue plasticity from WAT to BAT and in between. *Biochimica et Biophysica Acta (BBA) - Molecular Basis of Disease*. 1842(3):358–369. DOI: 10.1016/j.bbadis.2013.05.011.
- Liao, W., Nguyen, M.T.A., Yoshizaki, T., Favelyukis, S., Patsouris, D., Imamura, T., Verma, I.M. & Olefsky, J.M. 2007. Suppression of PPAR- γ attenuates insulin-stimulated glucose uptake by

- affecting both GLUT1 and GLUT4 in 3T3-L1 adipocytes. *American Journal of Physiology - Endocrinology and Metabolism*. 293(1):E219–E227. DOI: 10.1152/ajpendo.00695.2006.
- Lihn, A.S., Pedersen, S.B. & Richelsen, B. 2005. Adiponectin: action, regulation and association to insulin sensitivity. *Obesity reviews : an official journal of the International Association for the Study of Obesity*. 6(1):13–21. DOI: 10.1111/j.1467-789X.2005.00159.x.
- Lim, J., Liu, Z., Apontes, P., Feng, D., Pessin, J.E., Sauve, A.A., Angeletti, R.H. & Chi, Y. 2014. Dual mode action of mangiferin in mouse liver under high fat diet. *PLoS ONE*. 9(3):e90137. DOI: 10.1371/journal.pone.0090137.
- Lin, Y., Berg, A.H., Iyengar, P., Lam, T.K.T., Giacca, A., Combs, T.P., Rajala, M.W., Du, X., et al. 2005. The hyperglycemia-induced inflammatory response in adipocytes: The role of reactive oxygen species. *Journal of Biological Chemistry*. 280(6):4617–4626. DOI: 10.1074/jbc.M411863200.
- Lizcano, F. 2019. The beige adipocyte as a therapy for metabolic diseases. *International Journal of Molecular Sciences*. 20(20):5058. DOI: 10.3390/ijms20205058.
- Longo, M., Zatterale, F., Naderi, J., Parrillo, L., Formisano, P., Raciti, G.A., Beguinot, F. & Miele, C. 2019. Adipose Tissue Dysfunction as Determinant of Obesity-Associated Metabolic Complications. *International Journal of Molecular Sciences*. 20(9):2358. DOI: 10.3390/ijms20092358.
- Luong, Q., Huang, J. & Lee, K.Y. 2019. Deciphering White Adipose Tissue Heterogeneity. *Biology*. 8(2):23. DOI: 10.3390/biology8020023.
- Lynes, M.D. & Tseng, Y.-H. 2018. Deciphering adipose tissue heterogeneity. *Annals of the New York Academy of Sciences*. 1411(1):5–20. DOI: 10.1111/nyas.13398.
- Manach, C., Scalbert, A., Morand, C., Rémésy, C. & Jiménez, L. 2004. Polyphenols: food sources and bioavailability. *The American Journal of Clinical Nutrition*. 79(5):727–747. DOI: 10.1093/ajcn/79.5.727.
- Marnewick, J., Joubert, E., Joseph, S., Swanevelder, S., Swart, P. & Gelderblom, W. 2005. Inhibition of tumour promotion in mouse skin by extracts of rooibos (*Aspalathus linearis*) and honeybush (*Cyclopia intermedia*), unique South African herbal teas. *Cancer Letters*. 224(2):193–202. DOI: 10.1016/j.canlet.2004.11.014.
- Marnewick, J.L., Gelderblom, W.C. & Joubert, E. 2000. An investigation on the antimutagenic properties of South African herbal teas. *Mutation Research - Genetic Toxicology and Environmental Mutagenesis*. 471(1–2):157–166. DOI: 10.1016/S1383-5718(00)00128-5.
- Mazibuko, S.E., Muller, C.J.F., Joubert, E., de Beer, D., Johnson, R., Opoku, A.R. & Louw, J. 2013. Amelioration of palmitate-induced insulin resistance in C₂C₁₂ muscle cells by rooibos (*Aspalathus linearis*). *Phytomedicine : international journal of phytotherapy and phytopharmacology*. 20(10):813–9. DOI: 10.1016/j.phymed.2013.03.018.

- Mazibuko, S.E., Joubert, E., Johnson, R., Louw, J., Opoku, A.R. & Muller, C.J.F. 2015. Aspalathin improves glucose and lipid metabolism in 3T3-L1 adipocytes exposed to palmitate. *Molecular nutrition & food research*. 59(11):2199–208. DOI: 10.1002/mnfr.201500258.
- McDonough, P.M., Ingermanson, R.S., Loy, P.A., Koon, E.D., Whittaker, R., Laris, C.A., Hilton, J.M., Nicoll, J.B., et al. 2011. Quantification of hormone sensitive lipase phosphorylation and colocalization with lipid droplets in murine 3T3L1 and human subcutaneous adipocytes via automated digital microscopy and high-content analysis. *Assay and Drug Development Technologies*. 9(3):262–280. DOI: 10.1089/adt.2010.0302.
- van der Merwe, J.D., Joubert, E., Richards, E.S., Manley, M., Snijman, P.W., Marnewick, J.L. & Gelderblom, W.C.A. 2006. A comparative study on the antimutagenic properties of aqueous extracts of *Aspalathus linearis* (rooibos), different *Cyclopia* spp. (honeybush) and *Camellia sinensis* teas. *Mutation Research - Genetic Toxicology and Environmental Mutagenesis*. 611(1–2):42–53. DOI: 10.1016/j.mrgentox.2006.06.030.
- Meydani, M. & Hasan, S.T. 2010. Dietary Polyphenols and Obesity. *Nutrients*. 2(7):737–751. DOI: 10.3390/nu2070737.
- Micklesfield, L.K., Lambert, E. V., Hume, D.J., Chantler, S., Pienaar, P.R., Dickie, K., Puoane, T. & Goedecke, J.H. 2013. Socio-cultural, environmental and behavioural determinants of obesity in black South African women : review articles. *Cardiovascular Journal Of Africa*. 24(9):369–375. DOI: 10.5830/CVJA-2013-069.
- Mittal, B. 2019. Subcutaneous adipose tissue & visceral adipose tissue. *Indian Journal of Medical Research*. 149(5):571. DOI: 10.4103/ijmr.IJMR_1910_18.
- Mopuri, R. & Islam, M.S. 2017. Medicinal plants and phytochemicals with anti-obesogenic potentials: A review. *Biomedicine & Pharmacotherapy*. 89:1442–1452. DOI: 10.1016/j.biopha.2017.02.108.
- Morigny, P., Houssier, M., Mouisel, E. & Langin, D. 2016. Adipocyte lipolysis and insulin resistance. *Biochimie*. 125:259–266. DOI: 10.1016/j.biochi.2015.10.024.
- Mortimer, M., Visser, K., De Beer, D., Joubert, E. & Louw, A. 2015. Divide and conquer may not be the optimal approach to retain the desirable estrogenic attributes of the *Cyclopia* nutraceutical extract, SM6Met. *PLoS ONE*. 10(7):e0132950. DOI: 10.1371/journal.pone.0132950.
- Mosmann, T. 1983. Rapid colorimetric assay for cellular growth and survival: Application to proliferation and cytotoxicity assays. *Journal of Immunological Methods*. 65(1–2):55–63. DOI: 10.1016/0022-1759(83)90303-4.
- Muller, C.J.F., Joubert, E., Gabuza, K., De Beer, D., Fey, S.J. & Louw, J. 2011. Assessment of the Antidiabetic Potential of an Aqueous Extract of Honeybush (*Cyclopia intermedia*) in Streptozotocin and Obese Insulin Resistant Wistar Rats. In *Phytochemicals - Bioactivities and Impact on Health*. I. Rasooli, Ed. Croatia: InTech. 311–332. DOI: 10.5772/28574.
- Muller, C.J.F., Joubert, E., De Beer, D., Sanderson, M., Malherbe, C.J., Fey, S.J. & Louw, J. 2012.

- Acute assessment of an aspalathin-enriched green rooibos (*Aspalathus linearis*) extract with hypoglycemic potential. *Phytomedicine*. 20(1):32–39. DOI: 10.1016/j.phymed.2012.09.010.
- Muller, C.J.F., Joubert, E., Pfeiffer, C., Ghoor, S., Sanderson, M., Chellan, N., Fey, S.J. & Louw, J. 2013. Z-2-(β -D-glucopyranosyloxy)-3-phenylpropenoic acid, an α -hydroxy acid from rooibos (*Aspalathus linearis*) with hypoglycemic activity. *Molecular Nutrition & Food Research*. 57(12):2216–2222. DOI: 10.1002/mnfr.201300294.
- Muller, C.J.F., Malherbe, C.J., Chellan, N., Yagasaki, K., Miura, Y. & Joubert, E. 2018. Potential of rooibos, its major C-glucosyl flavonoids, and Z-2-(β -D-glucopyranosyloxy)-3-phenylpropenoic acid in prevention of metabolic syndrome. *Critical Reviews in Food Science and Nutrition*. 58(2):227–246. DOI: 10.1080/10408398.2016.1157568.
- Murakami, S., Miura, Y., Hattori, M., Matsuda, H., Malherbe, C.J., Muller, C.J.F., Joubert, E. & Yoshida, T. 2018. *Cyclopia* Extracts Enhance Th1-, Th2-, and Th17-type T Cell Responses and Induce Foxp3 + Cells in Murine Cell Culture. *Planta Medica*. 84(5):311–319. DOI: 10.1055/s-0043-121270.
- Mushtaq, S., Abbasi, B.H., Uzair, B. & Abbasi, R. 2018. Natural products as reservoirs of novel therapeutic agents. *EXCLI Journal*. 17:420–451. DOI: 10.17179/excli2018-1174.
- Musi, N. & Guardado-Mendoza, R. 2014. Adipose Tissue as an Endocrine Organ. In *Cellular Endocrinology in Health and Disease*. A. Ulloa-Aguirre & M.P. Conn, Eds. Boston, MA: Elsevier Inc. 229–237. DOI: <https://doi.org/10.1016/C2012-0-07127-X>.
- NCD-RisC. 2016. Trends in adult body-mass index in 200 countries from 1975 to 2014: a pooled analysis of 1698 population-based measurement studies with 19.2 million participants. *Lancet (London, England)*. 387(10026):1377–1396. DOI: 10.1016/S0140-6736(16)30054-X.
- Ng, M., Fleming, T., Robinson, M., Thomson, B., Graetz, N., Margono, C., Mullany, E.C., Biryukov, S., et al. 2014. Global, regional, and national prevalence of overweight and obesity in children and adults during 1980–2013: a systematic analysis for the Global Burden of Disease Study 2013. *The Lancet*. 384(9945):766–781. DOI: 10.1016/S0140-6736(14)60460-8.
- Nilsson, C., Raun, K., Yan, F., Larsen, M.O. & Tang-Christensen, M. 2012. Laboratory animals as surrogate models of human obesity. *Acta Pharmacologica Sinica*. 33(2):173–181. DOI: 10.1038/aps.2011.203.
- Niu, Y., Li, S., Na, L., Feng, R., Liu, L., Li, Y. & Sun, C. 2012. Mangiferin decreases plasma free fatty acids through promoting its catabolism in liver by activation of AMPK. *PLoS ONE*. 7(1):e30782. DOI: 10.1371/journal.pone.0030782.
- Nuttall, F.Q. 2015. Body Mass Index. *Nutrition Today*. 50(3):117–128. DOI: 10.1097/NT.0000000000000092.
- Ohta, T., Murai, Y. & Yamada, T. 2017. Usefulness of Obese Animal Models in Antiobesity Drug Development. In *Adiposity - Omics and Molecular Understanding*. InTech. DOI: 10.5772/64907.

- Orlando, P., Chellan, N., Louw, J., Tiano, L., Cirilli, I., Dlodla, P., Joubert, E. & Muller, C.J.F. 2019. Aspalathin-Rich Green Rooibos Extract Lowers LDL-Cholesterol and Oxidative Status in High-Fat Diet-Induced Diabetic Vervet Monkeys. *Molecules*. 24(9):1713. DOI: 10.3390/molecules24091713.
- Osayande, O.E., Azekhumen, G.N. & Obuzor, E.O. 2018. A comparative study of different body fat measuring instruments. *Nigerian Journal of Physiological Sciences*. 33(2):125–128.
- Ouchi, N. & Walsh, K. 2007. Adiponectin as an anti-inflammatory factor. *Clinica chimica acta; international journal of clinical chemistry*. 380(1–2):24–30. DOI: 10.1016/j.cca.2007.01.026.
- Palacios-Ortega, S., Varela-Guruceaga, M., Martínez, J.A., de Miguel, C. & Milagro, F.I. 2016. Effects of high glucose on caveolin-1 and insulin signaling in 3T3-L1 adipocytes. *Adipocyte*. 5(1):65–80. DOI: 10.1080/21623945.2015.1122856.
- Pandey, K.B. & Rizvi, S.I. 2009. Plant Polyphenols as Dietary Antioxidants in Human Health and Disease. *Oxidative Medicine and Cellular Longevity*. 2(5):270–278. DOI: 10.4161/oxim.2.5.9498.
- Pantsi, W.G., Marnewick, J.L., Esterhuyse, A.J., Rautenbach, F. & Van Rooyen, J. 2011. Rooibos (*Aspalathus linearis*) offers cardiac protection against ischaemia/reperfusion in the isolated perfused rat heart. *Phytomedicine*. 18(14):1220–1228. DOI: 10.1016/j.phymed.2011.09.069.
- Pasupuleti, M.K., Molahally, S.S. & Salwaji, S. 2016. Ethical guidelines, animal profile, various animal models used in periodontal research with alternatives and future perspectives. *Journal of Indian Society of Periodontology*. 20(4):360–368. DOI: 10.4103/0972-124X.186931.
- Patel, D.K. & Stanford, F.C. 2018. Safety and tolerability of new-generation anti-obesity medications: a narrative review. *Postgraduate Medicine*. 130(2):173–182. DOI: 10.1080/00325481.2018.1435129.
- Patel, O., Muller, C., Joubert, E., Louw, J., Rosenkranz, B. & Awortwe, C. 2016. Inhibitory interactions of *Aspalathus linearis* (rooibos) extracts and compounds, aspalathin and Z-2-(β -D-glucopyranosyloxy)-3-phenylpropenoic acid, on cytochromes metabolizing hypoglycemic and hypolipidemic drugs. *Molecules*. 21(11):1515. DOI: 10.3390/molecules21111515.
- Peeters, A., Barendregt, J.J., Willekens, F., Mackenbach, J.P., Mamun, A. Al & Bonneux, L. 2003. Obesity in Adulthood and Its Consequences for Life Expectancy: A Life-Table Analysis. *Annals of Internal Medicine*. 138(1):24. DOI: 10.7326/0003-4819-138-1-200301070-00008.
- Pheiffer, C., Dudhia, Z., Louw, J., Muller, C. & Joubert, E. 2013. *Cyclopia maculata* (honeybush tea) stimulates lipolysis in 3T3-L1 adipocytes. *Phytomedicine: international journal of phytotherapy and phytopharmacology*. 20(13):1168–71. DOI: 10.1016/j.phymed.2013.06.016.
- Piché, M.È., Auclair, A., Harvey, J., Marceau, S. & Poirier, P. 2015. How to Choose and Use Bariatric Surgery in 2015. *Canadian Journal of Cardiology*. 31(2):153–166. DOI: 10.1016/j.cjca.2014.12.014.
- Rharass, T. & Lucas, S. 2019. High Glucose Level Impairs Human Mature Bone Marrow Adipocyte

- Function Through Increased ROS Production. *Frontiers in Endocrinology*. 10. DOI: 10.3389/fendo.2019.00607.
- Rotondo, F., Ho-Palma, A.C., Remesar, X., Fernández-López, J.A., Romero, M.D.M. & Alemany, M. 2017. Glycerol is synthesized and secreted by adipocytes to dispose of excess glucose, via glycerogenesis and increased acyl-glycerol turnover. *Scientific Reports*. 7(1):8983. DOI: 10.1038/s41598-017-09450-4.
- Ruiz-Ojeda, F.J., Rupérez, A.I., Gomez-Llorente, C., Gil, A. & Aguilera, C.M. 2016. Cell models and their application for studying adipogenic differentiation in relation to obesity: A review. *International Journal of Molecular Sciences*. 17(7). DOI: 10.3390/ijms17071040.
- Saely, C.H., Geiger, K. & Drexel, H. 2012. Brown versus White Adipose Tissue: A Mini-Review. *Gerontology*. 58(1):15–23. DOI: 10.1159/000321319.
- Samuel, V.T. & Shulman, G.I. 2016. The pathogenesis of insulin resistance: integrating signaling pathways and substrate flux. *Journal of Clinical Investigation*. 126(1):12–22. DOI: 10.1172/JCI77812.
- Sanderson, M., Mazibuko, S.E., Joubert, E., De Beer, D., Johnson, R., Pheiffer, C., Louw, J. & Muller, C.J.F. 2014. Effects of fermented rooibos (*Aspalathus linearis*) on adipocyte differentiation. *Phytomedicine*. 21(2):109–117. DOI: 10.1016/j.phymed.2013.08.011.
- Sasaki, M., Nishida, N. & Shimada, M. 2018. A beneficial role of rooibos in diabetes mellitus: A systematic review and meta-analysis. *Molecules*. 23(4):839. DOI: 10.3390/molecules23040839.
- Schott, M.B., Rasineni, K., Weller, S.G., Schulze, R.J., Sletten, A.C., Casey, C.A. & McNiven, M.A. 2017. β -adrenergic induction of lipolysis in hepatocytes is inhibited by ethanol exposure. *Journal of Biological Chemistry*. 292(28):11815–11828. DOI: 10.1074/jbc.M117.777748.
- Schroeder, A., Mueller, O., Stocker, S., Salowsky, R., Leiber, M., Gassmann, M., Lightfoot, S., Menzel, W., et al. 2006. The RIN: An RNA integrity number for assigning integrity values to RNA measurements. *BMC Molecular Biology*. 7. DOI: 10.1186/1471-2199-7-3.
- Sepa-Kishi, D.M. & Ceddia, R.B. 2018. White and beige adipocytes: are they metabolically distinct? *Hormone Molecular Biology and Clinical Investigation*. 33(2). DOI: 10.1515/hmbci-2018-0003.
- Sharma, K., Arora, T., Joshi, V., Rathor, N., Mehta, A., Mehta, K. & Mediratta, P. 2011. Substitute of animals in drug research: An approach towards fulfillment of 4R's. *Indian Journal of Pharmaceutical Sciences*. 73(1):1. DOI: 10.4103/0250-474x.89750.
- Shilpa, K., Dinesh, T. & Lakshmi, B.S. 2013. An *in vitro* model to probe the regulation of adipocyte differentiation under hyperglycemia. *Diabetes and Metabolism Journal*. 37(3):176–180. DOI: 10.4093/dmj.2013.37.3.176.
- Shoelson, S.E., Herrero, L. & Naaz, A. 2007. Obesity, Inflammation, and Insulin Resistance. *Gastroenterology*. 132(6):2169–2180. DOI: 10.1053/j.gastro.2007.03.059.

- Smith, G.I., Mittendorfer, B. & Klein, S. 2019. Metabolically healthy obesity: facts and fantasies. *Journal of Clinical Investigation*. 129(10):3978–3989. DOI: 10.1172/JCI129186.
- Stander, M.A., Joubert, E. & De Beer, D. 2019. Revisiting the caffeine-free status of rooibos and honeybush herbal teas using specific MRM and high resolution LC-MS methods. *Journal of Food Composition and Analysis*. 76:39–43. DOI: 10.1016/j.jfca.2018.12.002.
- Standley, L., Winterton, P., Marnewick, J.L., Gelderblom, W.C.A., Joubert, E. & Britz, T.J. 2001. Influence of processing stages on antimutagenic and antioxidant potentials of rooibos tea. *Journal of Agricultural and Food Chemistry*. 49(1):114–117. DOI: 10.1021/jf000802d.
- Subash-Babu, P. & Alshatwi, A.A. 2015. Evaluation of Antiobesity Effect of Mangiferin in Adipogenesis-Induced Human Mesenchymal Stem Cells by Assessing Adipogenic Genes. *Journal of Food Biochemistry*. 39(1):28–38. DOI: 10.1111/jfbc.12101.
- Suganami, T., Nishida, J. & Ogawa, Y. 2005. A paracrine loop between adipocytes and macrophages aggravates inflammatory changes: Role of free fatty acids and tumor necrosis factor α . *Arteriosclerosis, Thrombosis, and Vascular Biology*. 25(10):2062–2068. DOI: 10.1161/01.ATV.0000183883.72263.13.
- Sun, J., Xu, Y., Deng, H., Sun, S., Dai, Z. & Sun, Y. 2010. Intermittent high glucose exacerbates the aberrant production of adiponectin and resistin through mitochondrial superoxide overproduction in adipocytes. *Journal of Molecular Endocrinology*. 44(3):179–185. DOI: 10.1677/JME-09-0088.
- Sun, K., Kusminski, C.M. & Scherer, P.E. 2011. Adipose tissue remodeling and obesity. *Journal of Clinical Investigation*. 121(6):2094–2101. DOI: 10.1172/JCI45887.
- Sun, N.-N., Wu, T.-Y. & Chau, C.-F. 2016. Natural Dietary and Herbal Products in Anti-Obesity Treatment. *Molecules (Basel, Switzerland)*. 21(10):1351. DOI: 10.3390/molecules21101351.
- Sweeting, A.N., Hocking, S.L. & Markovic, T.P. 2015. Pharmacotherapy for the treatment of obesity. *Molecular and Cellular Endocrinology*. 418:173–183. DOI: 10.1016/j.mce.2015.09.005.
- Tandon, P., Wafer, R. & Minchin, J.E.N. 2018. Adipose morphology and metabolic disease. *The Journal of Experimental Biology*. 221(Suppl 1):jeb164970. DOI: 10.1242/jeb.164970.
- Tanis, R.M., Piroli, G.G., Day, S.D. & Frizzell, N. 2015. The effect of glucose concentration and sodium phenylbutyrate treatment on mitochondrial bioenergetics and ER stress in 3T3-L1 adipocytes. *Biochimica et Biophysica Acta (BBA) - Molecular Cell Research*. 1853(1):213–221. DOI: 10.1016/j.bbamcr.2014.10.012.
- Thaker, V. V. 2017. Genetic and Epigenetic causes of obesity. *Adolescent medicine: state of the art reviews*. 28(2):379–405. Available: <http://www.ncbi.nlm.nih.gov/pubmed/30416642> [2019, November 26].
- Tokmakov, A.A., Kurotani, A., Takagi, T., Toyama, M., Shirouzu, M., Fukami, Y. & Yokoyama, S. 2012. Multiple Post-translational Modifications Affect Heterologous Protein Synthesis. *Journal of Biological Chemistry*. 287(32):27106–27116. DOI: 10.1074/jbc.M112.366351.

- Veeresham, C. 2012. Natural products derived from plants as a source of drugs. *Journal of Advanced Pharmaceutical Technology & Research*. 3(4):200. DOI: 10.4103/2231-4040.104709.
- Villaño, D., Pecorari, M., Testa, M.F., Raguzzini, A., Stalmach, A., Crozier, A., Tubili, C. & Serafini, M. 2010. Unfermented and fermented rooibos teas (*Aspalathus linearis*) increase plasma total antioxidant capacity in healthy humans. *Food Chemistry*. 123(3):679–683. DOI: 10.1016/j.foodchem.2010.05.032.
- Visagie, A., Kasonga, A., Deepak, V., Moosa, S., Marais, S., Kruger, M.C. & Coetzee, M. 2015. Commercial honeybush (*Cyclopia* spp.) tea extract inhibits osteoclast formation and bone resorption in RAW264.7 murine macrophages—An *in vitro* Study. *International Journal of Environmental Research and Public Health*. 12(11):13779–13793. DOI: 10.3390/ijerph121113779.
- Wang, H., Zhu, Y.Y., Wang, L., Teng, T., Zhou, M., Wang, S.G., Tian, Y.Z., Du, L., et al. 2017. Mangiferin ameliorates fatty liver via modulation of autophagy and inflammation in high-fat-diet induced mice. *Biomedicine and Pharmacotherapy*. 96:328–335. DOI: 10.1016/j.biopha.2017.10.022.
- Wang, Q.A., Scherer, P.E. & Gupta, R.K. 2014. Improved methodologies for the study of adipose biology: insights gained and opportunities ahead. *Journal of Lipid Research*. 55(4):605–624. DOI: 10.1194/jlr.R046441.
- Wang, S., Moustaid-Moussa, N., Chen, L., Mo, H., Shastri, A., Su, R., Bapat, P., Kwun, I., et al. 2014. Novel insights of dietary polyphenols and obesity. *The Journal of Nutritional Biochemistry*. 25(1):1–18. DOI: 10.1016/j.jnutbio.2013.09.001.
- Weyermann, J., Lochmann, D. & Zimmer, A. 2005. A practical note on the use of cytotoxicity assays. *International Journal of Pharmaceutics*. 288(2):369–376. DOI: 10.1016/j.ijpharm.2004.09.018.
- Wharton, S. 2016. Current Perspectives on Long-term Obesity Pharmacotherapy. *Canadian Journal of Diabetes*. 40(2):184–191. DOI: 10.1016/j.cjcd.2015.07.005.
- WHO. 2000. *Obesity: preventing and managing the global epidemic. Report of a WHO consultation*. DOI: ISBN 92 4 120894 5.
- WHO. 2018. *Obesity and overweight*. Available: <https://www.who.int/en/news-room/fact-sheets/detail/obesity-and-overweight> [2019, November 27].
- Wing, R.R., Venditti, E., Jakicic, J.M., Polley, B.A. & Lang, W. 1998. Lifestyle intervention in overweight individuals with a family history of diabetes. *Diabetes Care*. 21(3):350–359. DOI: 10.2337/diacare.21.3.350.
- Wisman, K.N., Perkins, A.A., Jeffers, M.D. & Hagerman, A.E. 2008. Accurate assessment of the bioactivities of redox-active polyphenolic in cell culture. *Journal of Agricultural and Food Chemistry*. 56(17):7831–7837. DOI: 10.1021/jf8011954.
- Wolfe, B.M., Kvach, E. & Eckel, R.H. 2016. Treatment of Obesity. *Circulation Research*.

118(11):1844–1855. DOI: 10.1161/CIRCRESAHA.116.307591.

- Wu, J., Boström, P., Sparks, L.M., Ye, L., Choi, J.H., Giang, A.-H., Khandekar, M., Virtanen, K.A., et al. 2012. Beige Adipocytes Are a Distinct Type of Thermogenic Fat Cell in Mouse and Human. *Cell*. 150(2):366–376. DOI: 10.1016/j.cell.2012.05.016.
- Yan, L.J. 2014. Pathogenesis of chronic hyperglycemia: From reductive stress to oxidative stress. *Journal of Diabetes Research*. 2014:137919. DOI: 10.1155/2014/137919.
- Yang, C.-Q., Xu, J.-H., Yan, D.-D., Liu, B.-L., Liu, K. & Huang, F. 2017. Mangiferin ameliorates insulin resistance by inhibiting inflammation and regulatiing adipokine expression in adipocytes under hypoxic condition. *Chinese Journal of Natural Medicines*. 15(9):664–673. DOI: 10.1016/S1875-5364(17)30095-X.
- Yoneshiro, T., Aita, S., Matsushita, M., Okamatsu-Ogura, Y., Kameya, T., Kawai, Y., Miyagawa, M., Tsujisaki, M., et al. 2011. Age-Related Decrease in Cold-Activated Brown Adipose Tissue and Accumulation of Body Fat in Healthy Humans. *Obesity*. 19(9):1755–1760. DOI: 10.1038/oby.2011.125.
- Yoshikawa, M., Shimoda, H., Nishida, N., Takada, M. & Matsuda, H. 2002. *Salacia reticulata* and Its Polyphenolic Constituents with Lipase Inhibitory and Lipolytic Activities Have Mild Antiobesity Effects in Rats. *The Journal of Nutrition*. 132(7):1819–1824. DOI: 10.1093/jn/132.7.1819.
- Zhang, Y., Liu, X., Han, L., Gao, X., Liu, E. & Wang, T. 2013. Regulation of lipid and glucose homeostasis by mango tree leaf extract is mediated by AMPK and PI3K/AKT signaling pathways. *Food Chemistry*. 141(3):2896–2905. DOI: 10.1016/j.foodchem.2013.05.121.
- Zoico, E., Rubele, S., De Caro, A., Nori, N., Mazzali, G., Fantin, F., Rossi, A. & Zamboni, M. 2019. Brown and Beige Adipose Tissue and Aging. *Frontiers in Endocrinology*. 10(JUN). DOI: 10.3389/fendo.2019.00368.
- Zwick, R.K., Guerrero-Juarez, C.F., Horsley, V. & Plikus, M. V. 2018. Anatomical, Physiological, and Functional Diversity of Adipose Tissue. *Cell Metabolism*. 27(1):68–83. DOI: 10.1016/j.cmet.2017.12.002.

7. Appendix

7.1 Aseptic technique

During cell culture, aseptic technique is important to prevent contamination of cells from foreign microorganisms (viruses, bacteria and fungi). Personal protective equipment, which included a clean laboratory coat, gloves, shoe covers, a face mask and arm sleeve covers were worn to reduce the risk of contamination. Cell culture procedures were carried out in a biosafety level 2 cabinet, which was cleaned with 70% ethanol prior to use. The work area was kept tidy and contained only the necessary reagents and consumables for the specific procedure to be conducted. All reagents and consumables such as flasks, pipettes and plates were wiped down with 70% ethanol. Consumables that were not properly sealed were considered non-sterile and therefore they were not used. Glass pipettes were sterilised with a Bunsen burner. To ensure a clean environment in and outside of the hood, incubators, the floor, work surfaces and equipment were cleaned twice a month with 1% Contrad. An hour thereafter, all these areas were wiped with 70% ethanol.

7.2 Reagents and kits

Table 7.1 List of reagents

Product name	Catalogue number	Supplier
3-(4,5-dimethylthiazol-2-yl)-2,5-diphenyltetrazolium bromide (MTT)	M2003	Sigma-Aldrich, St Louis, MO, USA
3-isobutyl -1-methyl-xanthine (IBMX)	I5879	Sigma-Aldrich, St Louis, MO, USA
3T3-L1 pre-adipocytes	CL-173	American Type Culture Collection (ATCC), Manassas, VA, USA
Chloroform	136112-00-0	Sigma-Aldrich, St Louis, MO, USA
Dexamethasone	D4902	Sigma-Aldrich, St Louis, MO, USA
Dimethyl sulfoxide (DMSO)	276855	Sigma-Aldrich, St Louis, MO, USA
Dulbecco`s modified Eagle`s medium (5.5 mM glucose) (DMEM)	22320030	Gibco, Thermo Fisher Scientific, Waltham, MA, USA
Dulbecco`s modified Eagle`s medium (25 mM glucose) (DMEM)	11995073	Gibco, Thermo Fisher Scientific, Waltham, MA, USA
Dulbecco`s phosphate buffered saline (DPBS)	17-513F	Lonza, Walkersville, MD, USA
Ethanol (for cleaning)	2875	Sigma-Aldrich, St Louis, MO, USA
Ethanol absolute, 200 molecular grade	E7023-500	Sigma-Aldrich, St Louis, MO, USA
Foetal bovine serum	16140071	Gibco, Thermo Fisher Scientific, Waltham, MA, USA
Hanks buffered saline solution (HBSS)	08-003A	Lonza, Walkersville, MD, USA
Glucose powder	D5030	Sigma-Aldrich, St Louis, MO, USA
Insulin	I92785	Sigma-Aldrich, St Louis, MO, USA
Isopropanol	I9516	Sigma-Aldrich, St Louis, MO, USA
Oil Red O (ORO)	1320-06-5	Sigma-Aldrich, St Louis, MO, USA
RNase free water	AM9937	Ambion, Austin, TX, USA

Sodium bicarbonate (NaHCO ₃)	M2645	Sigma-Aldrich, St Louis, MO, USA
Sterile TC water	59900C	Lonza, Walkersville, MD, USA
Qiazol reagent	79306	Qiagen, Hilden, Germany
Trypan blue	15050-065	Invitrogen, Carlsbad, CA, USA
Trypsin	17-161F	Lonza, Walkersville, MD, USA
TaqMan [®] universal PCR master mix II	4364338	Applied Biosystems, Foster City, CA, USA

Table 7.2 List of kits

Kits	Catalogue number	Supplier
DuoSet ELISA Ancillary Reagent Kit 2	DY008	R&D Systems, Minneapolis, MN, USA
Glycerol assay kit	MAK211	Sigma-Aldrich, St Louis, MO, USA
Mouse IL6 DuoSet ELISA	DY406	R&D Systems, Minneapolis, MN, USA
Mouse MCP1 DuoSet ELISA	DY479-05	R&D Systems, Minneapolis, MN, USA
Mouse TNF α DuoSet ELISA	DY410	R&D Systems, Minneapolis, MN, USA
RNeasy mini kit	74106	Qiagen, Hilden, Germany
Turbo DNase kit	AM1907	Ambion Inc, Austin, TX, USA
High Capacity cDNA kit	4368814	Applied Biosystems, Foster City, CA, USA

7.3 List of equipment and software

Table 7.3 List of equipment and consumables

Equipment	Catalogue number	Supplier
Agilent 2100 Bioanalyzer	76337	Agilent Technologies, Waldbronn, Germany
Biohazard safety cabinet, class II	EN 12469	Airvolution lab, Johannesburg, SA
BioTek [®] ELX 800 plate reader	7341000	BioTek Instruments Inc., Winooski, VA, USA
Carbon dioxide (CO ₂)	K239C	Air Products, Centurion, Gauteng, SA
CELLBIND 6-well plates	3335	Corning, Tewksbury, MA, USA
CELLBIND 24-well plates	3337	Corning, Tewksbury, MA, USA
CELLBIND 96-well plates	3300	Corning, Tewksbury, MA, USA
Eppendorf centrifuge 5810 R	5810000420	Sigma-Aldrich, St Louis, MO, USA
Cryotubes	430659	Corning, Tewksbury, MA, USA
Eppendorf tubes	30123301	Sigma-Aldrich, St Louis, MO, USA
Filter Pads	23385	Sigma-Aldrich, St Louis, MO, USA
Galaxy R CO ₂ incubator,	CO170R-120-0000	RS Biotech, West Lothian, UK
IKA vortex mixer	0030000753	IKA, Staufen, Germany
NanoDrop One ^C Microvolume UV-Vis spectrometer	ND-ONE	Thermo Fisher Scientific, Waltham, MA, USA
Olympus inverted light microscope	CKX 41	Melville, NY, USA
PCR plates	N8010560	Applied Biosystems, Foster City, CA, USA
Stainless steel beads (5mm)	69989	Qiagen, Hilden, Germany
T75 Flasks	708003	Nest Scientific, Rahway, NJ, USA

Table 7.4 List of software

Software	Description	Manufacturer
GraphPad Prism 7	GraphPad Software	La Jolla, CA, USA
BioTek plate reader	Gen5 software (version 1.05)	BioTek Instruments Inc., Winooski, USA
Microsoft office	Excel / Word / PowerPoint	Microsoft Corporation, WA, USA
SpectraMax [®] i3x Multi-Mode Microplate reader	SoftMax Pro 7 Software	Molecular Devices, Sunnyvale, CA, USA
ABI Thermal cycler	Software (SDS V1.4)	Applied Biosystems, Foster City CA, USA

7.4 Preparation of medium and buffers

Table 7.5 Preparation of medium

Medium	Reagents	Concentration	Volume (50 ml)
Growth medium	FBS	10%	5 ml
	DMEM	5.5, 25 or 33 mM	45 ml
Freezing medium	FBS	10%	5 ml
	DMEM	25 mM	41.5 ml
	DMSO	7%	3.5 ml
Differentiation media	DMEM	5.5, 25 or 33 mM	49.49 ml
	IBMX	0.5 mM	0.5 ml
	Insulin	1 µg/ml	0.005 ml
	Dexamethasone	1 µM	0.005 ml
Insulin Medium	Insulin	1 µg/ml	0.005 ml
	DMEM	5.5, 25 or 33 mM	49.995 ml

Media were freshly prepared on each day of differentiation and freezing

Table 7.6 Preparation of DMEM without phenol red

Medium	MW (g/mol)	Concentration	Amount/1L
DMEM powder	-	8.3 g/L	8.3 g
BSA (no fatty acids)	-	0.1%	1 g
NaHCO ₃	84.01	3.7 g/L	3.7 g
D-Glucose	180.16	4.5 g/L	1.5 g

Table 7.7 Sorenson's buffer

Reagent	Final Concentration	g/100 ml
Glycine	0.1 M	0.751 g
NaCl	0.1 M	0.584 g

*The pH of the buffer was adjusted to pH 10.5 with 0.1 mM NaOH

7.5 Assays

7.5.1 Preparation of the ORO and CV stains

A) ORO:

A 1% (w/v) ORO stock solution was prepared by dissolving 1 g of the ORO powder in 100 ml of isopropanol. This solution was placed on a magnetic stirrer overnight to dissolve most of the ORO powder. A 70% (v/v) working solution was prepared by adding 30 ml of distilled H₂O to 70 ml ORO stock solution. The ORO working solution was mixed by inversion and then sterile filtered to remove all the precipitates. The ORO working solution was stored at room temperature away from direct sunlight.

B) CV:

A 2% CV stock solution was prepared by dissolving 2 g CV powder in 100 ml of tissue culture grade H₂O. The CV stock solution was placed on a magnetic stirrer overnight (~16 hrs). A 0.5% working solution was prepared by adding 49.75 ml of distilled H₂O to 250 µl of the CV stock solution and then mixed by inversion. A fresh CV working solution was prepared for every experiment on the day of the experiment.

7.5.2 Preparation of the MTT

- 13 mg of MTT dye was weight and dissolved in 6.5 ml of DPBS to make a 2 mg/ml stock. Thereafter the solution was filter sterilised and stored at 4°C in a tube covered with foil.

7.6 Treatments

Table 7.8 Treatments

Extract /compound	Description	Supplier
Afriplex GRT™	Unfermented <i>Aspalathus linearis</i>	Afriplex (Pty) Ltd, Paarl, Western Cape, SA
Aspalathin	Major compound from <i>Aspalathus linearis</i>	High Force Research Ltd., Durham, England, UK
Crude polyphenol enriched fraction of <i>Cyclopia intermedia</i>	Unfermented <i>Cyclopia intermedia</i>	Babalwa Jack (Jack et al., 2017)
Mangiferin	Major compound from <i>Cyclopia</i>	Sigma-Aldrich, St Louis, MO, USA
Isoproterenol	β-Adrenoceptor agonist	Sigma-Aldrich, St Louis, MO, USA)

7.7 Supplementary data

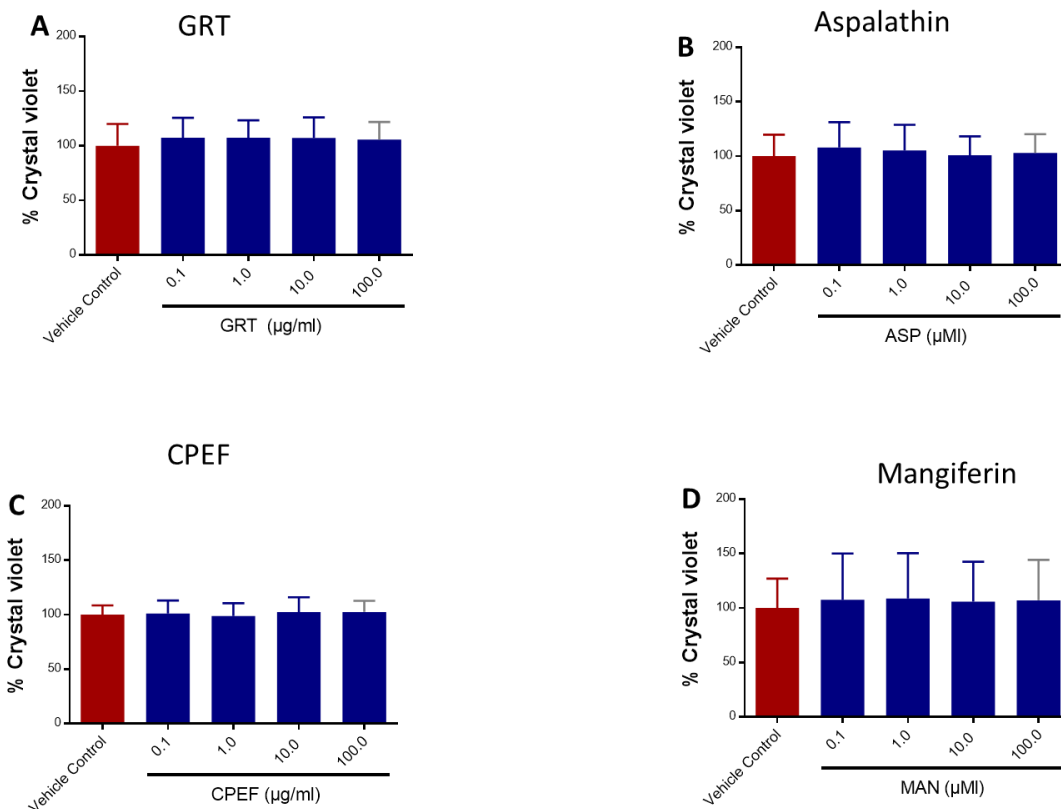


Figure 7.1 Effect of acute treatment on cell density.

3T3-L1 pre-adipocytes were differentiated in 33 mM glucose in the presence of treatment for 14 days, where after cell density was assessed using the crystal violet (CV) staining. CV was expressed relative to the vehicle control (DMSO), which was set at 100%. Results are expressed as the mean \pm SD of three independent experiments, each with n=3.

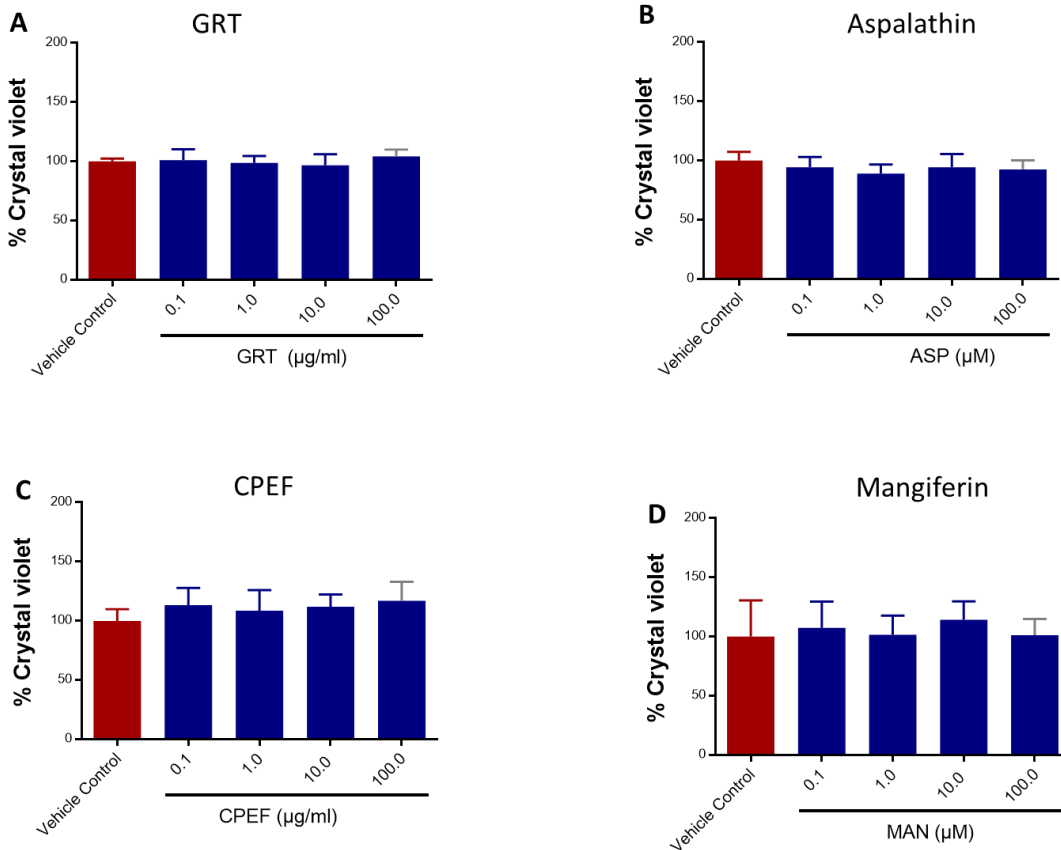


Figure 7.2 Effect of chronic treatment on cell density.

3T3-L1 pre-adipocytes were differentiated in 33 mM glucose in the presence of treatment for 14 days, where after cell density was assessed using the crystal violet (CV) staining. CV was expressed relative to the vehicle control (DMSO), which was set at 100%. Results are expressed as the mean \pm SD of three independent experiments, each with n=3.

7.8 Outputs from study

1. Conferences

- Oral Presentation

47th Conference of the Physiology Society of Southern Africa (18-21 August 2019, Eastern Cape) Differentiation in high glucose increases lipid accumulation, lipolysis and oxidative stress 3T3-L1 adipocytes. Mamushi MP, Jack B, Du Plessis SS & Pheiffer C.

9th Biomedical Research & Innovation Symposium (21 October 2019, Cape Town) The effect of *Aspalathus linearis* and *Cyclopia intermedia* on lipid accumulation, inflammation, oxidative stress and lipolysis in 3T3-L1 adipocytes. Mamushi MP, Jack B, Du Plessis SS & Pheiffer C

- Poster Presentation

13th Annual Early Career Scientist Convention (9-11 October 2019, Cape Town) Differentiation in high glucose increases lipid accumulation, lipolysis and oxidative stress 3T3-L1 adipocytes. Mamushi MP, Jack B, Du Plessis SS & Pheiffer C.

2. Publications

Adipose tissue as a possible therapeutic target for polyphenols: A case for *Cyclopia* extracts as anti-obesity nutraceuticals (2019). *Biomedicine & Pharmacotherapy*, 120, 109439. Jack, B. U., Malherbe, C. J., Mamushi, M., Muller, C. J., Joubert, E., Louw, J., & Pheiffer, C.